Enhancements to the Bond Between Advanced Composite Materials and Steel for Bridge Rehabilitation

by

John W. Gillespie, Jr.
Todd Douglas West

Center for Composite Materials
University of Delaware

December 2002

DELAWARE CENTER FOR TRANSPORTATION

University of Delaware
355 DuPont Hall
Newark, Delaware 19716
(302) 831-1446

Enhancements to the Bond Between Advanced Composite Materials and Steel for Bridge Rehabilitation

by

JOHN W. GILLESPIE, JR.
TODD DOUGLAS WEST

Center for Composite Materials
University of Delaware
Newark, Delaware 19716

DELAWARE CENTER FOR TRANSPORTATION
University of Delaware
Newark, Delaware 19716

This work was sponsored by the Delaware Center for Transportation and was prepared in cooperation with the Delaware Department of Transportation. The contents of this report reflect the views of the authors who are responsible for the facts and accuracy of the data presented herein. The contents do not necessarily reflect the official views of the Delaware Center for Transportation or the Delaware Department of Transportation at the time of publication. This report does not constitute a standard, specification, or regulation.

The Delaware Center for Transportation is a university-wide multi-disciplinary research unit reporting to the Chair of the Department of Civil and Environmental Engineering, and is co-sponsored by the University of Delaware and the Delaware Department of Transportation.

Delaware Center for Transportation
University of Delaware
Newark, DE 19716
(302) 831-1446

TABLE OF CONTENTS

Chapter 1: INTRODUCTION

1.1 Purpose of this Study

It is no secret that our nation's infrastructure is in need of repair. Many of the highways and bridges that serve our major cities were built during the 1950's and 1960's as part of the Dwight D. Eisenhower System of Interstate and Defense Highways. In much of the northeast, portions of the infrastructure significantly pre-date this network of roadways with ages of up to 100 years or more. Unfortunately, the life expectancy of such structures is only on the order of 50 years. Outmoded, outdated, inadequate, and even inferior design has limited a structure's usefulness and reduced this life expectancy; it is not uncommon to see bridges "posted" as a result of these design issues. Additionally, the increase in the volume, frequency, and weight of traffic beyond design assumptions has accelerated the effects of fatigue and aged the structures prematurely. Combining these factors with our reliance on motor vehicles for personal transportation, transport of goods, and the execution of commerce, the situation will get worse before it can improve.

Of these highway bridges, a majority was constructed using concrete bridge decks atop steel girders. Over the course of their lives, steel bridges require a minimum level of maintenance, including regular painting, to ensure their function for years to come. In many cases painting proves costly in materials and manpower therefore it is commonly not performed frequently enough or it is even neglected altogether. This improper maintenance introduces another enemy to the infrastructure in the form of corrosion that further weakens the already taxed structures.

The purpose of this study was to build upon previously developed techniques for the rehabilitation of steel bridge girders. The application of an advanced composite material to steel bridge girders through the use of adhesives has been explored as a rehabilitation option. The particular technique investigated in this work has been proven to restore lost stiffness and load capacity to weakened steel members (Gillespie, et al. 234-240) as well as reduce the rate of fatigue crack propagation in laboratory samples (Ammar 95-107). However, there are many areas that need to be addressed before the rehabilitation process can be deployed in the field.

The primary issue not addressed in the initial work were the effects of corrosion. Askeland tells us that corrosion is the result of the "metal reacting with oxygen or other gases" (15) and producing some type of byproduct through the chemical process of oxidation. In the case of steel corrosion, we commonly refer to the byproduct as rust. Not only will corrosion weaken the structural members, but it can also compromise the adhesive bond if it forms at the adhesive-steel interface. Above and beyond typical modes of corrosion, there is

the additional threat of galvanic corrosion through the joining of dissimilar materials. There are several measures that can be employed to reduce or eliminate the presence of corrosion; some of which were investigated and the results will be presented in Chapter 2.

Proper preparation of the bonding surfaces in any application involving adhesives is of paramount concern. The strength of the adhesive bond is directly proportional to the quality of the surfaces to which it is mated. First and foremost, all surfaces must be clean and free of impurities. Additionally, it is advantageous to have surfaces which are "roughened" slightly in some fashion. For example, a surface with small irregularities provides additional surface area for the adhesive to bond along with some mechanical resistance to shear at the bond interface. Conversely, a surface that is smooth or one that even has a slick finish does not produce nearly as strong of a bond because shear cracks can quickly propagate unimpinged along the length of the bond. Finally, the use of primers in surface preparation can greatly enhance the strength of the bond by creating a more consistent, complete, and durable bond. To this end, a variety of combinations of surface preparations were investigated in this research.

The long-term environmental durability of this type of structural rehabilitation is of concern as well. The majority of structures in this country experience a variety of climactic extremes. Conditions can range from 100 °F or greater with high levels of humidity in the summer months to temperatures well below freezing for extended periods in the winter months. The cyclic loading due to temperature variations introduces thermal fatigue effects, which take its toll on any structure as well. Additionally, each climactic extreme carries it's own unique impact to materials and structures. The impact of each mode to the durability of the bond was investigated through the use of wedge specimens in combination with the variety of surface preparations referred to above.

1.2 What is an Advanced Composite Material?

A composite material is one that attains its physical and mechanical characteristics through the integration of other materials. Generally, a composite material combines the most desirable characteristics of its constituents to create a superior material. A well-known example of a composite material is concrete which uses Portland cement, aggregates, water, and additional admixtures to create a more versatile material than any one of its components individually. Usually, an advanced composite material provides greater strength at lighter weights than traditional construction materials thus offering distinct advantages in many engineering applications.

Similarly, an advanced composite material combines two primary components, a matrix and a fiber, to attain additional performance not available in the components individually. A simple analogy to reinforced concrete best illustrates the behavior of composites. The fiber can be considered as the reinforcing steel

and matrix can be thought of as concrete. Additionally, the strength of the fiber lies in tension much like that of reinforcing steel. However a major difference is that the volume fraction of fiber in composites ranges from 50% to 70% versus volumes on the order of 1% and less in concrete. Additionally, the fiber has diameters on the order of 7-10 μm versus the 3/8 inch to 2 inches for reinforcing steel.

These new materials can be considered as a truly engineered material because the matrix and fiber can be selected from a variety of candidates to provide desired performance characteristics. The fiber orientation within the material can be altered to tailor material properties as needed. Additionally, a variety of manufacturing techniques is employed to create these materials, each one designed and suited to maximizing the performance and reducing the cost of the final product. Common examples of matrix materials include epoxies, phenolics, polyesters, and vinyl esters while aramid (Kevlar), carbon, glass, and graphite are frequently used as reinforcing fibers (Vinson 5-6). For the remainder of this report, the word "composite" will be used solely in reference to an advanced composite material unless otherwise noted.

Pertaining to this work, pultruded graphite composite was used. To fabricate this specific material, graphite fibers were aligned and pulled through a die. While passing through the die, the fibers were combined with a vinyl-ester matrix in liquid form to produce a unidirectional composite. The term "unidirectional" refers to the property that the primary strength of the material is found along one axis; in the case of the material used in this study, longitudinally. The final shape of the material was a thin rectangle of infinite length limited only by the length of the fibers used in production and the ability to transport the final product.

1.3 Previous Research

The rehabilitation of steel bridge girders through the application of advanced composite materials has been pioneered at the University of Delaware through various research projects. Mertz and Gillespie have explored a variety of composite reinforcement options that included plate, sandwich, wrap, pultruded channels, and pultruded strips (3-7). In strength testing, the girders repaired with a sandwich composite and the pultruded strips offered the greatest increase in flexural stiffness and load capacity alike. The pultruded strips were selected as the most viable rehabilitation scheme due to their commercial availability at low cost, the availability in a near infinite length, the ease of handling and implementation of the material, and the geometry constraints typically incurred when dealing with highway bridges. The infinite length is of a particular advantage because it eliminates the need for splices over the length of the rehabilitated member. Splices could introduce locations for fracture or fatigue crack initiation in the bond as a result of stress concentrations associated with the termination of a section of composite. Furthermore, splice locations would

provide additional interfaces that could be exposed to the adverse effects of the environment.

Mertz and Gillespie (1-7) explored options for attaching the selected materials to girders including various mechanical fasteners, resins, and adhesives. Mechanical fasteners were eliminated as an option because they offered no distinct incentive for using composite materials over traditional steel plates. Rajagopalan, Immordino, and Gillespie (222-230) developed a downselection methodology to evaluate and select adhesives that were the most advantageous for bonding composites to steel for a variety of conditions. Such criteria as pot life, glass transition temperature (T_g), and curing requirements, among others, were used as guidelines for the downselection. The study recommended Ciba Geigy AV8113 two-part epoxy for small to medium-scale repairs and Cytec® FM 235 or Ciba Geigy AV119 single component adhesives for larger applications.

It is desirable to use a two part epoxy whenever possible because most will cure within 16-24 hours under ambient conditions. However, the trade-off of this relatively simple curing cycle is a limited pot life (working time) of the adhesive, which can range anywhere from 90 seconds to 45 minutes. The single component adhesives offer a much longer pot life yet they often require elevated temperatures to ensure cross-linking of the polymers and, hence, a fully cured adhesive. Under laboratory conditions, it is relatively easy to perform a high-temperature cure; however, this task can be difficult to implement in the field. It is common practice to use heating blankets to cure concrete in colder climates or under winter conditions; this technique could conceivably be extended to assist in the curing of adhesive in the particular rehabilitation method. Wetzel (8) explored this option as well as induction heating, resistance heating, and radiant heaters as potential methods to adequately cure the adhesive. It was determined that these heating techniques were viable and the most effective method for obtaining the desired temperature within the adhesive bond line was dependant on the size and geometry of the rehabilitation.

The last, and quite possibly most important factor in the bonding of composites to steel is the surface preparation of both adherends. ASTM offers guides for the surface preparation of both metals and plastics for adhesive bonding. While there are many methods offered within these guides, they are mostly intended for small-scale laboratory applications. It is necessary to keep in mind that whichever surface preparation is selected, it must be easily implemented in the field on existing structures as well as be environmentally friendly. Additionally, McKnight as well as Rajagopalan explored the use of Dow Corning silane coupling agents to enhance bond characteristics. McKnight (251-287) found that the use of silanes with aluminum adhesive joints significantly increased the durability of the bond. Rajagopalan (222-230) found similar results in steel adhesive joints when exposed to both thermal fatigue and freeze/thaw tests. Dow Corning manufactures a number of silanes designed for use with a variety of adhesives.

Ultimately, actual field rehabilitation was simulated in the ATLASS structures laboratory at Lehigh University. University of Delaware researchers applied the devised technique on two of four steel bridge girders that were donated by PennDOT. The steel girders were part of a bridge originally built over Rausch Creek in central PA in the 1940's that was eventually replaced. Over time the corrosive effects of the mist spraying the girders caused such significant corrosion that the bridge had been shored for an undetermined amount of time. Several evaluation methods, including laboratory testing, indicated that the girders had lost as much as 32% of their original stiffness and overall strength. Testing after the rehabilitation showed a return of stiffness to nearly that of a virgin girder and increased the ultimate moment carrying capacity of the member to 113% of its original capacity (Mertz and Gillespie 14)

Previous work performed at the University of Delaware provided a starting point for this study. The composite material selected by Mertz and Gillespie (3-7) was carried through along with the Ciba-Geigy AV8113 from Rajagopolan, Immordino, and Gillespie (229). The technique developed and implemented for use with the full-scale rehabilitation by Gillespie, et al. (234) was also brought forward. Furthermore, McKnight's work with silanes and surface preparation proved critical to the continuation of this research.

1.4 Investigation Sequence

For this study, the sequence in which individual research stages were investigated was critical. Results obtained from one experimental phase directly impacted the test specimens and test procedure for subsequent phases. For this reason, the research was performed in the following order:

- Galvanic corrosion investigation
- Lap shear/ strength investigation
- Wedge specimen/ durability investigation
- Full-scale rehabilitation
- Full scale testing

It was determined early on that measures intended to eliminate galvanic corrosion would be an integral part of any rehabilitation. Because of this, performance of other aspects of the rehabilitation would depend upon the attenuation method used. If the research did not take this into account, it could have yielded misleading results or wasted resources and time on inaccurate information. For example, it was determined that a fiberglass scrim in the adhesive bond layer was the preferable solution to the galvanic corrosion issue. Since the scrim would be placed in the bond line, it was necessary to determine the performance of bond with the scrim in place. If there had been failures below expected strength levels, it would become necessary to devise a different method for eliminating the galvanic couple. Additionally, if testing had been

performed without the scrim in place, misleading values could have been obtained since it would be unknown if the scrim had any adverse affects on strength. Furthermore, an approach such as this had to be an integral part of the fabrication process and could not simply be added to the samples at a later stage.

Following this rationale, the downselection process was devised. First, galvanic corrosion testing was performed and the results led to the use of the fiberglass scrim in the bond line. The scrim was then incorporated into the fabrication of lap shear samples used during the bond strength investigation. Any preparation methods that were found to be inferior during the strength testing stage were then eliminated from any future stages. Next, wedge specimen samples for environmental durability testing were produced using all remaining preparation methods that emerged from the strength testing. Upon conclusion of the environmental durability, additional preparation methods were eliminated. Ultimately, preferred pretreatment combinations were selected based upon their performance throughout the stages, ease of field implementation, and applicability to the problem and then used for the full-scale rehabilitation.

Some facets of this investigation were unique to this study alone. Issues such as specifics regarding surface preparation, corrosion attenuation, galvanic corrosion, and environmental durability had not been previously considered. With a comprehensive understanding of all aspects of the rehabilitation process, a complete installation procedure will be established for future implementation in the field.

1.5 Experimental Overview

This section contains a brief description of each of the major test programs as presented in Section 1.4. A more comprehensive explanation of any implemented test procedures, methods, and/ or configurations will be presented more fully along with the corresponding test results in following chapters.

1.5.1 Galvanic Corrosion Testing

Galvanic corrosion is of major concern whenever dissimilar materials, especially dissimilar metals, are joined in any fashion. Materials are ranked in a table known as a galvanic series based upon their tendency to behave as an anode or a cathode in an electrochemical cell. If materials are at opposing ends of the galvanic series, their coupling increases the possibility of galvanic corrosion. Unfortunately, steel is anodic and graphite is cathodic therefore creating an unfavorable galvanic couple in the context of this application. However, it is important to note that aluminum is more anodic than steel and the combination of aluminum and graphite is commonplace in the aerospace industry. There are remediations in place for these applications and there have not been problems that have prevented the combination of those materials in aerospace

applications. Therefore the conclusion can be drawn that the union of steel and graphite will not pose a problem for this application provided appropriate measures are taken.

Galvanic corrosion requires the presence of an electric circuit otherwise known as an electrochemical cell. The hypothesis was formulated that an elimination of current flow through the thickness of an adherend implied an elimination of galvanically induced corrosion. The adhesive alone should be sufficient to act as an insulator between the materials, however it is not a fail-safe solution. Imperfections on the surface of the steel could create "hard-points" that could penetrate the adhesive layer and come in contact with the graphite. Additionally, there is no guarantee that the installation procedure will be reliable therefore leaving the possibility of voids in the adhesive layer that could allow a couple to form as well. It was decided that a fiberglass scrim placed within the bond line would behave as a "last resort" insulator. A "ground level up" screening process was implemented to measure the through thickness resistivities of the adherends under different bonding scenarios. A variety of representative rehabilitation models were assembled to assess the level of galvanic corrosion and the impact made by the corrective measures.

The elimination of galvanic corrosion between the adherends is critical because any corrosion of the steel beneath the bond line is not something that can be discovered during routine inspections. If any amount of corrosion is allowed to accumulate, the rehabilitation could fail in one of two ways. First, the corrosion could become so severe that it could completely compromise the adhesive-steel interface and effectively detach the composite from the girder. Secondly, a smaller layer of corrosion product could build up and the shear strength of the bond would no longer be a function of the adhesive it would become a function of the corrosion layer, which is significantly less than that of the adhesive.

Once again it is important to note that the elimination of the possibility for corrosion was the critical path in this research. Since the solution was most likely going to be integral to the fabrication process it was necessary that it was arrived at prior to the production of additional test samples. From there, the lap shear samples were prepared incorporating the scrim layer for the bond strength investigation. Following lap shear testing, wedge specimens were produced in accordance with the results of the previous two stages and environmental durability was tested. Only after environmental durability studies were complete was a full-scale rehabilitation performed.

1.5.2 Bond Strength Investigation; Lap Shear Samples

One of the most important aspects of an adhesive joint is its shear strength. When bonding composites to steel girders, the load in the steel girder is transmitted by shear through the adhesive layer and into the composite. Therefore, it is necessary to assess the shear strength of any adhesive prior to its implementation. An American Society of Testing and Materials (ASTM)

standardized lap shear procedure was implemented for the testing (ASTM D 3165). It is important to follow this standard with respect to fabrication and testing of the samples. Any deviation from the universally accepted standard would call any results into question. A matrix of adhesives, primers, and surface preparations was created for the lap shear testing. The approach for preparation of the surface of the steel was selected in accordance with standard DelDOT practice for preparation of steel prior to painting. Additionally, a DelDOT standard paint primer was included in the sample matrix.

1.5.3 Durability Investigation; Wedge Specimen Samples

Just as important an aspect as strength of an adhesive is the durability of the adhesive. If a bond is strong from a shear standpoint but is weak when exposed to a variety of environmental conditions, then the adhesive is ineffective. ASTM D 3762 standard wedge specimen test procedure was implemented for the screening of adhesive and surface preparation combinations. The key component in the surface preparation that enhanced the durability was the addition of a bond promoter (primer). The same combination of primers and adhesives that was used for the lap shear testing was also used for the durability testing.

1.5.4 Full-scale Rehabilitation

Following the individual test programs, a preferred technique for rehabilitation was defined. The optimal combination of material surface preparation, primer selection and application, corrosion protection methods, adhesive selection and application, and bonding procedure were integrated. It is important to note that two separate primers and two different adhesives were selected as part of the preferred option. This allows any user of this technique the opportunity to select which primer/ adhesive combination best suits their needs in terms of such variables as cost effectiveness, ease of use, availability, and integration with existing systems, procedures, and/or manpower.

Additionally, a critical aspect in the area of bridge rehabilitation with composites is the actual implementation of the repair. Any procedure can be performed in a laboratory; however, the ease with which the procedure is implemented in the field is the true test. Two full-scale girders, which were removed from service due to the effects of heavy corrosion, were rehabilitated in the University of Delaware structures laboratory. All recommended techniques that addressed individual aspects of the performance of the rehabilitation were incorporated into this methodology and procedure. A complete step-by-step procedure for performing field rehabilitation according to these parameters can be found in Chapter 5.

1.5.5 Full-scale Testing

Prior to their rehabilitation, the girders were placed in a test frame and tested under four point bend conditions to assess the loss of stiffness in the members due to the corrosion. Similarly, the girders were tested to determine the overall strength and stiffness restored after the rehabilitation. Future work will include the performance of the rehabilitation under fatigue conditions as well as the observed performance of the bond under a sustained load exposed to real-time environmental conditions outside of the lab through long term monitoring.

Chapter 2: GALVANIC CORROSION

2.1 Introduction

Galvanic Corrosion is defined as an increase in corrosion above the rate normally experienced by a material. Additionally, the American Society for Testing and Materials (ASTM) defines galvanic corrosion as an "accelerated corrosion of a metal because of an electrical contact with a more noble metal or nonmetallic conductor in a corrosive environment" (Hack, *Corrosion*_1). Hack states that the following three conditions must be met before galvanic corrosion can occur:

1. At least two different conductive materials must be present
2. An electrical connection joining the different materials must exist
3. An electrolyte must be present (*Corrosion* 1)

Once these conditions are met, the system becomes an electrical circuit known as a galvanic couple.

As is the case with any electrical circuit, the galvanic couple has both an anode and a cathode. Oxidation (corrosion) will occur at the anode, the more active of the two components, as the metal gives up electrons and ions enter the solution. Conversely, reduction takes place at the cathode, which is the more passive of the two materials, as the metal gains the ions from the solution.

A galvanic series is used to determine whether an electrode in a galvanic couple is an anode or a cathode. The galvanic series ranks alloys according to their corrosion potential, from more active to more passive, in a given environment. Each metal in the galvanic couple is determined to be either an anode or a cathode based upon its relative position to the other material in the galvanic series. The further apart the two metals are separated in the series, the larger the galvanic potential that exists between them. However, the galvanic series can only predict which metal is likely to see an elevated rate of corrosion, but not the amount of increase of that corrosion (Hack, *Corrosion* 29).

In the context of this research, it is seen when examining the galvanic series that the steel bridge girder is the anode while the graphite-based composite acts as the cathode. In fact, steel and graphite are nearly the most extreme cases of anodes and cathodes alike. When viewing the galvanic series, it is noted that the union of aluminum and graphite creates an even more extreme couple. The aerospace industry has been combining these elements for a number of years, and adverse effects have been avoided by suitable design approaches.

2.2 Background

There have been many different ways of experimentally determining the role galvanic corrosion plays in a composite-metal couple. A variety of experiments with different types of circuits have been conducted with different combinations of materials in a number of electrolytes. The fact that there has been such a broad range of experiments supports Hack when he states, "laboratory testing for galvanic corrosion involves so many variables, there are no standardized laboratory testing procedures" (Hack, *Corrosion*_19). Hack provides a number of possible tests that could be used to assess galvanic corrosion and offers criticism on advantages and disadvantages of each. Additionally, ASTM publishes a guide pertaining to galvanic corrosion testing that includes information on test specimens, test environment, procedure, specimen evaluation, and reporting results but stops short of recommending a standard test procedure. Keeping these facts in mind, several published tests have been reviewed.

The first experiment reviewed was most applicable to this research based on the types of materials screened and the environments studied. Aylor displayed significant galvanic corrosion in both nickel aluminum bronze (NAB) and HY80 steel when coupled with a graphite/epoxy composite in a marine environment and in accelerated electrochemical tests (81). The work also showed a correlation between the amount of exposed fiber and the level of corrosion. Additionally, it was shown that composites with no fiber exposed could still create a galvanic couple as the material absorbs the electrolyte and becomes saturated.

Another study by Bellucci investigated the effects of area ratio and environmental degradation of the composite on the rate of galvanic corrosion (281). In this study, two types of graphite-epoxy composite materials (GECM) were coupled with a number of ferrous and nonferrous metals. Bellucci found the galvanic current to be independent of anodic area and directly proportional to the cathodic area in couples between aluminum alloys, 4340-steel, and nickel aluminum bronze and GECM. Additionally, it was determined that the galvanic currents in the stainless steels and the titanium alloy were dependent upon both the anodic and cathodic surface areas. Finally, aging the composites in distilled water and 3.5% aqueous solution of NaCl was found to increase the effective cathodic area as the absorbed liquid separated the fiber from the matrix. As previously noted from this same study, the increase in cathodic area increased galvanic corrosion in some couples.

A group of researchers at BASF in Anaheim, CA suggest a problem beyond metallic corrosion in a metal-composite couple. Through their studies, it was shown that galvanic metal corrosion generated byproducts could also cause a deterioration of the matrix resins in composite materials. It was determined that all resins were affected, but it was shown that saponifiable resins were the most vulnerable to this type of attack (Boyd, et al. 1217). It was also shown that not all metals corroded at a rate that required protection; only metals with high levels of current such as aluminum and iron were of any concern.

Ultimately, they concluded that degradation of the matrix was not an issue. Recall the observed degradation was a direct result of galvanic corrosion byproducts. Preventative measures taken to eliminate corrosion on the metal surface were sufficient in eliminating galvanic corrosion and, hence, the composite degradation.

2.3 Joining of Components: Mechanical vs. Adhesive

As stated in Section 1.3, Gillespie, Mertz, et al. arrived at the conclusion that an adhesive joint was a preferred method of attaching the composite to the steel bridge girder. From a galvanic corrosion standpoint, an adhesive joint is preferred when joining dissimilar metals as well.

Consider a conventional mechanically fastened joint used with dissimilar metals as illustrated in Figure 2.1. Recall the criteria for galvanic corrosion as presented by Hack in Section 2.1. For reference, Metal A is the steel bridge girder, and Metal B is the graphite/epoxy composite. The first criterion has been satisfied merely by the presence of the composite repair. Next, the mechanical fastener fulfilled the second requirement by providing an electrical connection between the materials. Finally, the presence of any water (rain, seawater, accumulated moisture, etc.) will satisfy the third criterion by supplying the system with an electrolyte. By merely attaching the composite with a fastener, we have induced galvanic corrosion.

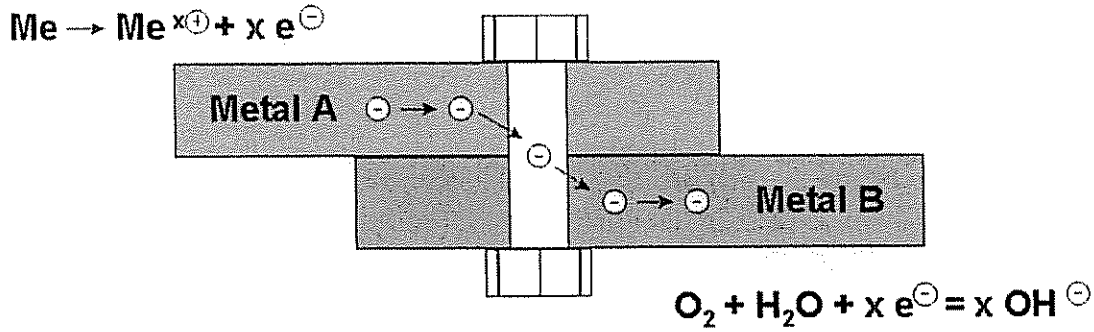

Figure 2.1 Conventional mechanically fastened joint.

Now, inspect a joint that has been bonded with an adhesive as in Figure 2.2. Once again, the presence of the steel bridge girder (Metal A) and the graphite/epoxy composite (Metal B) have satisfied the first requirement for galvanic corrosion. Similarly, it would not be an unreasonable assumption to state that the joint would be exposed to the same electrolyte-producing environment as the conventionally fastened joint thus satisfying the third criterion. However, the aspect that sets this type of joint apart is the adhesive bond. The adhesive layer is a non-conducting medium and therefore insulates

the steel from the composite. Because the components are insulated, no electrical connection exists. Since no electrical connection exists, Hack's 2nd criterion is not satisfied and therefore there is no threat of galvanic corrosion.

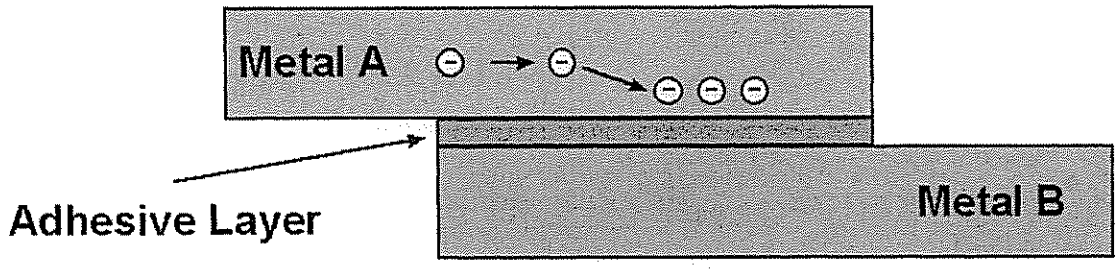

Figure 2.2 Adhesively bonded joint.

2.4 Introduction of a Fabric Scrim Layer

In theory, the connection created with an adhesive will completely eliminate galvanic corrosion, however, theory doesn't necessarily hold true in practice. The elimination of the galvanic couple through the adhesive joint is based upon the primary assumption that there are no holidays or voids in the adhesive layer, otherwise known as the bond line. This could prove to be a faulty assumption because any "human factor" must be considered as a potential source of deviation from the expected result. Additionally, the surface of the steel may be irregular due to varied levels of corrosion across its surface, localized damage due to impacts, or any other number of possible causes. These surface variations could generate "hard points" or locations where the steel pushes through the adhesive and comes in contact with the composite surface. This would once again introduce a mechanism for galvanic corrosion. In response to the possibility of galvanic corrosion existing due to the listed reasons, it was determined that a fabric barrier, or scrim layer, could be used to inhibit the flow of electrons from the steel to the composite as shown in Figure 2.3. This approach has been used successfully in the aerospace industry to eliminate galvanic corrosion between aluminum and carbon reinforced polymer composites.

Similar to the adhesive layer, the presence of the fabric scrim cannot be relied upon to stop galvanic corrosion altogether. The material used as the scrim has been constructed by weaving tows of fiber into a fabric. "Holes" located between adjacent tows of fiber are inherent to the weaving process. Once again, these holes can be potential locations for galvanic corrosion to occur. One possibility is where the steel or composite pokes through the holes in the scrim and comes in contact with the other material. Another concern is the electrolyte saturating the fabric and creating an electric circuit in that fashion. To avoid either undesirable condition, the scrim must be sealed to fill any holes

and to isolate the fabric from the environment. To accomplish this, the scrim can be installed in one of two ways.

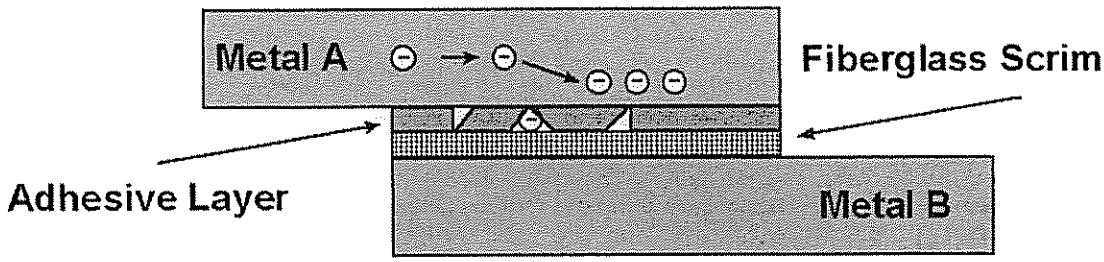

Figure 2.3 Adhesively bonded joint with glass fabric scrim layer.

The first opportunity to introduce the scrim is during the fabrication stage of the composite. Because the composite is made through the pultrusion process, it would be relatively simple to add an additional layer of fiber, in this case the fabric, at the production stage. The fabric would be fed through the same die as the graphite fiber and located at one of the exterior surfaces. This is a very desirable option because the composite will be manufactured under controlled conditions and a high level of quality assurance can be guaranteed.

The second possibility involves adding the fabric scrim during the installation process. As will be explained in greater detail in Chapter 5, the rehabilitation process calls for a film of adhesive to be applied to both the steel and composite adherends. After the adhesive layer is applied to the girder, a section of fabric can be smoothed out over the surface of the girder prior to the attachment of the composite. When the composite is then bonded to the girder, the adhesive on both the girder and the composite repair will be forced to fill in any spaces within the fabric and "wet-out" or saturate the material. This preventative measure will all but eliminate the possibility of galvanic corrosion within the rehabilitation.

2.5 Experimental Procedure

Based on the information found in the literature listed in Section 2.2, the conclusion was made that the potential for galvanic corrosion existed with this particular rehabilitation scheme. The concepts presented in Sections 2.3 and 2.4 suggest that galvanic corrosion could be eliminated through the presence of both the adhesive layer and the glass barrier. However, this theory must be proven experimentally before one can be satisfied that all possibility of galvanic corrosion has been eliminated.

It was determined that the most probable location for a galvanic couple to exist was at the surfaces of two adherends. Based on this potential couple, electron exchange would have to occur through the interface, or more specifically the

bond line. The possibility for a galvanic couple being created through Edge Effects is a secondary concern that can be easily remedied by adding a heavy bead or fillet of adhesive during the installation procedure. This theory was tested during the second phase of galvanic corrosion experimentation discussed in Section 2.5.2.

Two individual experiments were conducted to illustrate both the presence of corrosion and effective means for eliminating such corrosion. The first experiment involved screening the constituent materials for their ability to conduct electrical current. This was supported by a second test scheme, which was devised to apply the theories and lessons from the first experiment under simulated field conditions.

There will be references made to specific sample fabrication processes and material components throughout Section 2.5. Please note that the selection of preferable surface preparation, primers, and adhesives used in the fabrication of the galvanic corrosion samples will be discussed at length in Chapter 3. Additionally, a description and illustration of the test sample fabrication process can be found in Chapter 3 as well.

2.5.1 Experiment One: Component Screening

A simple electrical test was devised to determine the Through Thickness resistivity of the two adherends. Resistivity is defined as the measured electrical resistance of the material divided (normalized) by the specimen thickness. Additionally, this quantity is inversely proportional to conductivity therefore it can be seen that high resistivity values are desirable when one wants to electrically isolate components. This value of resistivity provided a standard value to compare results across specimens with varying thickness. The Through Thickness resistance of each individual specimen was measured using a digital multi-meter with plate style test leads. From the measured resistance and the recorded thickness of each sample, the resistivity was then obtained for comparison purposes.

Initially pin-type test leads were used to measure resistances, however the sharp points of the leads led to inconsistent results when used with the composite. It was determined the points of the leads would occasionally "miss" graphite fibers and come in contact with only the matrix. Considering this measurement was on the microscopic level and the actual application was on the macroscopic level, 1/2 in square test leads were fabricated for resistance measurements. By using the square test leads, a more applicable global behavior of the samples was obtained by providing contact to a larger surface area.

2.5.1.1 Specimen Selection

When measuring the through thickness resistivities of the specimens with respect to this research, it was imperative that the materials tested were similar, if not identical, to that which will be used in the field. Additionally, it was necessary that all possible combinations of steel and composite specimens be considered. Table 2.1 lists surface preparation methods for the samples used in the first galvanic corrosion test.

The first main group of samples, labeled E through M, encompassed all of the composite material samples. Type E was the composite in the condition as it was received and was selected to serve as a baseline for comparison to all other composite samples. Note that the bonding surface of the composite requires abrasion and solvent cleaning in order to enhance the bond strength therefore sample Type F was selected to simulate this. Similarly, an option exists to bond a second layer of composite directly on top of the first in situations where additional strength is required. Type G was created to model the behavior of a layer of composite that had both sides abraded and cleaned to facilitate bonding.

Table 2.1 First galvanic corrosion specimen preparation matrix.

Composite Specimen Prep Methods	
E	As received
F	One face abraded and cleaned
G	Two faces abraded and cleaned
H	Two faces abraded, cleaned, and painted with conductive paint
J	Adhesive (Ciba-Geigy AV8113) layer on surface
L	One face abraded, cleaned, and scrim from wet lay-up
M	One face abraded, cleaned and adhesive layer with embedded scrim
Steel Specimen Prep Methods	
N	As received
P	One face bead blasted and cleaned
Q	Two faces bead blasted and cleaned
R	Two faces bead blasted, cleaned, and painted with conductive paint
S	One face bead blasted, cleaned, and with silane primer
T	One face bead blasted, cleaned, silane primer, and adhesive layer
U	One face bead blasted, cleaned, silane primer, and adhesive layer with scrim

It was assumed that the adhesive layer would act as an insulator and isolate the composite electrically from the steel. In order to verify this assumption, a layer of Ciba-Geigy AV8113 adhesive was applied to the surface of the composite material in a quantity that would be expected in an actual rehabilitation. Based

on this, sample Type J was selected. In the event there is not complete adhesive coverage in the rehabilitated state, it is theorized that a fiberglass scrim layer could be added to the system to serve as a "safety net" and serve as an insulator as well.

It is important to note that the scrim could be fabricated integral to the surface of the composite or it could be added as a separate component during the rehabilitation process. The samples for Type L were fabricated by bonding a layer of fiberglass scrim to the surface of composite samples using a vinyl esther resin and the SCRIMP, Siemann's Composite Resin Infusion Molding Process, technique. This simulates the addition of the scrim during the material fabrication stage. It follows that sample Type M models the addition of the scrim during the rehabilitation process as it was embedded in a layer of adhesive.

The second group of samples, labeled N through U, incorporated all samples with steel as its main component. These samples were similar in composition their composite counterparts. Sample Type N was the steel in its "as received" state and served as a control sample. Sample Types P and Q were steel with one and two faces bead blasted and cleaned with a solvent respectively.

In addition to abrading the surface of the steel through the use of a bead blast to improve bond characteristics, a silane primer was selected to further improve the bond between the adhesive and steel. Based on this, sample Type S incorporated steel with an abraded and cleaned surface with a layer of silane primer. Type T was identical to Type S with the addition of a layer of the Ciba-Geigy adhesive. Finally, Type U incorporated the major aspects of Type S, an abraded, cleaned and primed piece of steel, with Type M, an adhesive layer with an embedded scrim, to create the last sample.

Note that samples H and R incorporate an application of graphite based conductive paint to the surface of the constituent materials. This was originally included in the study to test the performance of the paint in the event additional testing was required where the entire surface of the material was to be considered "active" during the test. If necessary, the resulting resistivities could later be subtracted from results of additional experiments on the premise that the conductive paint introduced some additional resistance to the system.

2.5.1.2 Experimental Results

Results from the resistivity screening of the samples were expected to be predictable. It was anticipated that the composite in the "as received" state would offer some level of resistance due to the nature of the finished surfaces, but it would still conduct a majority of current. As the surface finishes of the composites were abraded therefore exposing more area of graphite the conductivity was expected to increase. When the surfaces were covered with an adhesive layer, a scrim layer, or both, the conductive graphite fibers should be insulated therefore yielding infinite resistivities. Similar results were expected

from the steel samples with parallel preparation methods. Finally, the steel samples with the layer of silane primer should have exhibited minimal levels of resistance above the cleaned samples.

As was expected, the sample types J, L, M, T, and U showed no sign of current transfer and therefore had infinite resistivities. Additionally, the "as received" steel samples, type N, exhibited a slight level of resistance, 85.4 Ω/ in thickness, attributable to surface oxidation or the presence of machining oils from the mill. After the impurities were removed from the surfaces using a high-pressure bead blast and a solvent cleaning, the resistivities decreased. Measured values were 16.7 Ω/ in and on the order of zero Ω/ in, or near infinite conductivity, for one and two cleaned surfaces respectively.

Similarly, the conductivity of the composite samples was expected to increase as their surfaces were cleaned as well; however the exact opposite occurred. The "as received" composite samples recorded resistivities averaging 42.6 Ω/ in. When only one face was cleaned, the resistivities practically tripled to 121.9 Ω/ in and reached a maximum of 310.0 Ω/ in with both surfaces bead blasted and cleaned with a solvent.

Upon investigation, the source of this unexpected result resided in the preparation method. Recall that a high-pressure bead blast was employed when removing the smooth finish from the surface of the composite. Under a microscope, it was discovered that the use of the bead blaster was damaging the graphite fibers at the surface of the composite sample. The once continuous fibers were literally being chopped into multiple short pieces of fiber by the cleaning method. Because the fibers were now discontinuous, they were no longer conducting current as they initially had, hence the increase in resistivity. More importantly, the strength of the composite relies on the fibers being continuous along their length. By chopping the fibers, the composite's strength can no longer be guaranteed. In effect, the performance of the rehabilitation was ultimately being compromised by the cleaning method.

Figures 2.4 and 2.5 illustrate the effect the cleaning method had on the fibers in the composite. In the photographs, the fibers are visible as dark lines while the lighter regions are the matrix. Figure 2.4 depicts the surface condition of the composite as received from the manufacturer. Note the continuity of the fibers as well as their parallel alignment. Figure 2.5 shows the adverse effect of a 50-psi bead blast on the fibers near the surface. Note the visible pitting of the surface and discontinuity of the fibers illustrated by the light portions interrupting the dark, continuous fibers. Again observe the parallel alignment of the fibers in this unidirectional composite.

As a result of this study, a variety of surface preparation methods for the composite were investigated. First, the composite was abraded by hand using Scotch Brite® pads to remove the polished surface finish. The resistivities were again measured and found to be 26.9 Ω/ in and 13.7 Ω/ in for one and two faces cleaned respectively; these results were in line with what was originally

expected. Figure 2.6 illustrates the range of resistivity measurements for the composite based on the different surface preparation methods.

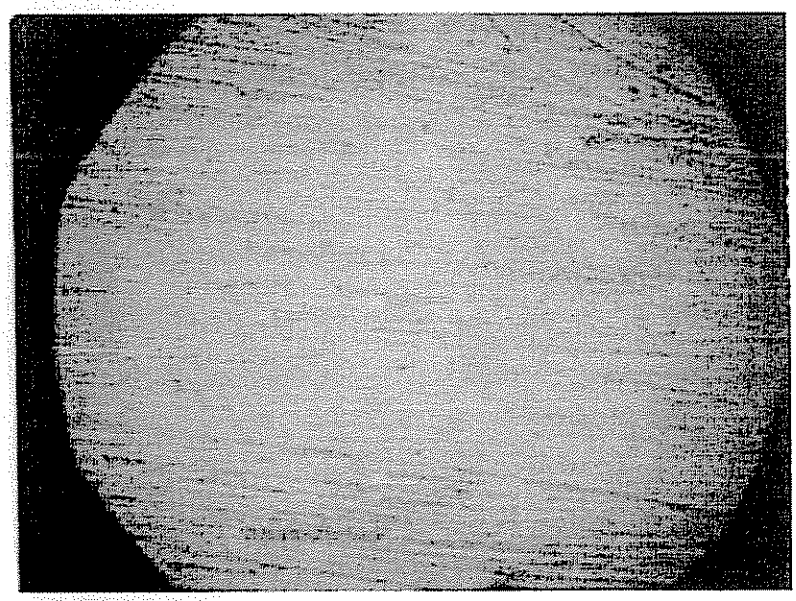

Figure 2.4 Surface condition of composite as received from manufacturer magnified 200X.

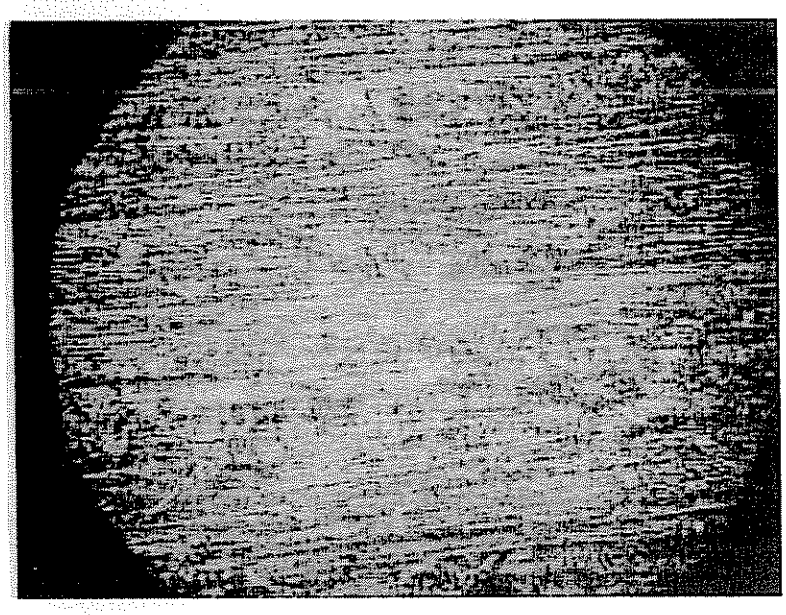

Figure 2.5 Surface condition of composite after 50-psi bead blast magnified 200X.

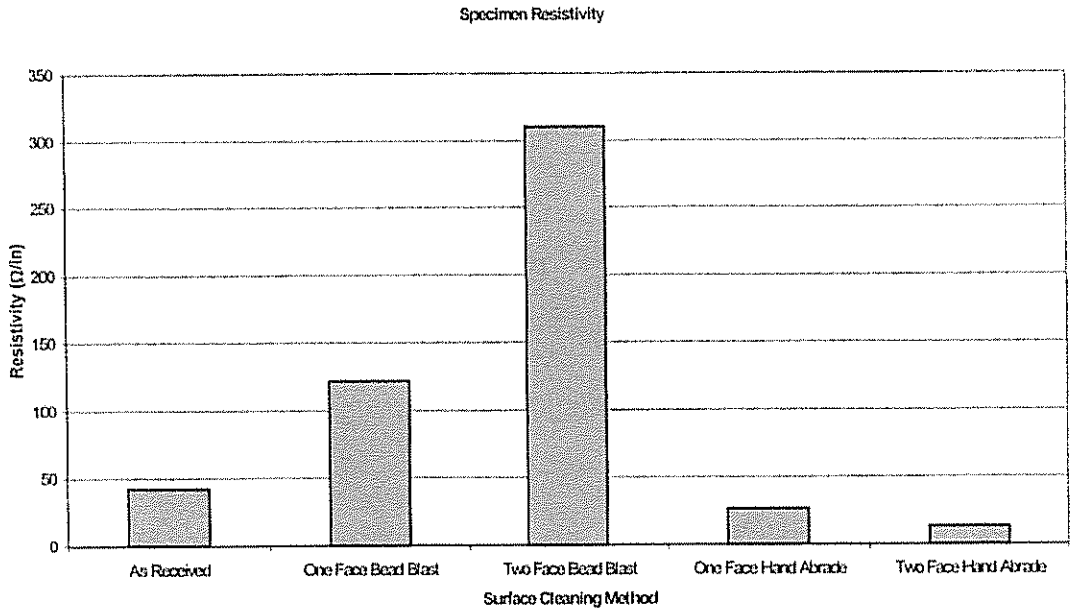

Figure 2.6 Resistivity comparison for composite samples across surface cleaning method.

The hand abrasion surface preparation method was fine for small-scale laboratory purposes, however a more practical approach needed to be established if field installation was to be possible. Bead blasting was still determined to be the most effective method for cleaning a large quantity of composite in the field. However, if this method was to be implemented, care must be taken to ensure that no damage was imparted to the composite during cleaning. A series of controlled tests were conducted using the bead blaster to determine the optimum cleaning procedure. Glass beads type MS-XH which range in diameter from 177 – 297 microns (0.0069 – 0.0116 in) was used. Based on their description in a supplier's catalog, they "function without embedment, pick-up, contamination, or other damage to the surface under treatment." It was learned that pressures between 20 and 30-psi with the nozzle spaced two to three inches from the surface of the material combined for the ideal cleaning parameters. In the course of his research, Ammar constructed a recirculating bead blast chamber that, when used in combination with a selectable pressure air compressor, would provide a practical means of surface preparation in the field while following the criteria set forth in this section.

2.5.2 Experiment Two: Long-Term Exposure

The second galvanic corrosion experiment was designed to simulate extreme environmental conditions that the proposed rehabilitation may encounter over its lifetime. A test matrix of eleven samples was established to examine different mechanisms and/ or modes of corrosion, potential protections, and to represent a variety of installations. The samples were cyclically exposed to a corrosive wet/ dry environment, specifically, a 10% aqueous NaCl solution. Each cycle lasted 24 hours and consisted of approximately 12 hours soaking in the solution and 12 hours air-drying.

The salt-water solution was designed to simulate dissolved highway de-icing salts saturating the repair. This was determined to be most probable extreme corrosion-causing environment that the rehabilitation would experience. The selection was based upon the fact that DelDOT uses common NaCl as a roadway de-icing salt during the winter. Additionally, the concentration of the solution was selected based upon a literature survey and a desire to provide as harsh an environment yet remain within the bounds of conventional research.

A commercially available polyethylene storage box was used to contain the samples and the conditioning solution. Figure 2.7 shows this container prior to the beginning of the experiment. This particular box was selected because it had molded slots in all four walls to receive full-height dividers that were used to keep the samples separate. Additionally, the divider slots had molded numbers and letters corresponding to their location to allow for identification of samples without concern of the markings accidentally being destroyed.

A high-density polyethylene (HDPE) sheet was cut to the dimensions of the box, drilled randomly with 3/8-inch holes, and placed in the bottom of the storage box prior to installing the dividers and placing the samples. This sheet was to act as a moveable floor or shelf on which the samples would rest so they could be lifted out of the bin for the drying period. The holes allowed the solution to pass through the HDPE sheet and drain back into the box to be retained for the duration of the experiment. A length of 100 lb break strength cord was looped continuously through four holes in the corners of the HDPE sheet to act as a lifting mechanism to remove the samples. Both the drilled HDPE sheet and the cord can be seen in Figure 2.7. Once lifted out of the bin, three lengths of coil stock were inserted through pre-drilled holes on either side of the box to act as joists or supports for the shelf and samples for the duration of the drying period. Figure 2.8 illustrates the position of the samples during a drying period.

Throughout the course of the exposure, qualitative and quantitative measurements were recorded periodically to detail the evolution of the corrosion. The qualitative assessments documented the appearance of the specimens and the amount of corrosion product present while the quantitative methods tracked the change in sample mass over the course of the study. The mass of the individual samples was expected to increase over time due to the absorption of moisture as well as the development of corrosion on any steel

surface. Additionally, the increase in mass over time was expected to be proportional to the amount of steel exposed per sample.

Upon conclusion of the exposure period, all composite parts were removed to allow inspection of the interfaces between the composite and the steel. The steel-composite interfaces were investigated for the presence of corrosion in an attempt to assess the performance of the counter-corrosion measures. Additionally, all steel plates were cleaned of all corrosion and then weighed to quantify a total mass lost. Finally, the composite control samples were mechanically tested to determine whether there were any adverse effects to the structure, and hence the mechanical properties, of the material over the course of exposure.

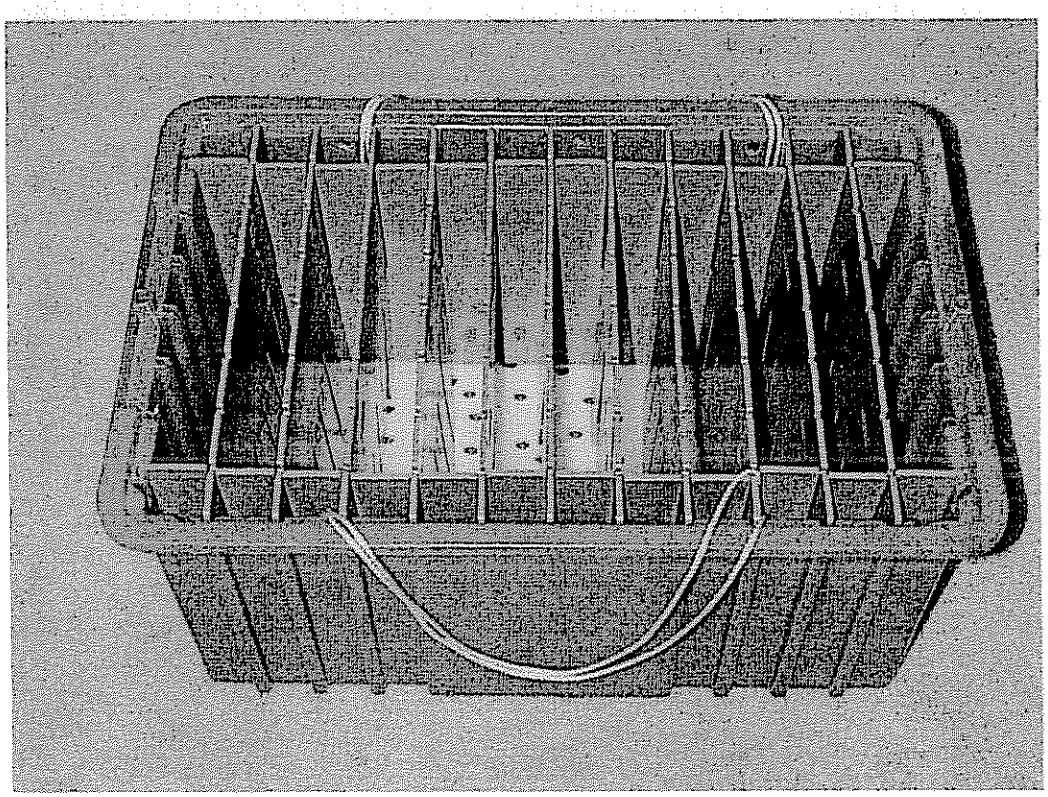

Figure 2.7 Empty storage box for samples and electrolyte used during second galvanic corrosion test.

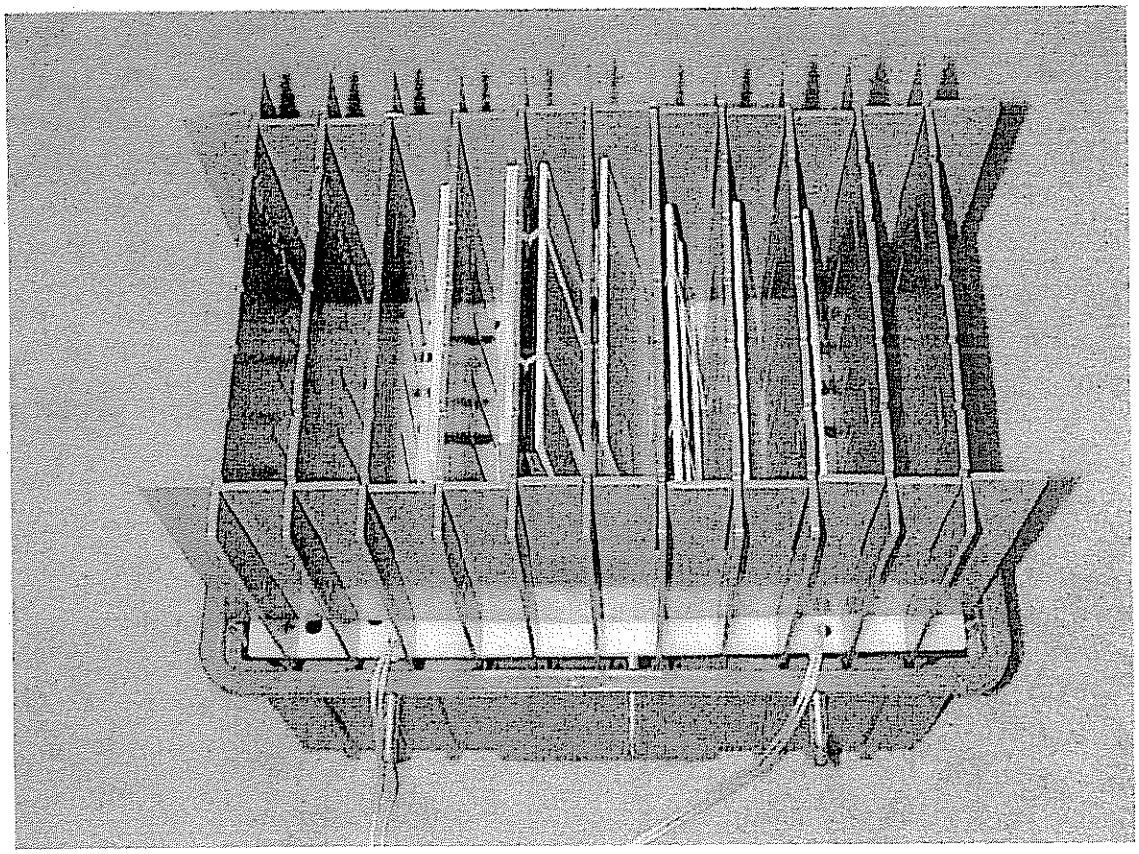

Figure 2.8 Storage box with samples in "drying position" for the second galvanic corrosion test

2.5.2.1 Specimen Selection

The primary goal of this particular stage of testing was to demonstrate both the potential for corrosion, specifically galvanic corrosion, and the effectiveness of the selected corrosion countermeasures. Akin to the requirements placed on the test specimens from the experiment of Section 2.5.1, it was imperative that the materials tested were similar, if not identical, to that which will be used in the field.

The preferred rehabilitation can be thought of as a laminate with three plies. The first ply was the steel adherend, the second was the adhesive layer with the embedded scrim, and the final layer was the composite adherend. Since each ply of this "laminate" would behave differently when exposed, it was necessary to have at least one control sample for each component. This would allow their individual contributions to be separated out from the overall test results if necessary. It was assumed that the fiberglass scrim would be completely encased in adhesive in the final state and it was therefore unnecessary to have its own control specimen. A typical exposure sample would be fabricated in a panel consisting of one 6 in square A36 steel plate, Ciba-Geigy AV8113

adhesive, and four 1 1/2 in x 6 in "strips" of composite, therefore those quantities were specifically selected as controls. In order to create the adhesive controls, a quantity was pressed into thin sheets and cured to comprise the final control sample.

Next, it was necessary to consider the performance of the samples at the bond interface. The through thickness direction of the rehabilitation was the most probable location for galvanic corrosion to occur and the most critical from a performance standpoint as well. If the electrolyte were allowed to penetrate the region between the steel and composite, conditions would be ripe for corrosion. If corrosion were to take place, the entire rehabilitation would be compromised. Therefore this class of samples became known as "Through Thickness Samples" and consisted of five combinations representing four potential types of installation cases.

The first two were simply composite bonded to steel, one with and one without the intermediate layer of fiberglass scrim. Next were two samples that attempted to simulate a void or holiday in the adhesive layer. They were fabricated by placing a full layer of adhesive on the surface of the composite, to ensure wetting out of the scrim, followed by a thin strip of adhesive placed around the perimeter of the steel plate. The uncovered center of the steel plate acted as the void in the system. The final sample in this class was merely composite clamped to the surface of the steel to simulate a worst-case scenario during the installation process in which no adhesive or scrim was present between the two adherends. This was expected to serve as a galvanic corrosion control sample as well since this mechanism was essentially being forced due to the configuration of the sample. The behavior of this sample could specifically be compared to that of the steel control sample to assess the contribution due to galvanic corrosion.

The last set of three samples was known as the "Edge Effect Samples." They were designed to investigate the performance of the rehabilitation at the edges of the composite adjacent to steel. The behavior of the system at the edges was isolated by using four 1 1/2 in square pieces of composite with a 6 in square steel plate. The first sample was simply the four composite squares bonded to the steel with a scrim layer in place. The second sample was identical to the first except that a heavy bead of adhesive, also called a fillet, was placed around the edges of the composite in an attempt to insulate the composite from the steel. Similar to the final Through Thickness sample, the last Edge Effect sample was again pieces of composite clamped to the surface of the bare steel using rubber bands.

All non-mating surfaces of any sample with a component of steel were coated with a rust inhibiting paint. This was an attempt to ensure that only one surface would actively corrode as a means of simplifying results during and after the course of the exposure. Table 2.2 lists the nomenclature used for the individual samples over the course of this study.

Table 2.2 Galvanic corrosion exposure sample identification matrix.

Through Thickness Samples	
TT-A	Through Thickness; Adhesive Only
TT-AS	Through Thickness; Adhesive and Scrim
TT-V1	Through Thickness; Void Sample I
TT-V2	Through Thickness; Void Sample II
TT-C	Through Thickness; Clamped Composite to Steel
Edge Effect Samples	
EE-F	Edge Effect; Adhesive Fillet on Composite Edge
EE-AS	Edge Effect; Adhesive and Scrim with Exposed Composite Edge
EE-C	Edge Effect; Clamped Composite to Steel
Control Samples	
A-L	Adhesive Control
C-L	Composite Control
S-L	Steel Control

2.5.2.2 Interim Results

Periodic qualitative observations and quantitative measurements were made during the course of the exposure. Below is a list of those findings up to and including the first 54 exposure cycles.

- Qualitative Observations
  1. Buildup of corrosion sediment in solution
  2. Increased amount of corrosion of steel adjacent to composite in samples with bonded (see Figure 2.9) or clamped composite (see Figure 2.10) early in exposure potentially attributable to galvanic corrosion effects or crevice effect of composite retaining solution
  3. "Streaking" of corrosion on samples possibly due to solution run-off during drying phase as shown in Figure 2.11
  4. Black and rust colored corrosion product represented in Figure 2.11
  5. Rapid development of corrosion (i.e. bare steel surfaces fully corroded in less than 7 cycles)
  6. Heavy build-up of corrosion as exposure term lengthens
  7. Signs of blistering and cracking of corrosion product

8. Staining of composite from corrosion product suspended in solution as shown in Figure 2.12
9. Composite samples exhibiting iridescent staining on bottom edges in Figure 2.13 possibly due to capillary action of absorption and salt staining at absorption front

- Quantitative Observations
  1. Increase in values of mass for most samples and most significant in those samples with large proportions of exposed steel as expected due to the formation of corrosion product on surface of steel
  2. All samples, other than control samples, showing slight variation in mass possibly due to variation in relative moisture content at individual weighing sessions or build-up of corrosion precipitate or sediment on material surfaces
  3. Composite control samples effectively maintaining constant mass
  4. Adhesive control sample showing slight variation in mass values

Figure 2.14 illustrates the change in mass of the samples over the first 54 cycles.

As the exposure period continued, the effects of the corrosive environment became more apparent. Specifically, the corrosion product continued to build on the samples with exposed areas of steel. The blisters that had previously formed on some samples ruptured allowing the corrosion to advance to the point of significant scaling of the product from the sample surface. With respect to the samples that simulated the actual field repair, very little changed over the course of the exposure. Outside of some cosmetic changes, no visible problems were observed; most importantly, the bond appeared to be in tact throughout the course of this specific experiment.

Initially, the mass of the Through Thickness samples increased minimally over time and practically remained constant over the first 125 cycles. Beyond this point, the mass increased slightly which can be attributed to scaling of the corrosion resistant paint, which allowed limited corrosion to form. The only exception to this was the clamped sample, which was essentially bare steel with minimal protection provided by the composite. Its mass remained near constant approximately through the first 50 cycles then increased at a greater rate than the other samples through the experiment's conclusion. Figure 2.15 illustrates these trends.

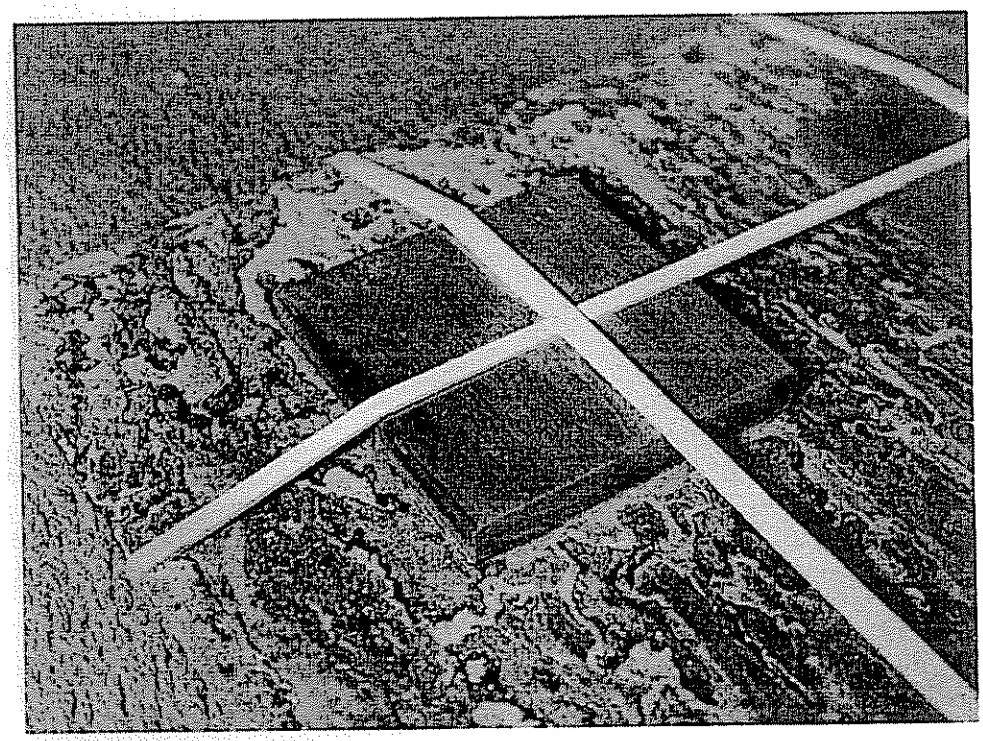

Figure 2.9 Variation of corrosion in regions adjacent to a composite square, specifically the cut edges, illustrated by sample EE-C.

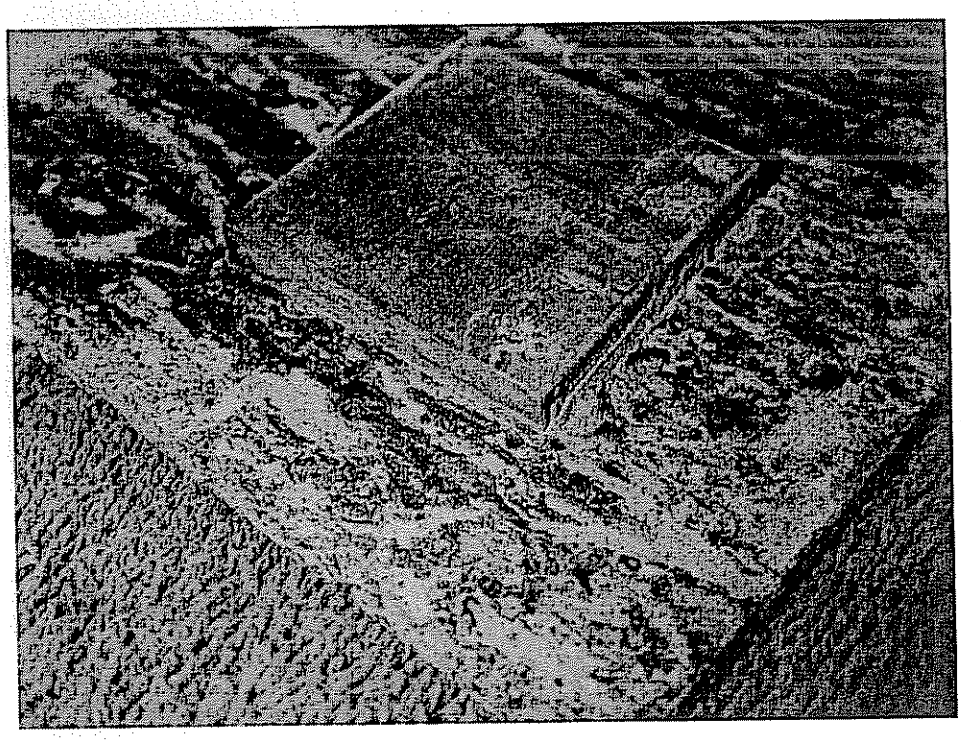

Figure 2.10 Variation of corrosion in regions adjacent to a composite square as illustrated by sample EE-AS.

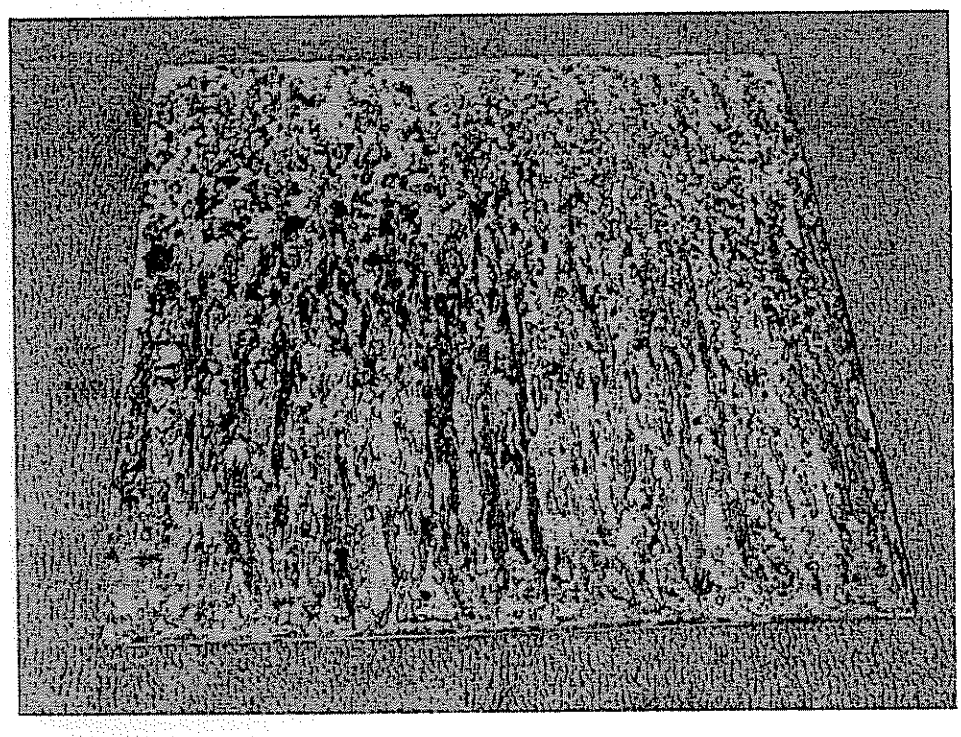

Figure 2.11 Streaking of corrosion product and different corrosion colors as experienced by Sample S-L.

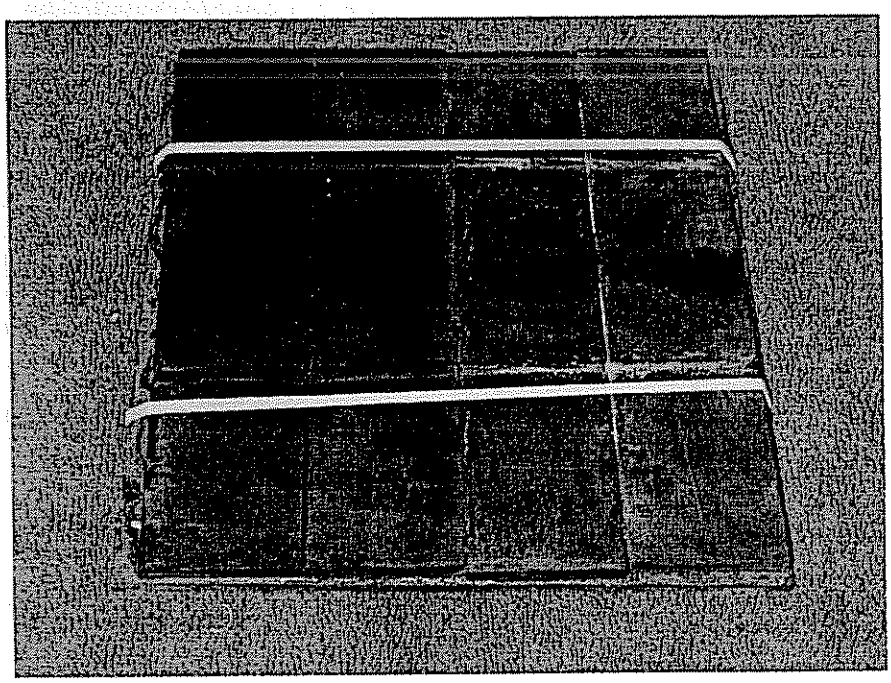

Figure 2.12 Staining of composite material on sample TT-C by aqueous corrosion precipitate.

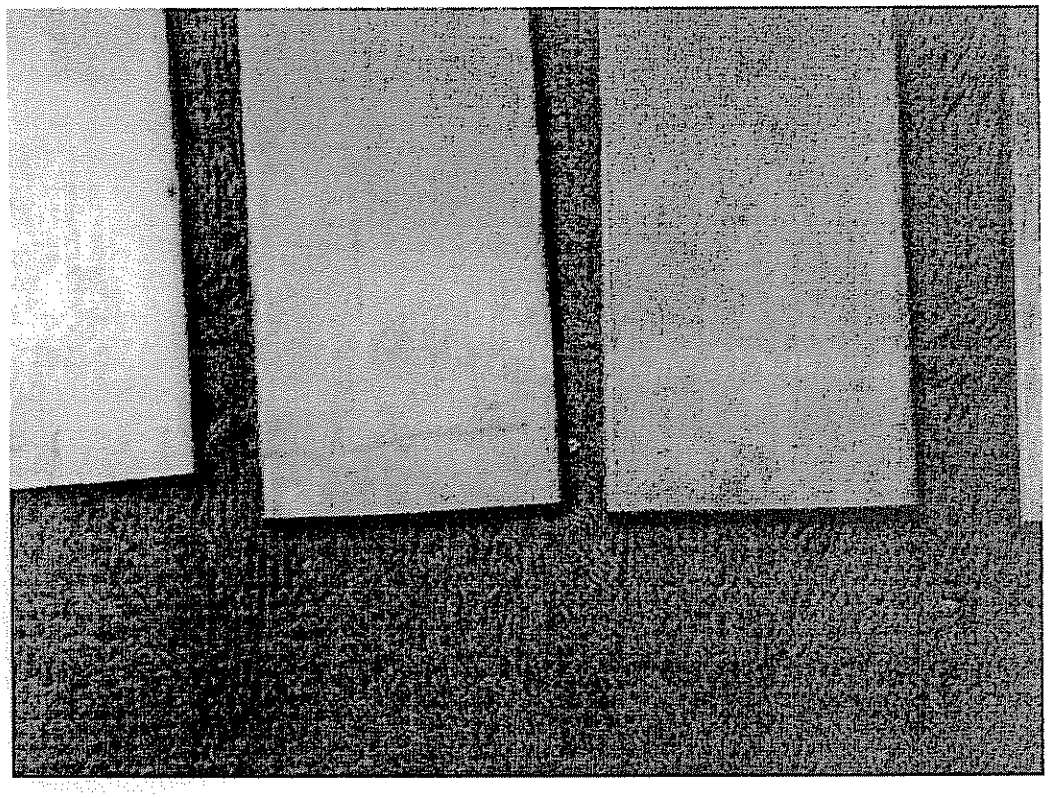

Figure 2.13 Iridescent staining at cut end of composite control samples (C-L).

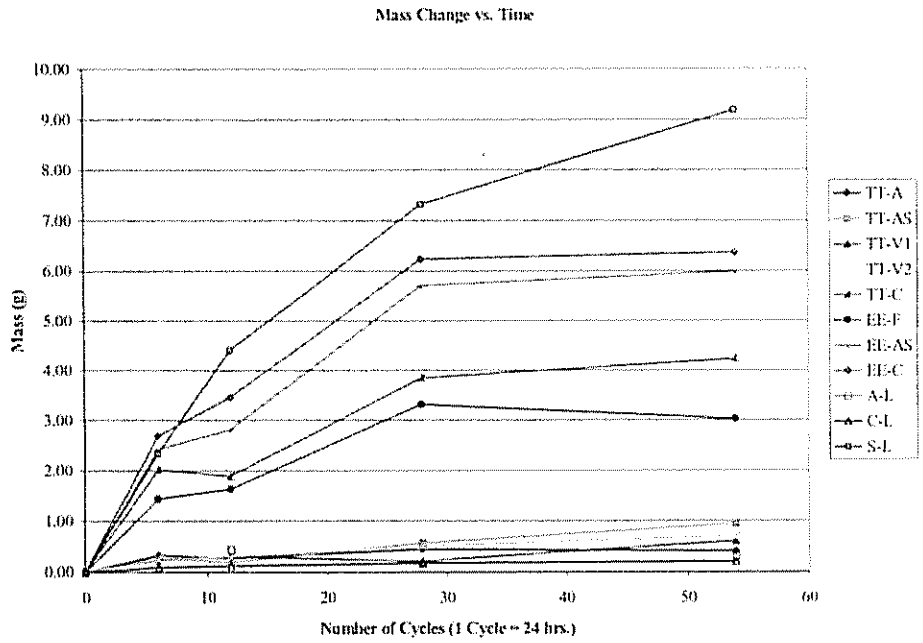

Figure 2.14 Mass change vs. time of exposure samples through 54 cycles.

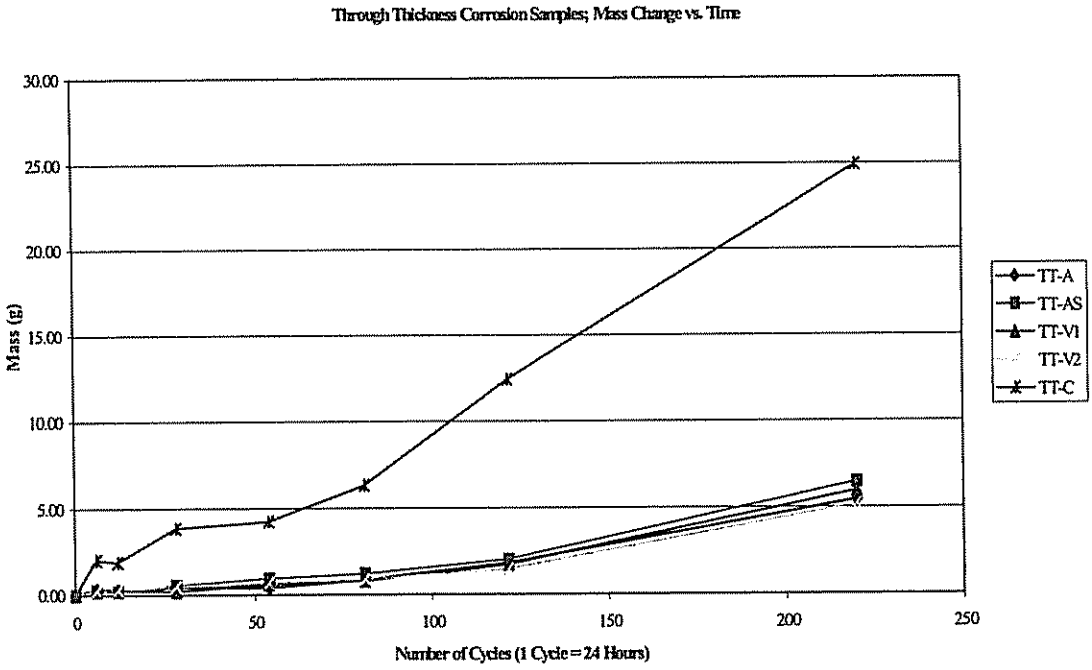

Figure 2.15 Mass change vs. time of exposure for through thickness corrosion samples.

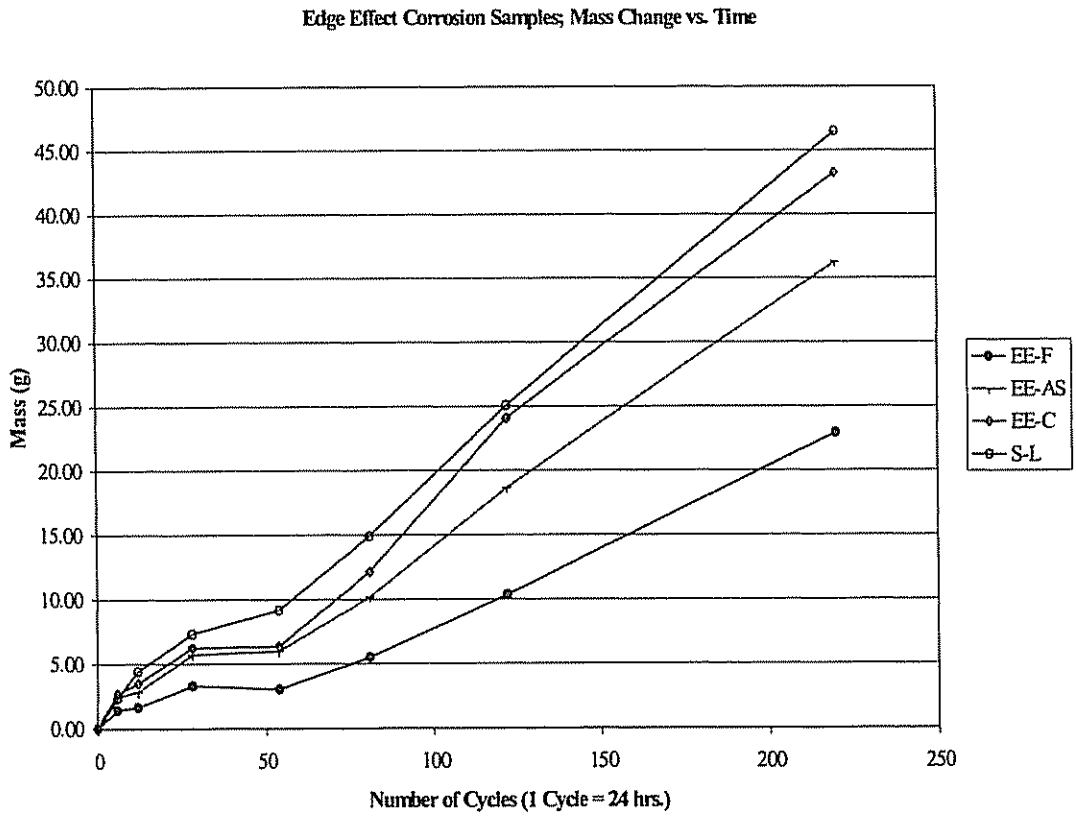

Figure 2.16 Mass change vs. time of exposure for edge effect and steel control corrosion samples.

Samples with a large amount of exposed steel, specifically the Edge Effect samples and the steel control sample, gained mass at a higher rate than the Through Thickness samples which was expected. These samples gained mass initially at a high rate, attained a plateau from cycles 28 to 54, and then increased at a greater rate from cycle 54 to the conclusion of testing. Figure 2.16 illustrates these observations.

This increase in corrosion rate can be traced to the qualitative observation of the cracking and partial scaling of the corrosion layer as shown in Figure 2.17. Consider that the initial layer of corrosion developed to a certain depth *d* into the thickness of the steel. At some point in time, practically all the available steel to fuel the corrosion reaction was consumed therefore stalling the process. This can be likened to the function of ASTM A588 weathering steel. With weathering steel, a certain amount of steel on the surface is sacrificial and is expected to corrode a specific amount. This hardened corrosion layer is designed to be retained on the structure's surface and therefore act as a protective barrier to the steel beneath. In the case of our samples, the protective layer was compromised due to the cracking, therefore exposing bare steel beneath. This uncorroded steel surface provided further fuel to the corrosion reaction.

Therefore, the increase in mass can be traced to the addition of more corrosion product to the samples.

2.5.2.3 Qualitative Experimental Results

Upon completion of the exposure of the samples, their final conditions were assessed and final mass readings were taken. Ultimately, the period of exposure was uneventful. Outside of corrosion levels on bare steel exceeding expectations, nothing extraordinary happened to the samples. Additionally, final inspection indicated that corrosion had indeed occurred under the surface of the clamped samples and had started to lift the composite out of contact with the steel. Note that all exterior edges of the steel plates experienced some slight corrosion. After all qualitative and quantitative measurements were taken; the samples were separated into their constituent parts for evaluation.

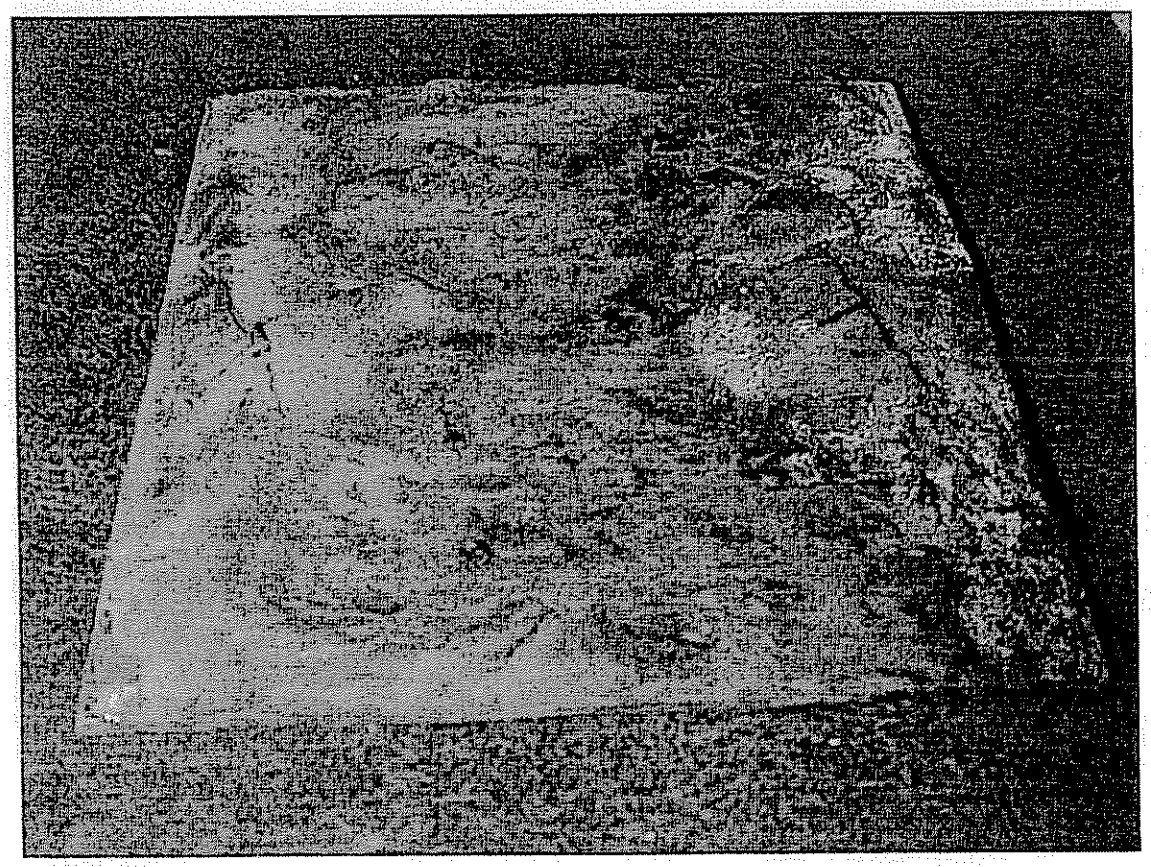

Figure 2.17 Heavy corrosion with blisters and cracks formed on surface of steel control sample, S-L.

2.5.2.3.1 Control Specimens

The behavior of the steel control sample was fairly predictable; it saw full corrosion as would be expected on any ferrous metal exposed to a similar environment. However, the level of corrosion exceeded expectations in the form of blistering and cracking of the corrosion surface (see Figure 2.17). Based on this elevated level of corrosion, the conclusion could be drawn that the samples were exposed to an aggressive environment, which was the goal of the selection of the 10% aqueous NaCl solution.

Slight rust colored staining of the surface of the composite was observed as a result of suspended corrosion product settling on the samples. However, there were some unexpected results obtained from the composite control samples as well. It was observed early on that there was some iridescent coloring of the surface of the material (see Figure 2.13). This discoloration appeared to generate at either end of the sample where it had been cut and had progressed inward potentially attributable to capillary effect of the fibers drawing the fluid. It is hypothesized that this could either be a build up of precipitated NaCl or even matrix degradation, which could lead to the separation of the fibers from the matrix. This mechanism would have the same detrimental effect as the debonding of reinforcing steel in concrete. Mechanical testing performed on the samples indicated there was no reduction of strength of the material as a result of the exposure. These results are discussed at length in Section 2.5.2.5.

There were no visible outward effects as experienced by the adhesive control samples. There was minimal surface staining of the adhesive by the suspended corrosion precipitate, however no changes in the physical properties of the adhesive were noted over the course of the exposure.

2.5.2.3.2 Through Thickness Samples

Recall that there were two main types of Through Thickness samples, those that were fully bonded, and those that were not. The fully bonded group included the adhesive only sample (TT-A) as well as the sample with both an adhesive and scrim (TT-AS). The second group included both partially bonded samples, those that contained a void (TT-V1 and TT-V2), and the clamped sample (TT-C). Note that the preferred surface pretreatment was applied to all samples that were bonded to any degree.

During the inspection stage following exposure it was learned that no bonds were compromised in the fully bonded samples. The composite was then separated from the steel substrate to allow inspection of the interface. It is important to note that all bonds failed cohesively in the composite and not adhesively at the surface of either adherend, which is indicative of bond integrity. A cohesive failure occurs when the composite material itself fails through its section and there is composite material still bonded to the other adherend as shown in Figure 2.18.

Despite this mode of failure, there were isolated locations where the adhesive was removed completely from the surface of the steel during the separation process. This revealed white metal beneath the adhesive that supported theories that corrosion would not be a concern at interior interfaces. Figures 2.19 and Figure 2.20 show locations along the adhesive "seam" between composite strips where the adhesive was separated from the steel surface. This photograph was taken several days after opening the sample therefore some light maroon corrosion has begun to form on the unprotected steel.

Along some of the edges of the samples it could be seen where some water had begun to penetrate the interfaces. Figures 2.21 and 2.22 show that the adhesive and steel were slightly discolored and some minor surface corrosion had begun to form. It is important to note that the corrosion had only advanced to a stage through 200-plus cycles that was equivalent to bare steel exposed for 7 cycles. Even though the corrosion was limited, this penetration could ultimately lead to significant corrosion and potentially failure of the bond therefore it requires being addressed. Fortunately, it can easily be remedied by applying a heavy fillet of adhesive at all edges to effectively isolate the interface and eliminate penetration. This method was proven to be effective in the Edge Effect samples as will be discussed in the following section.

Next, samples TT-V1 and TT-V2 were examined. External observations were in line with those made on the fully bonded samples. Again, the bond was broken to allow investigation of the surface of the steel plates. Upon opening the partially bonded samples it was learned that the technique employed to create a void-type installation defect were not effective and the voided samples essentially became fully bonded samples. In other words, the void was essentially filled in. Despite the disappointment of learning the samples were not what had been expected, several positive lessons were taken from these particular items:

- The adhesive used has excellent workability properties. Despite using what was believed to be an inadequate amount of adhesive, the limited amount of adhesive present successfully flowed and filled the entire voided region. This assures researchers that voids will be successfully filled and that the installation process has some level of redundancy.
- Upon investigating the steel adherend, it was again shown that there was no corrosion within the interior of the sample. Essentially the same results were obtained with these samples as with the first two of this type. This observation further reinforces the experimental results through repeatability.

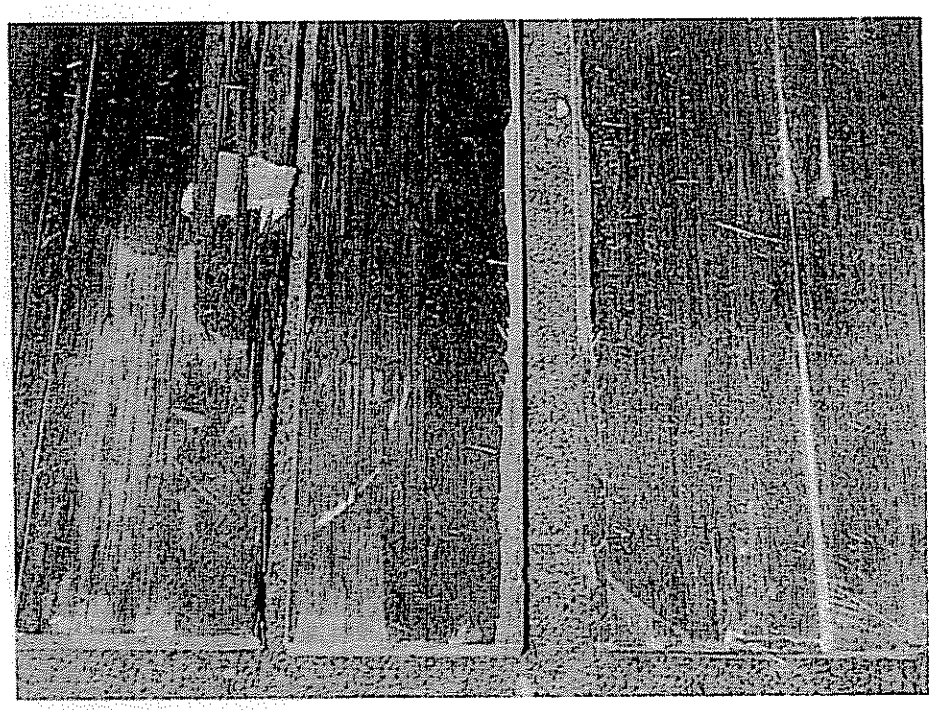

Figure 2.18 A cohesive bond failure illustrated by sample TT-V1. Note the loose fibers and part of the composite still bonded to the surface of the steel (right.)

Figure 2.19 Interior exposed areas of white metal steel at bond interface of sample TT-A.

Figure 2.20 Close-up of exposed areas of white metal steel at bond interface of sample TT-A.

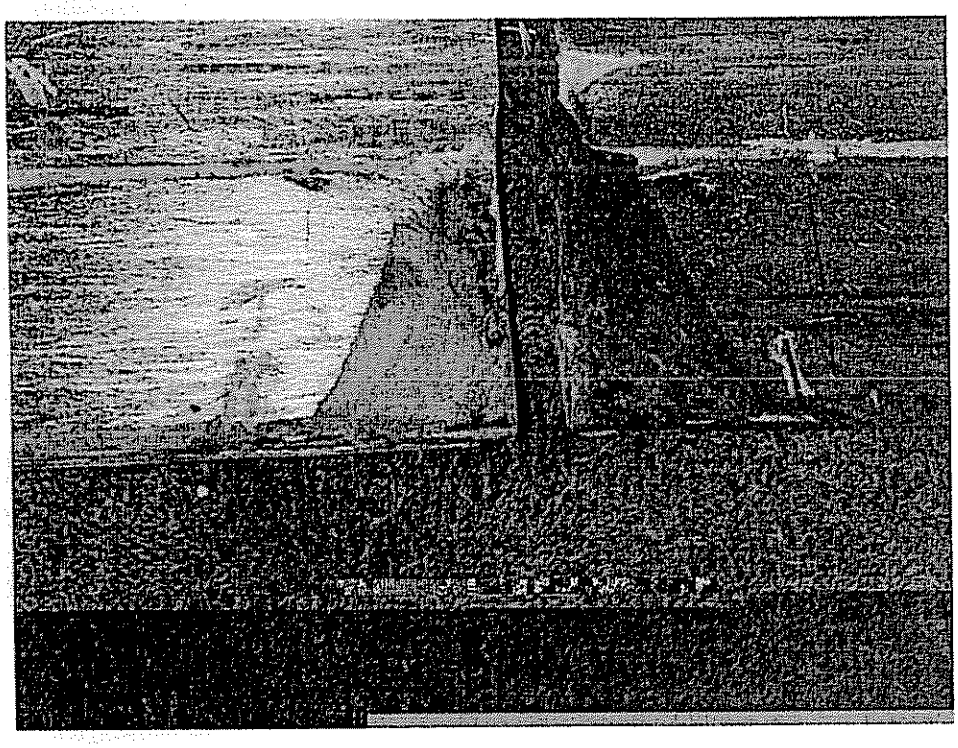

Figure 2.21 Corrosion at steel-composite interface at corner of sample TT-A.

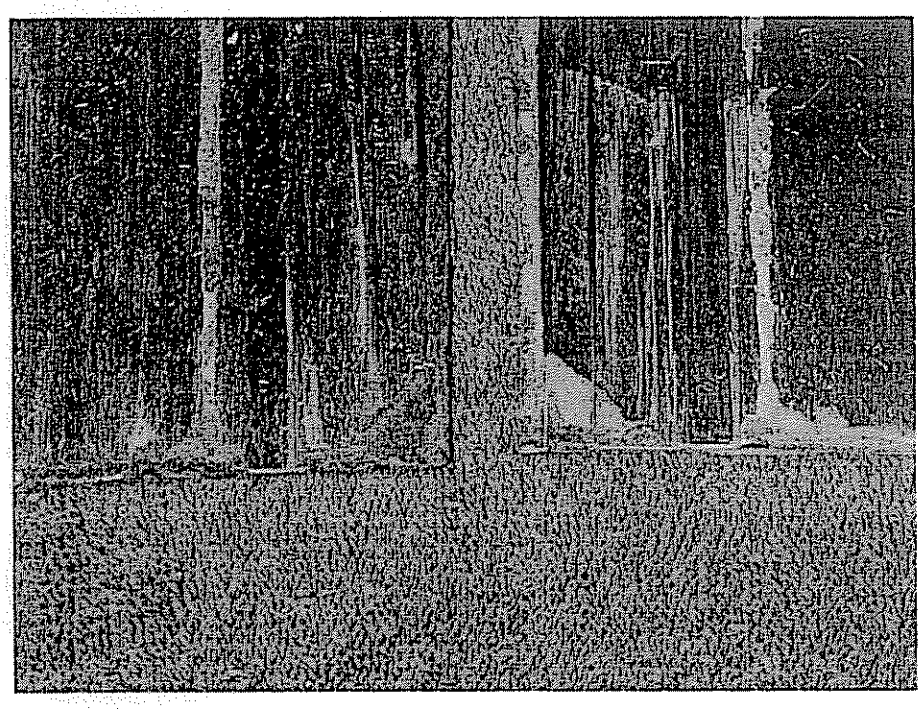

Figure 2.22 Corrosion at steel-composite interface along edges of sample TT-A.

The Through Thickness testing of sample TT-C provided the most interesting results. It was evident that there was corrosion at the material interface. The corrosion had progressed to such a state that the clamped composite was actually lifted off of the surface of the steel. When separated, the corrosion product was left attached to the surface of both the steel and the composite illustrated in Figure 2.23. The corrosion pattern and color was slightly different from the corrosion on the surface of the bare steel. This could be an indication of either galvanic corrosion or crevice type corrosion. Each adherend was cleaned and compared with controls to assess the level and types of corrosion.

2.5.2.3.3 Edge Effect Samples

Similar to the Through Thickness samples, the Edge Effect samples also had a fully bonded and un-bonded group. The bonded group contained the typically bonded sample with exposed edges and the fillet Edge Effect sample. Obviously, the clamped Edge Effect sample would be characterized in the unbonded group.

Again, all bonds performed extremely well. Upon separating the samples, there was some observed discoloration near the exposed edges of sample EE-AS indicative of water that had penetrated the bond line as seen in Figure 2.24. However, the picture of sample EE-F with the beaded edge in Figure 2.25 showed no such signs of water penetration as expected. Additionally, a pure observation with no statistical support, it appeared as if the beaded samples were more difficult to remove than those with the exposed edge. This potentially suggests an initial weakening of the bond that had not been

protected at the edges with a bead of adhesive. When comparing the two pictures, it is clearly visible that there is more composite still bonded to the surface of the steel from sample EE-F (Figure 2.25) indicating a cohesive failure as opposed to the apparent adhesive failure of sample of sample EE-AS (Figure 2.24).

The final exposure sample to be examined was the clamped Edge Effect sample, EE-C. There were no new observations made with this sample when compared to all of the other samples. Its performance was equivalent to its Through Thickness counterpart.

2.5.2.4 Quantitative Experimental Results

Quantitative measurements were recorded in addition to the qualitative observations made over the course, and at the conclusion, of the exposure period. All specimens gained mass over the experiment, which was to be expected. A majority of the mass gain was a result of the development of corrosion product on the surface of any exposed steel. In addition to the change in mass due to corrosion, mass gain was additionally attributed to the absorption of liquid by the composite and/ or adhesive as well as the build-up of corrosion sediment on the surface of all samples. Control samples of both adhesive and composite were exposed simultaneously to provide values for absorption. Additionally, an attempt was made to wipe the sediment clean from the sample surfaces prior to weighing to minimize that effect. However, it can be assumed that all specimens had an equal amount of build-up therefore any increase in mass attributable to remaining sediment can be neglected in the final analysis.

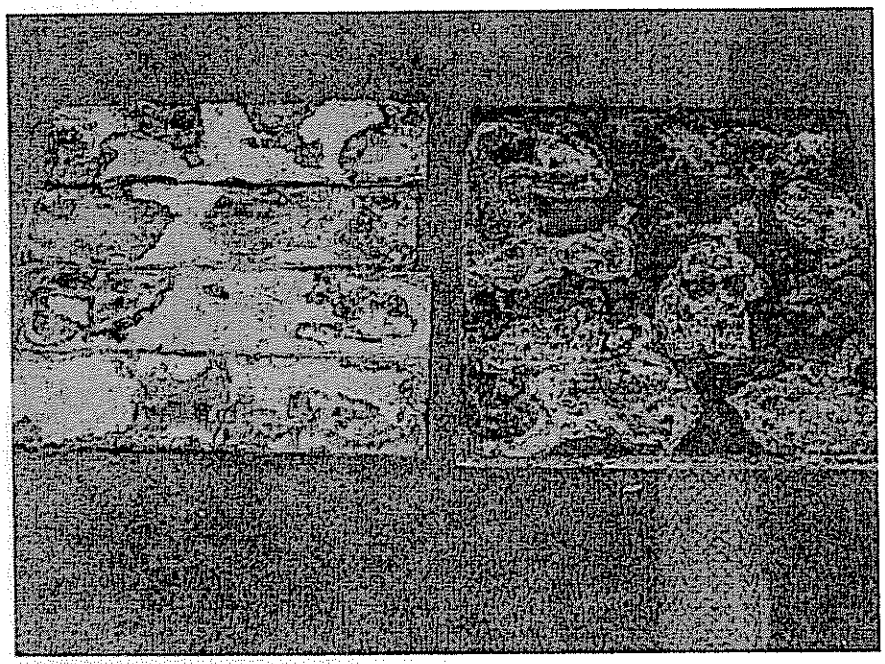

Figure 2.23 Opened sample TT-C showing corrosion product attached to both steel and composite adherends as well as a deviation in the color of corrosion product from other samples.

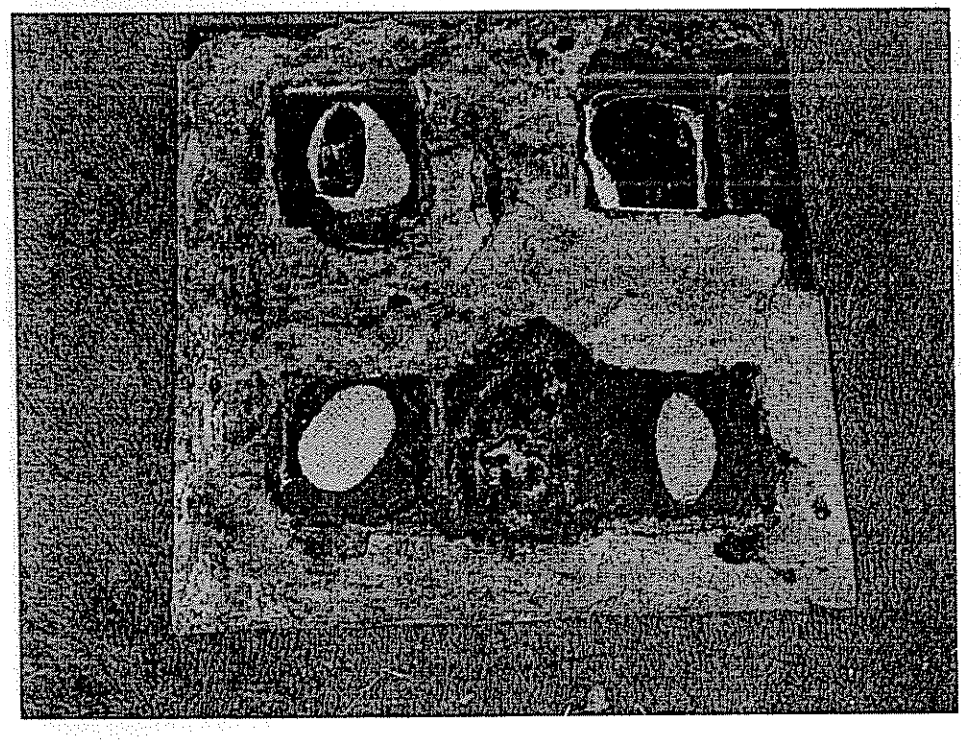

Figure 2.24 Sample EE-AS with composite removed showing penetration of electrolyte via corrosion around edges of each square.

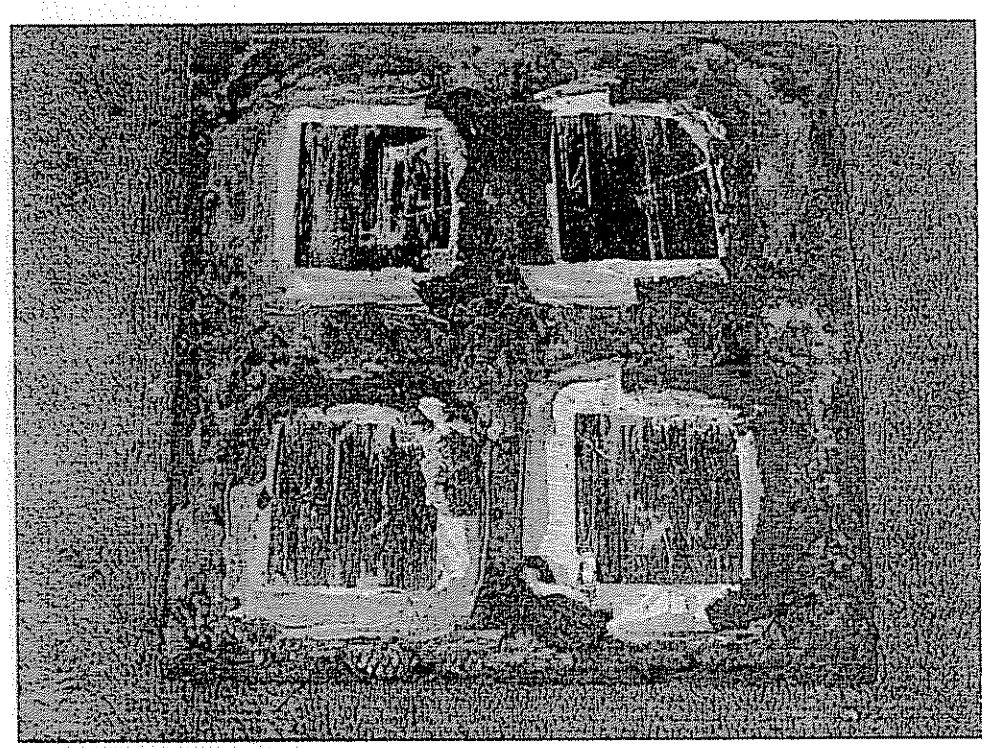

Figure 2.25 Sample EE-F with composite squares removed. Cohesive failure illustrates effectiveness of adhesive bead in preventing corrosion from weakening bond.

In order to assess the performance of an individual sample relative to another, a basis for comparison must be established. The most logical criterion was to compare the change in mass, Δ_m, by each steel plate after the exposure period had concluded and after all samples had been cleaned. Because all of the samples didn't necessarily have the same initial volume of steel, the change in mass must be taken as a percentage of the initial mass, m_i, of each sample. Equation Eq. 2-1 was used to determine the change in mass, Δ_m, where m_c was defined as mass change, either gained or lost, by an individual sample.

$$\Delta_m = \left| \frac{m_i - m_c}{m_i} * 100\% \right| \qquad \text{Eq. 2-1}$$

During the analysis, the following assumptions were made:

1. Mass change, m_c, was directly proportional to the level of corrosion
2. The free edges and back surface of all samples corroded at the same rate and can therefore be neglected
3. It follows that all samples had the same "active" surface area
4. All steel plates had the same initial thickness

5. The adhesive and composite had constant rates of absorption in all samples and was equal to that of the respective control samples and could either be subtracted or neglected

Because none of the "active" surface area of any Through Thickness sample was directly exposed to the corrosive solution, comparison between those samples was straightforward. The change in mass, Δ_m, of one sample was merely compared to another sample to assess relative performance. However, comparison between the Edge Effect samples was not as simple.

Recall that the Edge Effect samples were intended to investigate the behavior of the corrosion where the free edge of the composite interfaced with the steel. Because of this feature, a significant area of bare steel was directly exposed to the 10% aqueous NaCl solution. However, this exposed area, A_e, varied from sample to sample and was defined by equation Eq. 2-2 as the difference between the total area of a given plate, A_t, and the area covered by either the composite or adhesive, A_c.

$$A_e = A_t - A_c \qquad \text{Eq. 2-2}$$

It followed that the mass lost, m_l, could be divided by this exposed area, A_e, to provide mass lost per unit area, λ, as shown in equation Eq. 2-3, to allow for comparison between samples.

$$\lambda = m_l / A_e \qquad \text{Eq. 2-3}$$

Similarly, this exposed area can also be expressed as a percentage of the total area of the plate using equation Eq. 2-4:

$$\%A_e = \frac{A_t - A_c}{A_t} * 100\% \qquad \text{Eq. 2-4}$$

From this percentage, a theoretical mass change, $m_{c\text{-}theory}$, for each Edge Effect sample was computed equation Eq. 2-5

$$m_{c-theory} = \%A_e * m_{c-SL} \qquad \text{Eq. 2-5}$$

where $m_{c\text{-}SL}$ was defined as the mass lost by the steel control sample. This quantity was used to assess the performance of the individual Edge Effect

samples. Any deviation from this theoretical mass lost could be attributable to galvanic corrosion.

Finally, a ratio of mass lost, m_l, to mass gained, m_g, could be used to compare the relative performance of all of the samples. The mass change, gain or loss, can be assumed to be a function of the steel plate only since the change in mass through absorption by the other controls was subtracted from the total mass gained by each sample. Similarly, the steel was the only component of the samples that fueled the oxidation reaction.

2.5.2.4.1 Control Specimens

The control specimens played a critical role in this stage of the analysis. They provided baseline data that was necessary to evaluate the performance of the rest of the samples in the experiment. By determining the mass lost by the steel control sample (S-L) on a basis of mass per unit surface area, the relative contribution of corroding steel could then be determined for all other samples. Additionally, any change in mass by the composite and adhesive control samples (C-S and A-S respectively) could similarly be deducted from the mass change of the other samples as well. Then, any remaining change in mass, presumably loss, could be attributable to other sources such as galvanic corrosion or other mechanisms.

At the end of the experiment, it was measured that the adhesive and composite controls gained 0.28 g and 0.42 g respectively or 1.35% and 0.24% of their corresponding initial mass. Recall that these values were deducted from the total weight gained to isolate the behavior of the steel plate alone. It was recorded that the steel control gained 46.50 g, or 0.86% of its initial weight. After removal of the corrosion product, it was revealed that sample S-L had lost 124.86 g, or 21.3% of its initial mass. Recall that a ratio of mass lost to mass gained by the steel could be used as a tool to quantify levels and possibly mechanisms of corrosion. The steel control sample established a baseline ratio of 2.687. It is assumed that the mass lost by the steel from each would be directly proportional to mass gained through corrosion since the plate was the fuel for the oxidation reaction.

2.5.2.4.2 Through Thickness Specimens

Recall that the qualitative observations revealed that the only corrosion of the fully bonded Through Thickness samples occurred at the edges of the steel plate and slightly on the back of the samples. This minimal corrosion resulted in slight gains of mass ranging from 0.82% to 1.04% of initial weight, with an average of 0.92%. This quantity represents the amount of corrosion seen by all samples on the edges and backs of the steel plates since the "active" surface did not corrode. Recall that our "partially bonded" sample class no longer exists due to the voided area filling with adhesive. Even though the samples were treated as

individuals during the experiment, during the analysis, they can be considered to all be from the same group and therefore the average of their results can be applied.

All bonded samples, including those with the scrim layer, were then separated into their constituents and the steel plates were cleaned of all corrosion as well as any remaining paint, adhesive, scrim, and composite. The mass of the steel plates was again recorded and compared to the mass of the plates before exposure. It was discovered that the four bonded Through Thickness samples had lost an average of 8.18% of their mass with a standard deviation of 0.97%. Considering that the sample S-L had lost 21.3% of its weight, this value of 8.18% seemed to be high considering the relatively minimal amount of steel exposed. In other words, it was unexpected to see such a large percentage of mass lost by samples where the "active" steel surface was primarily isolated from the corrosive environment relative to the steel control sample whose "active" surface was completely exposed to the NaCl solution. Similarly, the average ratio of mass lost to mass gain by the bonded samples was almost three and a half times that of the steel alone at 9.043.

The quantitative results yielded by the clamped Through Thickness sample was more in line with what was expected based on the results of the other samples. It gained 4.00% by the end of the exposure term, which was more than the bonded samples yet, less than the steel control. This could be traced to the fact that some quantity of corrosion product had fused to the surface of the composite as well thereby reducing the overall mass gained by the steel. After separation and cleaning, the amount of corrosion product attached to the composite was 5.07% for a total mass gain by the system of 9.07%. After cleaning, the steel plate alone had lost 14.2% mass and had a ratio of 1.562 of mass lost to mass gained.

It was unexpected to see the clamped sample have a larger mass gain and lower mass lost when comparing to the steel control sample. Based on the concept of galvanic corrosion, it was expected to see more corrosion on the steel from this sample than by the steel alone. This behavior therefore resulted in a ratio of mass gained to mass lost that was much lower than the steel control alone. This phenomenon is addressed at length in Section 2.5.2.4.5.

2.5.2.4.3 Edge Effect Samples

A similar procedure was followed for evaluating the behavior of the Edge Effect samples as what was used with the Through Thickness samples. Recall that equation Eq. 2-5 was used to obtain a theoretical value for both mass gained by the sample as well as mass lost by the constituent steel plate based on the area of exposed steel relative to the steel control sample. Table 2.3 contains the predicted values in grams with the actual values and a percent difference from the theory for each quantity. For comparison purposes, the mass gained and lost by the steel control sample was included as well.

Table 2.3 Predicted and actual change in mass for edge effect samples.

Sample	Area (in^2)	Gain (t)	Gain (a)	% Diff	Loss (t)	Loss (a)	% Diff
EE-F	16.54	21.10	22.70	7.38%	56.70	75.83	33.70%
EE-AS	27.10	34.67	35.63	2.77%	93.18	107.14	14.98%
EE-C	27.73	35.45	41.44	16.90%	95.28	125.36	31.57%
S-L	36.44	N/A	46.50	N/A	N/A	124.96	N/A

This table illustrates the unpredictable nature of corrosion, specifically galvanic corrosion. An attempt to predict mass gained by the samples based on the area of exposed steel was relatively accurate. Only sample EE-C deviated greater than 10% from predicted to actual. However, the mass lost by each sample demonstrated how difficult it truly is to quantifiably predict corrosion behavior. Ironically, the mass lost by sample EE-AS was most closely predicted while the other two samples deviated over 30% from theory.

From the results of the Through Thickness samples, and by inspection, we would have expected sample EE-C to exhibit the lowest ratio of mass lost to mass gained. This held true and it virtually matched the behavior of the sample S-L therefore giving no indication of any other mechanism than traditional corrosion.

2.5.2.4.4 Interim Conclusions

Based on the quantitative results from the second galvanic corrosion experiment, interim conclusions were made. The results with respect to the steel plate of each sample are found in Table 2.4. The quantities contained in the table are represented by the following variables:

- A_t: Total area of steel plate
- A_e: Exposed area of steel plate
- m_i: Initial mass of steel plate
- m_g: Mass gained over course of exposure
- $\%_g$: Mass gained expressed as a percentage of m_i
- m_l: Mass lost by the steel plate after cleaning
- $\%_l$: Mass lost expressed as a percentage of m_i
- *Ratio*: Ratio of mass lost to mass gained by steel plate

Table 2.4 Results from second galvanic corrosion experiment.

Sample	A_t	A_e	m_i	m_g	$\%_g$	m_l	$\%_l$	Ratio
TT-A	34.02	34.02	548.66	4.74	0.86%	50.63	9.23%	10.690
TT-AS	34.30	34.30	553.27	5.78	1.04%	42.64	7.71%	7.381
TT-V1	34.54	34.54	557.06	5.28	0.95%	39.47	7.09%	7.481
TT-V2	33.91	33.91	546.91	4.48	0.82%	47.61	8.71%	10.620
TT-C	36.51	36.51	588.87	23.56	4.00%	83.37	14.16%	1.562
EE-F	36.45	16.54	587.88	22.70	3.86%	75.83	12.90%	3.341
EE-AS	36.35	27.10	586.25	35.63	6.08%	107.14	18.28%	3.007
EE-C	36.37	27.73	586.69	41.44	7.06%	125.36	21.37%	3.025
S-L	36.44	36.44	587.69	46.50	7.91%	124.96	21.26%	2.687

The results that provide the clearest conclusions are the quantities for percent mass gained and percent mass lost. For both quantities, all of the bonded Through Thickness samples had near equivalent mass gained and mass lost, while the Edge Effect samples behaved as might have been expected.

First, the mass gained and mass lost by the bonded Through Thickness samples were on the same order. Considering the only difference between any of these samples was the presence of the fiberglass scrim, this would be expected. Recall that samples with prefabricated voids that were intended to isolate the performance of the fiberglass scrim were not actually present as discussed in Section 2.5.2.3.2. It followed that the clamped through thickness sample exhibited greater mass gained and lost as a result of the steel being directly in contact with both the electrolyte and the graphite composite.

Similarly, the Edge Effect samples were appropriately represented by the same quantities. The percentages of mass gained and mass lost appear to be proportional to the area of the steel exposed, which was to be expected. Since the changes in mass, both gained and lost, were a function of the area of exposed steel and the corresponding oxidation reaction, these results were expected as well. Finally, and not surprisingly, the steel control sample demonstrated both the highest percentage of mass gained and lost.

To ultimately assess the performance of the adhesive bonded samples, the clamped samples from both sample classes were compared to their bonded counterparts. Specifically consider any of the bonded through thickness samples with TT-C and samples EE-AS and EE-C. It is clear with the Through Thickness samples that the clamped sample gained four times the mass of any of the bonded samples while losing one and a half times the mass. This is a direct result of the level of corrosion since the mass gained was in the form of oxidation and mass lost was the amount of steel consumed in that reaction. It is reasonable to conclude that the adhesive effectively isolated the steel from the composite and eliminated any corrosion and galvanic corrosion specifically.

The results are more apparent when considering the Edge Effect samples. Both the EE-AS and EE-C samples had the same amount of initial steel surface area, surface area covered, and hence surface area exposed. It is clearly and conclusively shown that the clamped sample again gained and lost more mass that the bonded sample as a direct result of the corrosion. It can be further concluded that this difference was attributable to galvanic corrosion as a result of the direct contact of the composite to the steel. Finally, it was shown through these samples that the adhesive and scrim effectively eliminated galvanic corrosion.

As an aside, it was accidentally proven that galvanic corrosion exists between the adherends. After separation of the samples and cleaning their surfaces, the constituents were stored together for future inspection and photographing. A slight amount of corrosion product coated the surface of the cleaned steel plates. In some cases, the exposed fibers from the split composite caused by the cohesive failure of the bond were in direct contact with the steel plate. In these areas of direct contact the amount of the corrosion was observed to be greater than on the parts of the steel not in contact with the composite. This further supports the conclusion that the selected repair method effectively eliminated galvanic corrosion since the characteristic mode of corrosion illustrated by these base components was not observed in any of the samples.

2.5.2.4.5 Commentary on Quantitative Results

Unfortunately, there were some unexpected results were obtained by studying the mass history of each sample. From initial inspection, the ratio of mass lost to mass gained for the fully bonded Through Thickness samples would lead one to surmise that the adhesively bonded samples did not perform as well as the clamped sample. The bonded samples had an average ratio of mass lost to mass gained of 9.043 compared to the relatively low 1.562 of the clamped Through Thickness sample. This was the inverse of what was expected since the composite clamped to the steel is clearly less desirable from a galvanic corrosion standpoint. However, one must consider the change in mass for each sample and not simply the ratio of the mass changes. Further investigation into the experiment reveals potential flaws inherent in the test methodology that may have lead to these unexpected results in terms of the ratio.

The variable mass results could potentially be explained by a systematic "washing away" of the corrosion product from sample surfaces during the wet/ dry cycling. Fluid flow over the surface of the samples was forced during the act of lifting the samples from the storage vessel for the drying period. The forced flow could potentially be strong enough to remove loose corrosion particles from the samples. This accounts for the presence of large amounts of corrosion sediment in the bottom of the container, the presence of corrosion precipitate on the surface of the samples, and ultimately, the variation of the ratio of mass gained to mass lost.

Assume that the composite in the clamped Through Thickness sample effectively protected the corrosion product from being separated from the steel plate. As the assembly was lifted, the aqueous solution washed over the surface of the composite while separating the corrosion product from all the other samples. Therefore, it is reasonable to conclude that its mass recordings are representative and accurate

Conversely, this dislocated corrosion product affects the results of the remaining samples with a steel component in two ways. First, the recorded mass gained by the samples is low because some of the gained mass became suspended in the solution. Second, the mass lost values are artificially high because the removed corrosion product now exposed new steel that could be consumed in the oxidation reaction. The combination of these factors is believed to contribute to the inconclusive results.

2.5.2.5 Mechanical Testing of Composite Samples

The final area of investigation from the long-term exposure experiment was to characterize the material properties and strength of the composite. Recall that literature suggests that both conditioning in NaCl as well as galvanic corrosion can adversely affect the strength of composites. Because of these factors, it was necessary to evaluate how the selected composite performed under the given exposure conditions.

Short beam shear tests (ASTM D 2344) and three point bending tests (ASTM D 790) were performed on both the conditioned composite samples as well as virgin samples and their performances were compared. Both groups of testing were performed on an Instron 4484 Universal Testing Machine under standard conditions and at room temperature. The machine was equipped with a PC interface connected directly to the load cell to measure load and displacement ten times per second during the experiment. The tests were run with a fixed crosshead rate of 0.05 in/min.

2.5.2.5.1 Short Beam Shear Test Results

Recall the composite used in this study was a unidirectional graphite fiber composite. Nominal short beam shear test samples had a length of 2.000 inches, width of 0.500 in, and a thickness of 0.211 in. Based on previous research and ASTM D 2344, a span to thickness ratio of 4 to 1 was selected for a span of 0.844 inches. The specification recommended total length to thickness of 6 to 1, or 1.266 inches in the context of this study, however, 2.000 was used for machinability reasons. Additionally, sample widths varied from 0.498 in to 0.555 in due to the machining processes as well.

The breaking load, P_B, was recorded in pounds for each sample and the apparent shear strength, S_H, was calculated in psi using the following equation:

$$S_H = 0.75 P_B / bd \qquad \text{Eq. 2-6}$$

Table 2.5 lists all specimen size and test results for the samples that were conditioned while Table 2.6 contains the same information for the virgin samples. An average S_H for both sets of samples was calculated for comparative purposes. The conditioned samples had an average S_H of 8.99 ksi with a standard deviation of 0.16 ksi while the virgin samples averaged 9.34 ksi with a standard deviation of 0.09 ksi. These results compare very favorably and indicate no loss of strength in the composite due to exposure since the strength of virgin samples feel within three standard deviations of the conditioned samples. Note that all samples tested failed through a shearing in their respective gross cross section.

Table 2.5 Conditioned composite sample short beam shear test data.

Specimen	*b* (in)	*d* (in)	P_B (lb)	S_H (ksi)
C-1	0.555	0.211	1435.1	9.19
C-2	0.507	0.211	1267.6	8.89
C-3	0.547	0.212	1410.2	9.12
C-4	0.529	0.212	1324.0	8.85
C-5	0.537	0.212	1381.2	9.10
C-6	0.526	0.212	1295.8	8.72
C-7	0.549	0.212	1404.5	9.05
C-8	0.549	0.212	1402.9	9.04
Average	0.537	0.212	1365.2	9.00
Std. Dev.	0.016	0.001	61.1	0.16
Coef. of Var.	2.57E-04	2.14E-07	3738.9	0.03

Table 2.6 Virgin composite sample short beam shear test data.

Specimen	*b* (in)	*d* (in)	P_B (lb)	S_H (ksi)
V-1	0.498	0.211	1317.6	9.40
V-2	0.501	0.211	1307.1	9.27
V-3	0.535	0.211	1394.9	9.27
V-4	0.552	0.211	1464.9	9.43
Average	0.522	0.211	1371.1	9.34
Std. Dev.	0.026	0.000	73.8	0.09
Coef. of Var.	6.950E-4	0.000	5444.9	7.47E-3

2.5.2.5.2 Three-Point Bending Test Results

The test samples used in three point bending (ASTM D 790) were similar in geometry to those used in the short beam shear tests of Section 2.5.2.5.1 except they required a significantly greater length to ensure a flexural failure. Carlsson and Pipes suggest a span to depth ratio of 16 to 1 for this type of composite material (101) yielding a span length of 3.376 in for our samples. Since the conditioned samples had a nominal length of 6.000 inches, the full-length sample was tested in flexure at this span. However, it was soon revealed that this span was too short because all tested samples failed through interlaminar shear. Therefore a 24 to 1 span to depth ratio was selected requiring a span of 5.064 inches. At this span length, the expected tension failure of the outer fibers was experienced by all samples. Additionally, sample widths ranged from 0.516 in to 0.549 in due to variability in machining. The test configuration used for the three point bending flexural tests mirrored that of the short beam shear tests except it was modified for a longer gage length.

The maximum load, P_{max}, was recorded in pounds for each sample at failure and applied to equation Eq. 2-7 to determine the maximum stress, σ_{max}, in psi for each sample.

$$\sigma_{\max} = \frac{3PL}{2bd^2} \qquad \text{Eq. 2-7}$$

Additionally, the incremental change in load, ΔP, in pounds and change in deflection, $\Delta\delta$, in inches were calculated from the data in the mid range of the load history for each sample. Those values were then used with equation Eq. 2-8 to determine the modulus of elasticity, E, in psi for each specimen.

$$E = \frac{L^3}{4bd^3}\frac{\Delta P}{\Delta \delta} \qquad \text{Eq. 2-8}$$

Note that the equation used in determining the modulus of elasticity does not take into consideration the effects of shear deformation. Carlsson and Pipes state, "large span to thickness ratios, L/h, are required to minimize the influence of shear deformation" (105) while independent research demonstrated that L/h = 24 supported that statement. Table 2.7 lists all specimen size and test results for the samples that were conditioned while Table 2.8 contains the same information for the virgin samples.

Note that all of the material that was independently conditioned in the 10% aqueous NaCl bath was consumed during the short beam shear and the first round of three point bending tests. Therefore some of the composite that was clamped to the surface of the Through Thickness samples was cleaned and used to fabricate the samples used in three-point bending at the new span length.

This decision forced by necessity actually allowed an additional mechanism to be tested that had not originally been considered.

Recall that Boyd, et al. demonstrated that galvanic corrosion byproducts could degrade the matrix of the composite thereby exposing the fibers and resulting in reduced composite strength (1218-1224). Since galvanic corrosion was forced by clamping the composite directly to the surface of the steel, it can be assumed that the potential for damage to the fibers exists. Typically, the fibers will fail in compression before tension. It follows that exposing potentially degraded fibers to compression during testing would be logical to force weak-mode failure. However, for this particular application the composite is considered to be a tension member and there is no reason to believe that there will be any mechanism to directly impart compression to the surface of the composite. Therefore, it was determined that the tension face of the test samples would be the face that was clamped to the steel. During the testing, an additional sample was placed in the test frame with the clamped side in compression and it failed interlaminarly supporting this theory.

Table 2.7 Conditioned composite sample three-point bending test data.

Specimen	b (in)	d (in)	P_{max} (lb)	σ_{max} (ksi)	ΔP (lb)	$\Delta\delta$ (in)	E (Msi)
C-1	0.516	0.211	431.7	145.2	322.9	0.1512	15.1
C-2	0.533	0.210	437.3	143.7	373.7	0.1712	15.1
C-3	0.528	0.210	401.1	133.1	356.0	0.1618	15.4
C-4	0.542	0.211	451.8	144.6	380.1	0.1672	15.3
Average	0.530	0.211	5.2	430.5	0.2	144.51	15.1
Std. Dev.	0.011	0.001	0.000	21.3	6.8E-3	0.73	0.1
Cof. Var.	1.176E-4	3.333E-7	0.000	455.2	4.6E-5	33.06	20.1

Table 2.8 Virgin composite sample three-point bending test data.

Specimen	b (in)	d (in)	P_{max} (lb)	σ_{max} (ksi)	ΔP (lb)	$\Delta\delta$ (in)	E (Msi)
V-1	0.540	0.211	488.9	157.1	312.5	0.1422	14.8
V-2	0.547	0.212	500.1	157.1	336.6	0.1448	15.2
V-3	0.519	0.211	459.1	153.5	324.6	0.1519	15.0
V-4	0.549	0.211	490.5	155.0	383.3	0.1635	15.5
Average	0.539	0.211	5.2	484.7	0.2	156.42	15.2
Std. Dev.	0.014	0.001	0.0	17.7	4.9E-3	1.21	0.4
Cof. Var.	1.882E-4	2.50E-7	0.0	314.6	2.4E-5	3.13	102.2

An average maximum stress, σ_{max}, was calculated for each set of samples as well as corresponding standard deviations for each quantity for comparative purposes. The conditioned samples had an average σ_{max} of 144.5 ksi with a standard deviation of 0.7 ksi while the virgin samples exhibited an average of 156.4 ksi with a standard deviation of 1.2 ksi. The results correlate nicely, however they do suggest a slight decrease in load carrying capacity by the conditioned samples. This decrease could be attributed to the failure mode, which was tension in the outer fibers. Recall that the degradation of tensile strength of the fibers weakened through the mechanisms of galvanic corrosion. In light of the fact that the composite will be protected from galvanic corrosion in the field, and this slight decrease in ultimate strength is not of concern.

Similarly, an average modulus of elasticity, E, was computed for each set of samples along with their standard deviations. For this testing, the conditioned samples averaged 15.1 Msi while the virgin specimens averaged 15.2 Msi with standard deviations of 0.1 and 0.4 Msi respectively. These values are virtually identical and suggest there was no adverse effect on the composite from the conditioning or the effects of galvanic corrosion.

2.6 Conclusions

The purpose of this chapter was to investigate the potential for and the elimination of galvanic corrosion. The theories of galvanic corrosion were introduced and discussed. Additionally, scholarly research applicable to this study was evaluated and summarized. It was concluded that the composite material selected when combined with the steel bridge girder posed the threat of galvanic corrosion. Furthermore, preventative measures were necessary to eliminate conditions favorable to its development. Based on the properties of adhesives, it was assumed that the adhesive joint would effectively isolate the components electrically. However, installation defects, saturation of the

components, and interaction at the edges of the materials posed additional threats. Therefore several solutions were proposed and evaluated for their effectiveness through two separate tests.

The first test was designed to demonstrate the probability of current flow through the thickness of the materials as well as the ability to eliminate it. By effectively eliminating current flow, one of the three components required for galvanic corrosion would be eliminated. After establishing the conductivity of the constituents, a variety of modifications to the materials were tested. As theorized, the materials were completely insulated electrically through the addition of a layer of adhesive. However, in situations where there may not be adhesive present, it was proposed to include a fiberglass scrim in the bond line or manufactured in the surface of the composite. In theory, this scrim would provide an "insurance policy" for eliminating conductivity.

A three-ounce 120 fiberglass scrim was bonded to the surface of the composite samples using a vinyl ester resin and the SCRIMP manufacturing process. After the adhesive had cured, the new samples were again tested for conductivity and it was shown that the addition of the scrim was effective in eliminating current flow. Aside from the formal test matrix, a panel of composite and steel with the scrim bonded in the adhesive layer, fabricated for other tests, was checked for conductivity and it too was found to have infinite resistivity.

An unexpected enhancement to the rehabilitation process was also discovered during this first test. Through the range of sample types tested, it was learned that the surface preparation of the composite was actually damaging the material. A variety of combinations of surface cleaning methods were tested and it was concluded that a 20-30 psi bead blast with the nozzle 2-3 in from the surface of the material provided optimum results.

The second test conducted during this phase of the research involved conditioning eleven representative samples through wet-dry cycling in a 10% aqueous NaCl bath. The samples were selected to evaluate the behavior of the rehabilitation through the thickness of the repair, at the edges of the components, as well as establishing baseline performance of the constituent materials through control specimens. The samples were immersed for approximately 12 hours to promote saturation of the materials and then allowed to air dry for an additional 12 hours. Both qualitative and quantitative results were recorded as part of this study. Ultimately, mechanical tests were performed on the composite material alone in order to evaluate the effect of the exposure on this particular material.

This particular test provided some dramatic qualitative results. The level of corrosion on any bare steel exceeded expectations. There were some locations in which it appeared that there were mechanisms contributing to the corrosion other than the standard oxidation reaction. While it is believed that galvanic corrosion played a role in these differing qualitative results, other mechanisms such as crevice effects could not be ignored.

When the bonded samples were separated, the expected and the most promising results were obtained. First and foremost, the composite failed cohesively instead of adhesively at the interface indicating that the chosen bonding scheme withstood the effects of the long-term saturation. Additionally, at some areas where the adhesive did pull away from the steel, an uncorroded, white metal surface was revealed. This observation dramatically illustrated that corrosion at the bond interface had effectively been prevented.

The quantitative results were not as definitive as the qualitative results and the data required more investigation in order to draw conclusions. Ultimately, it was illustrated that the samples that were bonded adhesively, both with and without a scrim and for both sample classes, exhibited lower levels of mass loss than their clamped counterparts. Mass loss was previously shown to be directly proportional to the level of corrosion therefore it can be concluded that the adhesive layer and the adhesive and scrim combination effectively isolated the two components and protected against galvanic corrosion. Even though the behavior of the Edge Effect samples was fairly accurately predicted by the performance of the control samples the results obtained for Through Thickness samples were not what might have been expected. Furthermore, it was difficult to draw correlations between similar Through Thickness and Edge Effect samples.

Conversely, the results from the mechanical testing to characterize the composite material provided excellent results. Both short beam shear (ASTM D 2344) and three point bending (ASTM D 790) were conducted as a part of the testing. Both conditioned and virgin samples were tested using either test procedure. From the short beam shear testing, the conditioned samples had an apparent shear strength, S_H, of 8.99 ksi while the virgin samples exhibited 9.34 ksi. After calculating standard deviations for both sample groups, thee conditioned and virgin samples were statistically equal.

The three point bending tests provided similarly encouraging results. The maximum bending stress, σ_{max}, for the conditioned samples was 144.5 ksi and the virgin samples averaged 156.4 ksi. When the standard deviations were determined, it was found that the conditioned samples had slightly inferior performance to the virgin samples however the difference was minimal. Additionally, the modulus of elasticity of the two groups of samples was practically identical with the conditioned samples averaging 15.1 Msi and the virgin samples averaging 15.2 Msi.

As a whole, the discoveries revealed in this chapter are significant. Galvanic corrosion was identified as a potential mode of failure for the rehabilitation, tests were designed to illustrate this and isolate its mechanisms, and preventative measures were developed, tested, and experimentally proven to work. Additionally, enhancements to the preparation of the materials were made which further improves the integrity and reliability of such a rehabilitation method. These results can be used by practicing engineers and state DOT's to demonstrate that corrosion is not an issue in the context of this repair scheme.

Chapter 3: STRENGTH INVESTIGATION

3.1 Introduction

After determining that galvanic corrosion was not an issue for this rehabilitation scheme, the next area of concern was the performance of the adhesive bond to steel. Performance is qualified by strength testing, discussed in this chapter, and durability testing, discussed in Chapter 4, of the primer/ adhesive system. Rajagopalan, Immordino, and Gillespie (222-230), Ammar (50-54), and Mertz and Gillespie (1-5) have performed extensive tests in an attempt to determine optimum adhesives for a variety of infrastructure applications. In conjunction with other research at the University of Delaware, Wetzel (8) and others have investigated methods for elevated temperature curing of the adhesives in the field. Elevated temperature may be required to achieve optimal adhesive properties or simply to reduce the cure time. Additionally, Ragopalan, Immordino, and Gillespie (223-224) and McKnight (194-284) among others have done extensive work in the area of adhesion promoters and surface preparation.

Based on the survey of the aforementioned literature, the evaluation of industry practices, as well as considering factors unique to this problem, a number of adhesives and primers were screened for use in this phase of the research. Next, combinations of the applicable adhesives and primers were established for testing. Within some of the adhesive/ primer groups, alternate material preparation methods were addressed to evaluate their impact on bond strength.

ASTM standard lap shear specimens (ASTM D 3165) were fabricated and tested for each of the selected sample types. Average shear strengths were compared between groups to assess relative performance. Shear strength is known to be a function of bond line thickness and that it may vary in the field. Consequently, the thickness of the bond line for each sample was measured. This enabled direct comparison between sample types and to assess the sensitivity of shear strength to bond line thickness for adhesive selection.

3.2 Adhesive Selection

The following criteria were used in order to select adhesives for evaluation in this work:

- ASTM D-1002 Shear Strength
- ASTM D-638 Tensile Strength and Modulus
- Pot Life
- Workability

- Glass Transition Temperature (T_g)
- Room Temperature Cure
- Availability
- Shear Elongation

These criteria consider the design, ease of erection, cost, and performance of retrofit applications. Long-term durability was another important criteria and is discussed in Chapter 4.

The ASTM strength characteristics were significant for obvious reasons; it is desirable to have adequate performance of the rehabilitation. Specifically, Edberg and Ammar previously established minimum shear strength of 600 psi through finite element models for adhesively bonding composite materials to steel bridge girders (this stress level would be specific to each individual bridge design). There was not a specified minimum tensile strength established, rather this information was used to help differentiate performance of the studied adhesives. Shear modulus and elongation to failure were properties that were regarded to be of secondary concern. Steel rehabilitation offers significant shear areas over relatively thin bond lines so load transfer will be efficient for the typical range of adhesives. However at stress concentrations (e.g. splices and terminations) it is desirable to have adhesives with high elongation to failure as this class of materials will be tough and more resistant to fatigue crack growth in the adhesive.

Pot life is significant in this application because it controls the overall size of a practical rehabilitation. It is imperative that all components are in place before the adhesive cures. A longer pot life naturally provides more working time and therefore allows a larger rehabilitation to be performed. A minimum of 30-40 minutes is recommended for a team to complete a 20-30 foot installation. Workability ties directly into pot life with respect to its significance. If an adhesive proves difficult to work with it follows that a specific installation would take longer to be completed than an identical repair with a more "user friendly" adhesive. It follows that the longer it takes to perform a repair of specified area or length, the more significant the pot life of the adhesive becomes. Therefore it is desirable to have and adhesive that is easy to work with.

The glass transition temperature, T_g, is another property of the adhesive that is of significance. The rehabilitation is of no use if the adhesive softens and loses stiffness and strength above T_g. Maximum temperatures for civil engineering applications are on the order of 130°F and that was selected as our minimum value for T_g. Adhesives that cure at room temperature and provide values of T_g greater than our service temperature are highly desirable. Due to the physical nature of the installation, it is greatly simplified if an adhesive can fully cure without the aid of external heating devices. The use of heating blankets and other means of providing adequate heat to guarantee proper curing of concrete

are industry practice, however, the complexity and cost of the rehabilitation is reduced through an adhesive with a room temperature cure.

Finally, the availability of the adhesive is something that needs to be taken into consideration. It serves no purpose to recommend a rehabilitation that requires a component that is not readily or widely available. Therefore the adhesive selected should be one that is commercially available from a number of suppliers and in a variety of geographic locations to facilitate implementation of this repair scheme.

Based on these criteria, three adhesives were selected for consideration and Table 3.1 illustrates how their manufacturer data compares. Ciba-Geigy AV8113 epoxy was specifically recommended for this application (Rajagopolan, Immordino, and Gillespie 229) therefore it was considered to be the preferred adhesive. Similarly, Mertz and Gillespie (8) and Gillespie, et al. (234) used it in their work in steel rehabilitation, which laid the foundation for this study. Another epoxy, SikaDur 30, was considered because it was part of a proprietary composite rehabilitation system designed by Sika. Finally, Plexus MA 425 was investigated because of other benefits inherent to a methacrylate adhesive (i.e. high elongation and toughness). All three of the adhesives tested were two-part adhesives that were readily available and currently used in various industries.

Table 3.1 Manufacturer data listing the selection criteria of the three screened adhesives.

Criteria	Ciba-Geigy AV8113	SikaDur 30	Plexus MA425
ASTM D-1002 Shear Strength	2660 psi 18 MPa	3600 psi 24.8 Mpa	1500-1800 psi 10.3-12.4 MPa
ASTM D-638 Tensile Strength	2280 psi 15.7 MPa	3600 psi 24.8 Mpa	2000-2500 psi 13.8-17.2 MPa
ASTM D-638 Tensile Modulus	15.6 ksi 108 MPa	650 ksi 4482 MPA	40-50 ksi 276-345 MPa
Pot Life	60 minutes	70 minutes	30-35 minutes
Glass Transition Temperature (T_g)	194°F 90°C	130°F 55°C	218°F 103°C
Room Temperature Cure Time	16 hours	24 hours	80-90 minutes (75% strength)
Tensile Elongation	25%	1%	120%-140%
Cost per 5 gal.	Resin: $350 Hardener: $515	$563 for complete kits	Resin: $436 Hardener: $585
Availability	Yes	Yes	Yes

The Ciba-Geigy AV8113 adhesive components were available in quarts or in five-gallon units and mixed in a 1:1 ratio by mass. For industrial applications, meter-mixing equipment can be used to automate the mixing phase. The resin was a stiff, ochre colored paste while its accompanying hardener was an ice blue colored material. When mixed, the epoxy was a characteristic green color and was slightly stiffer than the hardener by itself. It spread fairly readily, but was very tacky and sometimes difficult to work with.

Conversely, the SikaDur 30 was very easy to work with. It consisted of a 3:1 ratio and was sold in 3/4-gallon kits that consisted of two pre-measured containers to ensure the proper mix. Both parts of the adhesive were gray; one (the larger part) was a very light gray and the other (the smaller component) was significantly darker. The adhesive appeared to have some small aggregate, possibly sand, as a component that made the material grainy. It had the consistency and workability of a cement paste or grout. Considering that the adhesive was originally part of Sika's CarbuDur system used in strengthening concrete with composites, it was not surprising that the adhesive had these physical properties.

The Plexus MA 425 adhesive required a 10:1 ratio of adhesive to activator and was sold in 380 ml pre-measured cartridges, in five-gallon containers of each component, and even in 50-gallon drums for larger applications. The 380 ml cartridge was rather innovative. It had the appearance of a caulking tube that had a second smaller concentric, or co-axial, tube in the center. The creamy white colored resin filled large outer tube while the ice blue colored hardener was contained in the narrow middle tube. A long mixing nozzle with interior baffles to combine the two components was attached to one end of the cartridge. The whole assembly was then placed in a proprietary caulk gun equipped with two plungers. When the trigger was squeezed, both plungers moved simultaneously forcing the components into the nozzle in the correct proportion. After mixing, the adhesive was bright blue in color, less viscous than both the Ciba Geigy and Sika adhesives, and had excellent workability.

3.3 Primer Selection

There is a great deal of literature on the topic of surface preparation for adhesive bonding. The literature survey concluded that some type of primer must be used to create a bond that is both strong and has environmental durability. In selecting primers for this work, it was necessary to select primers that were compatible with the types of adhesives being used on steel. Specifically, a primer designed for use with epoxies was required by both the Ciba-Geigy and Sika adhesives while Plexus manufactured a primer specifically for use with its MA425. Additional criteria included methods of application, drying requirements, present applications, environmental compatibility, as well as cost and availability. Primers from a number of companies (3M, Dow, Essex, Plexus) and a number of applications (industrial, automotive, structural) were considered, however, the following three were best suited to the application. Table 3.2 lists the manufacturer data for the selected primers with respect to the aforementioned criteria.

McKnight (284-287) Rajagopalan (226-229), and Kinloch (*Structural* 269-312) have all demonstrated the benefits of using a silane-based primer. Therefore silane Z-6040 for epoxies from Dow Corning was selected as the preferred primer. The priming solution was made by mixing 1% by weight of the silane with de-ionized water that had a pH in the range 4.5-5.0 and stirring for a minimum of 30 minutes.

The second primer used in this research was a silane-based chemical recommended by Dow called Q1-6106. This compound contained a melamine based hexamethoxymethylmelamine resin. Melamines are sometimes referred to as urea-formaldehydes and primarily serve as crosslinking catalysts (Sax 737). In other words, the melamine-based chemical was in the primer as a transport mechanism to ensure that the silane was in the proper "location" to carry out its function. This chemical was clear in color and had the consistency of Karo syrup. The Q1-6106 was mixed 5% by weight with methanol and stirred for a minimum of 30 minutes to form the primer.

Plexus PC 120 primer was recommended by the manufacturer for use with its MA 425 adhesive. Again, this Plexus product offered some user-friendly features. First, the primer was available in a ready to use state; there was no mixing involved, just open the container and apply. More significantly, however, was the fact the primer was red in color. This pigment was very useful in showing what surface area had been primed and what areas had not been coated to ensure complete coverage.

In addition to the traditional "adhesive primers," a paint primer was also evaluated. It was considered because every attempt to customize the installation process to current DelDOT procedures would facilitate future implementation. DelDOT paint specifications 605616, 605619, and 605620 call for the use of a micaceous iron oxide based moisture-cured urethane paint system. Approved primers for this system are Wasser MC-Miozinc and Xymax Bridge Zinc. Since both were approved equals, only the Wasser MC-Miozinc was used.

Table 3.2 Manufacturer data listing the selection criteria of the three screened primers.

Criteria/ Properties	Z-6040 Silane	Q1-6106 Adhesion Promoter	Plexus PC120 Primer
Appearance	White to slightly yellow	Clear	Red
Physical Form	Low-viscosity liquid	Slightly viscous fluid	Low-viscosity liquid
Viscosity	3	850	2
Specific Gravity at 77°F	1.07	1.19	0.81
Refractive Index	1.428	1.510	N/A
Flash Point, closed cup (°F)	>213	120 (minimum)	53
Type	Glycidoxy (epoxy) functional methoxy silane	100% active coupling agent	Proprietary chemical primer and conditioner
Primary Uses	Coupling agent to improve adhesion of organic resins to inorganic surfaces	Coupling of reinforcing agents to plastics; adhesion promoter for plastics and metals	Coupling agent to be used in conjunction with Plexus MA420 adhesive
Mixing Agents	1% by mass with de-ionized water	5% by mass with methanol	None
Mixing Procedure	Min. 30 minutes	Min. 30 minutes	None
Recommended Drying Procedure	15 minute air dry	15 minute air dry	Air Dry
Cost for five gallon pail	$544	$718	$390

3.4 Sample Preparation and Bonding Schemes

Prior to bonding, all adherends were prepared using the same baseline bonding scheme. This particular combination consisted of the following:

- Bead blast of the steel bonding surface to near-white metal to remove any corrosion, oils, or mill byproducts
- Bead blast of the composite bonding surface to remove the smooth finish per the guidelines set forth in Section 2.5.1.2
- Solvent wipe of both adherends to remove any residual particles from bead blasting process
- Apply Ciba-Geigy AV8113 adhesive and allow 24 hour room temperature cure

Variations of the baseline bonding scheme were then established to evaluate adhesive/ primer combinations. Each combination was given an identifier as follows:

A: Baseline

B: Baseline with Z-6040 primer coat and 15-minute air-dry

C: Baseline with Z-6040 primer coat and 15-minute air-dry with 30 minute oven drying at 112 °F

D: Baseline with Z-6040 primer coat and 15-minute air-dry with 30 minute oven drying at 200 °F

Q: Baseline with Q1-6106 primer coat and 15-minute air-dry

P: Baseline prep substituting Plexus MA 425 adhesive and PC 120 primer with 15-minute air-dry

DD: DelDot approved Wasser MC-Miozinc paint primer

Sika: Identical to prep method "B" with the substitution of SikaDur 30 adhesive for the Ciba-Geigy AV8113

Note that care must be taken when applying the primer coat to ensure only a thin layer has been applied. If the primer layer is too thick, cohesive failure within the primer may occur and limit shear strength. Following all 15-minute periods of air-drying, the steel plates were dried with forced air prior to bonding or prior to oven drying to ensure no unintentional build-up of primer.

3.5 Sample Fabrication

Recall the results from Chapter 2 that recommend the use of a 3-ounce 120 fiberglass scrim layer to be used with this rehabilitation. Considering that the composite had already been purchased, it was necessary to introduce this scrim layer during the sample fabrication stage. A standard procedure was developed for fabricating the test samples used in this research. The methods discussed here were applied in the fabrication of all lap shear samples as well as the wedge

test samples of Chapter 4 and the samples for the second galvanic corrosion test of Section 2.5.2.

(1) Cut steel, composite, and fiberglass to desired (or required) size. For this research, both the steel and fiberglass were 6 in squares while the composite was 6 in long by 1 1/2 in wide.

(2) Apply baseline preparation from section 3.4 with the exception of applying the adhesive.

(3) Assemble all required parts including, but not limited to, alignment jig, C-clamps, Teflon® release spray, release film, adhesive mixing tools, and adherends (see Figure 3.1).

(4) Apply any desired primers.

(5) Coat inside of alignment jig with Teflon® release spray.

(6) While the primer is drying, measure adhesive per manufacturer's specifications (Figure 3.2) and mix (Figure 3.3).

(7) Spread an even coat of adhesive across the entire surface of the steel plate (Figure 3.4). Even though excess adhesive will be "squeezed out" during clamping process, take care not to apply too much adhesive.

(8) Place steel plate with adhesive in alignment jig.

(9) Smooth fiberglass scrim over surface of steel plate (Figure 3.5) removing any trapped air bubbles. Ensure scrim is in contact with adhesive (Figure 3.6).

(10) Apply an even coat of adhesive over the surface of the composite strips (Figure 3.7) again taking care not to apply too little or too much adhesive.

(11) Place composite strip on top of scrim and align with edge of jig (Figure 3.8).

(12) Repeat steps 10 - 11 until assembly is complete (Figure 3.9).

(13) Place a piece of release film on top of finished assembly (Figure 3.10) to prevent samples from bonding to forcing plate or additional panels.

(14) Ensure that no components have rotated or slipped during individual steps (Figure 3.11). It is of utmost importance to ensure alignment of composite pieces in the test panel due to the fiber orientation and corresponding strength characteristics.

(15) Repeat steps 7 - 14 to fabricate desired number of test panels. It is of paramount importance to complete all assemblies and clamping procedure within the working time of the adhesive.

If the adhesive cures prior to clamping, the possibility exists for irregularities in the bond line thickness affecting test results.

(16) After all panels have been assembled (two in this view), place forcing plate on top of final layer of release film (Figure 3.12). The plate serves as a bearing plate to evenly distribute the clamping force over the surface of the samples to ensure all components are seated and to "squeeze out" and excess adhesive.

(17) Tighten C-clamps in the four corners of the assembly (Figure 3.13).

(18) After tightening all four clamps and some of the adhesive has squeezed out, go back and tighten the clamps again. As the adhesive is forced out, the thickness of the clamped system has been reduced therefore reducing the pressure from the clamps. It is necessary to maintain maximum pressure on the system until the adhesive has fully cured.

(19) After the adhesive has cured, remove the panels and fabricate the test specimens (Figure 3.14). Note the green adhesive between the strips of composite. This illustrates that it is not necessary to put adhesive on the edges of the composite because the pressure from clamping squeezes it into the voids.

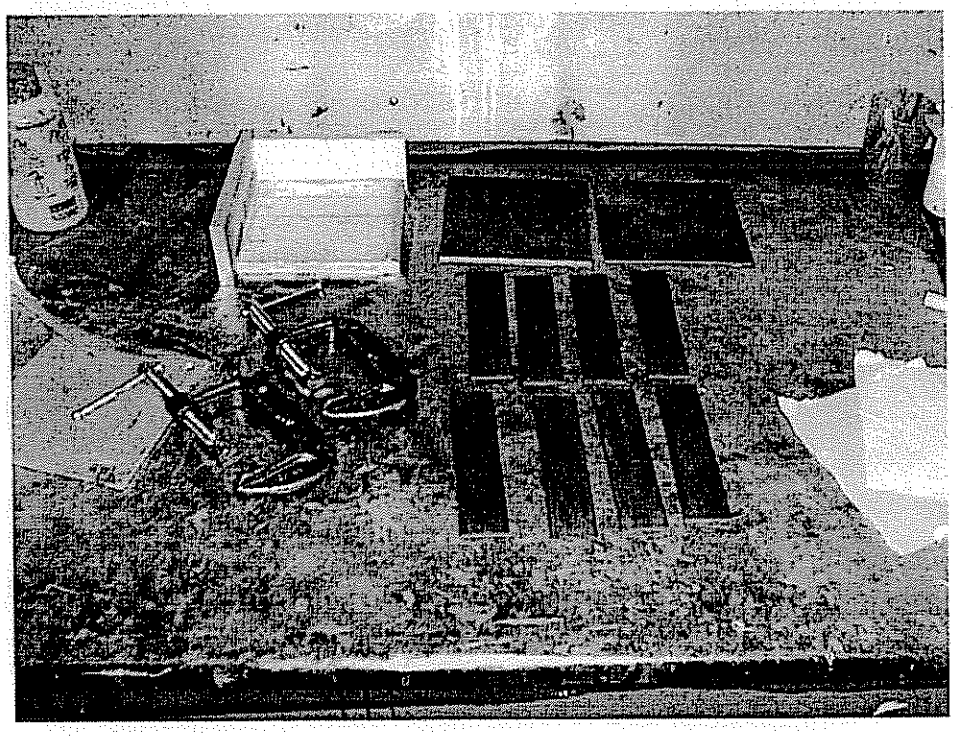

Figure 3.1 Supplies used in test panel fabrication.

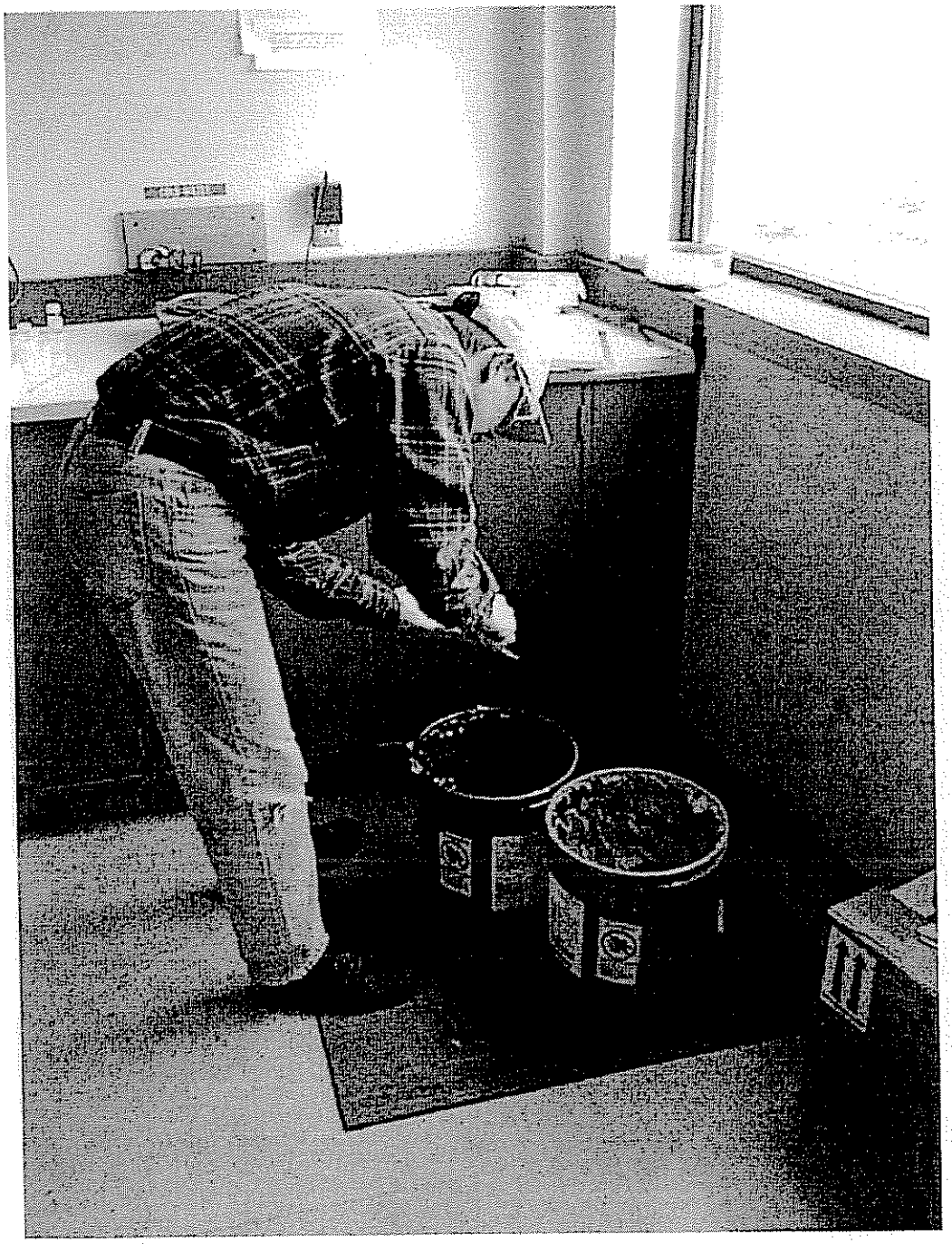

Figure 3.2 Measuring the two parts of the Ciba-Geigy AV 8113 adhesive. Note the different colors of the adhesive components.

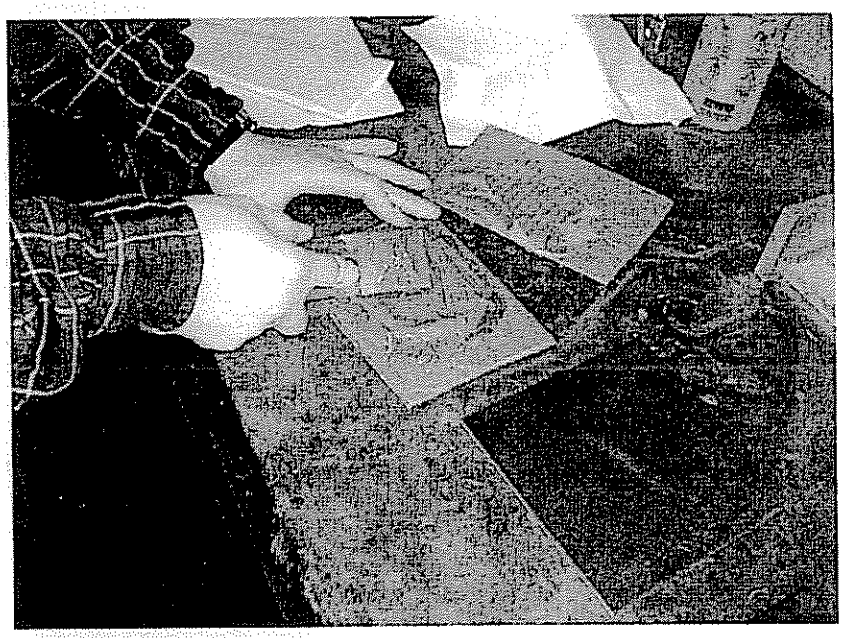

Figure 3.3 Mixing the two-part Ciba-Geigy AV 8113 adhesive.

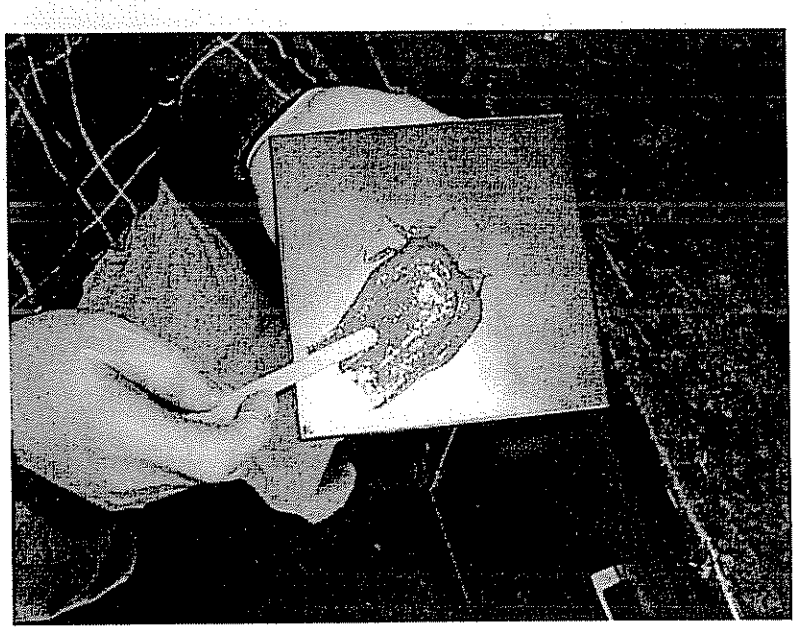

Figure 3.4 Spreading the mixed adhesive over the surface of the steel plate.

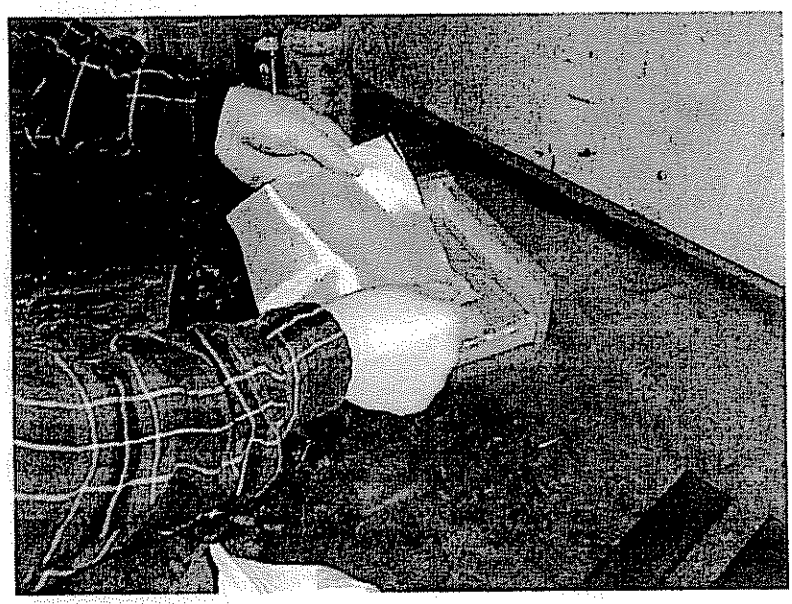

Figure 3.5 Placing the fiberglass scrim on top of the steel plate with adhesive.

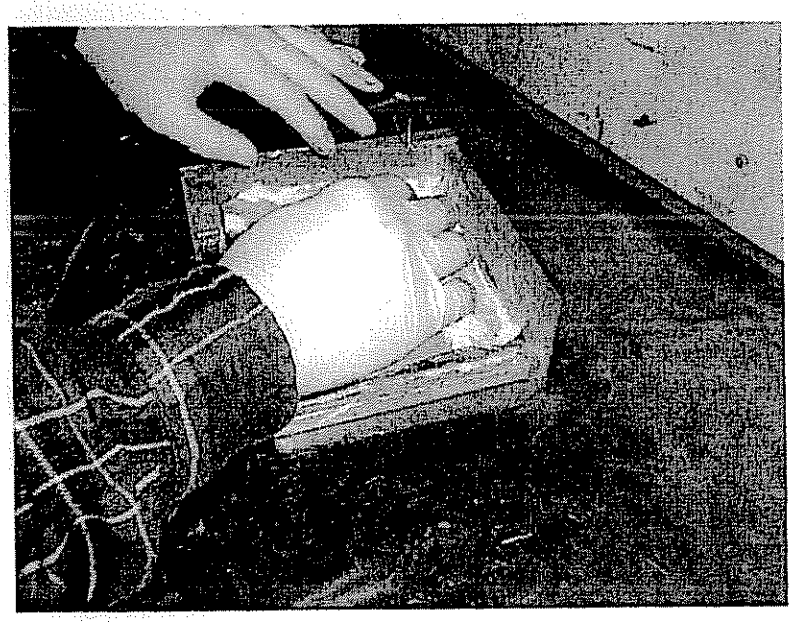

Figure 3.6 Smoothing the scrim to eliminate all voids and to ensure contact with the adhesive.

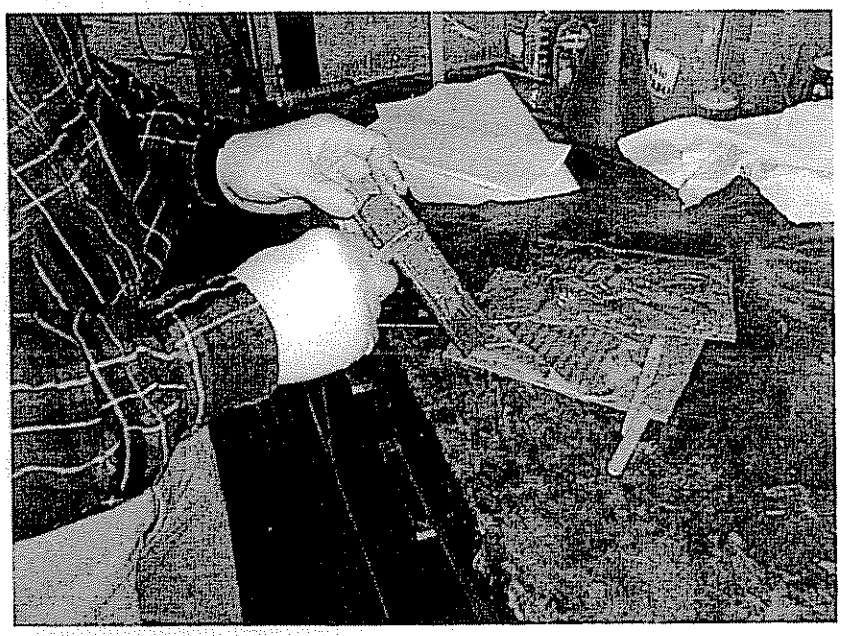

Figure 3.7 Applying the adhesive to a composite strip.

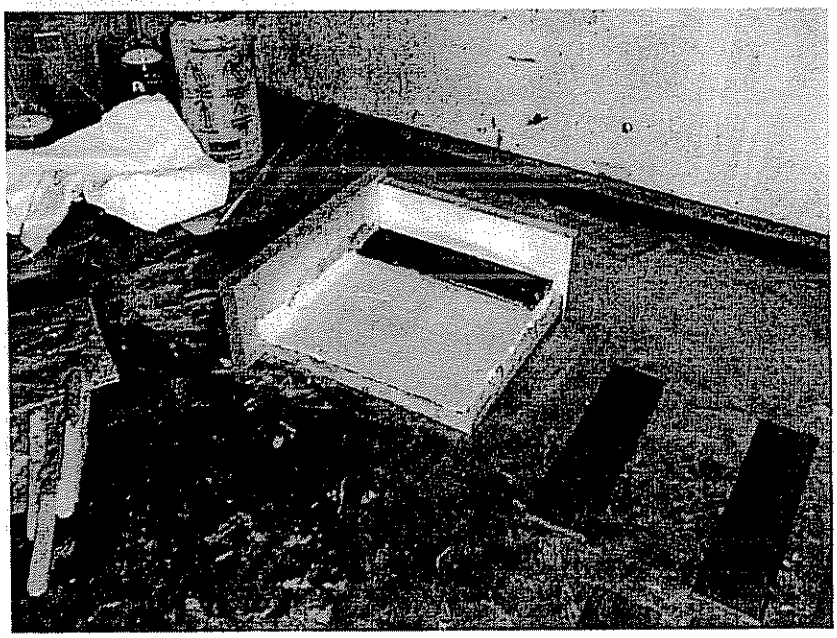

Figure 3.8 Composite strip placed on scrim and aligned with edge of jig.

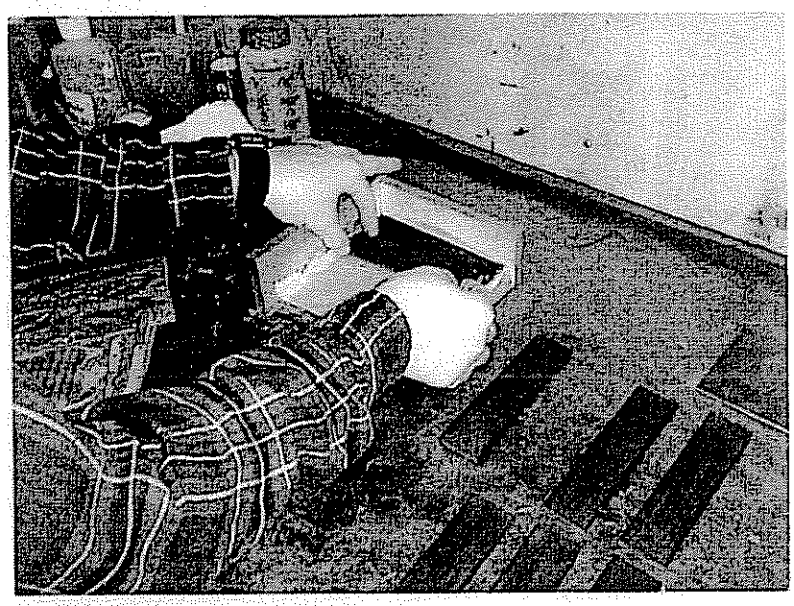

Figure 3.9 Adding additional composite strips to steel plate.

Figure 3.10 Placing release film over completed panel to prevent bonding to additional panel or forcing plate.

Figure 3.11 Securing composite strips and ensuring that none have slipped or rotated out of desired alignment.

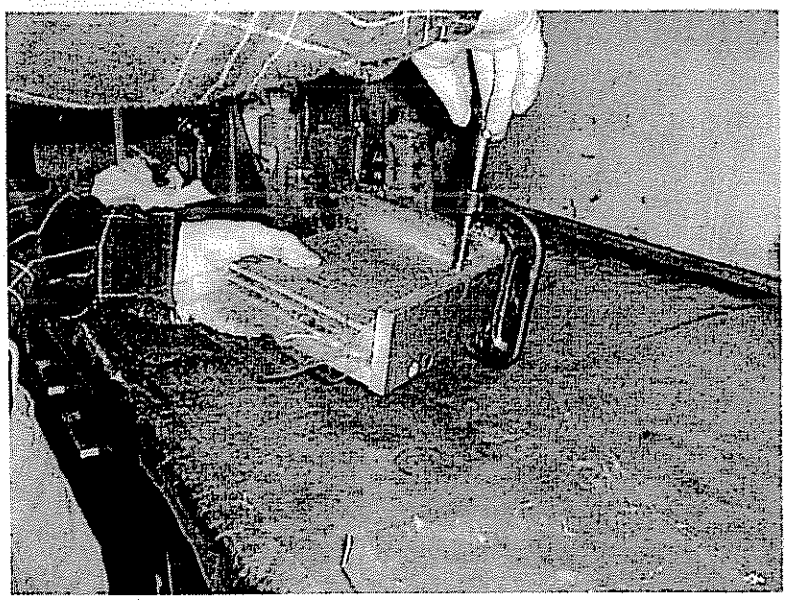

Figure 3.12 Installing forcing plate and tightening first C-clamp.

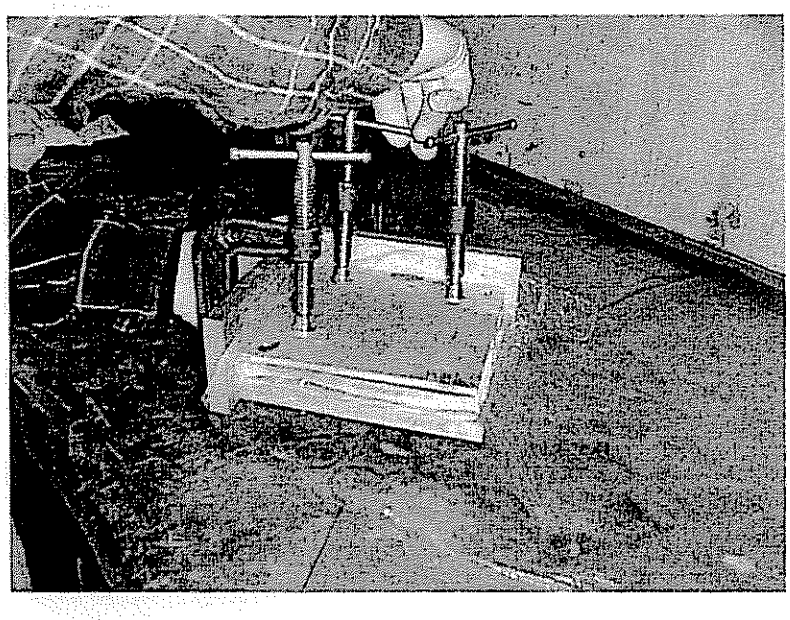

Figure 3.13 Tightening C-clamps in all four corners of alignment jig. Note the green adhesive beginning to "squeeze out" of panel edge.

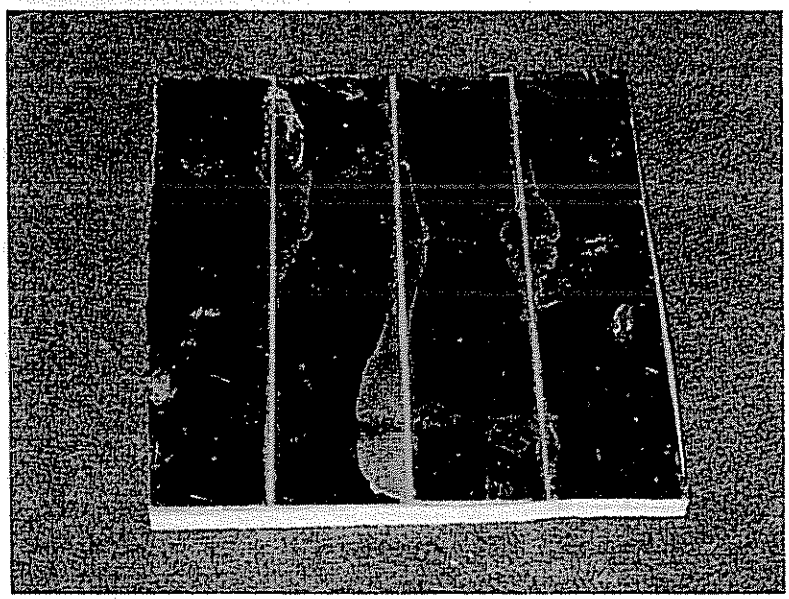

Figure 3.14 The fully cured test panel ready for machining.

Each panel yielded four (4) individual lap shear samples that were cut out of the center of each strip of composite bonded to the steel. The samples had nominal dimensions of 6 in in length, 1 in width, and with a 1/2 in lap. The lap was formed by making one cut on each adherend, offset by 1/2 in, to the bonding surface of the other adherend ensuring that the adhesive had been fully severed. The adhesive must be completely cut, to ensure a shear failure in the adhesive.

Initial testing was performed on identical test samples following the same preparation methods given above with the exception of the scrim layer. It was necessary to evaluate the performance the adhesive without the scrim to determine if the presence of the fiberglass diminished the shear capacity of the bond. Only preparation methods A through D were fabricated and tested without the scrim. The results were then compared between corresponding prep methods to determine what effect the addition of the scrim layer would have on shear strength, if any. For clarification in identifying the samples, the letter "S" was added to the sample ID to designate those samples that had a scrim layer.

3.6 Experimental Procedure

Prior to testing, the dimensions of the lap for each sample were measured and the shear area, A_s, was then calculated as the product of the length and width for each sample. The length, l, of the lap was measured at either outside edge of the sample in inches and averaged. Similarly, the width, b, of the lap was measured in inches at three points along its length and averaged. All samples were tested using an Instron 1120 Universal Testing Machine at standard atmospheric conditions. The breaking load, P, in pounds was recorded for each sample and was divided by the shear area to compute the shear stress, τ, in psi for each sample. After each sample had been tested, the thickness of each bond line was measured using a microscope with a graduated eyepiece and recorded.

Additionally, the failure loci were recorded for each sample. Each individual failure locus was classified as a percentage of total contribution for each of the following types:

(1) Adhesive to steel

(2) Adhesive to composite

(3) Cohesive in adhesive

(4) Cohesive in composite

(5) Cohesive in scrim

(6) Cohesive in DelDOT paint primer

(7) DelDOT paint primer adhesively to steel

Table 3.3 is a matrix illustrating the different failure modes with respect to the different sample groups in which they occurred. The adhesive failures were defined as a clean separation of adhesive from the surface of either adherend (Figures 3.15 and 3.16). When an adhesive failure was experienced, the potential for a fiberglass scrim tear was present as depicted in Figure 3.17. The scrim tore because adhesion failed on either face of the scrim to some degree instead of completely on one face therefore subjecting the fabric to tensile

forces. In most cases, there was adhesive remaining on either adherend indicating a cohesive failure in the adhesive.

A cohesive failure in the adhesive is illustrated in Figure 3.18 where the adhesive is visible on both fracture surfaces. Conversely, a cohesive failure in the composite is shown in Figure 3.19 where remnants of the composite adherend are attached to the steel adherend. The last cohesive failure mode was cohesive in the scrim. Initially it had appeared that the mode had been adhesive to the scrim with a clean separation of the adhesive from the scrim surface. This would indicate an inadequate bond because the scrim wasn't completely wet out. Despite the appearance of a fully adhesive failure, inspection under a microscope revealed that there were fine remnants of fiber embedded in the adhesive therefore demonstrating the cohesive failure mode.

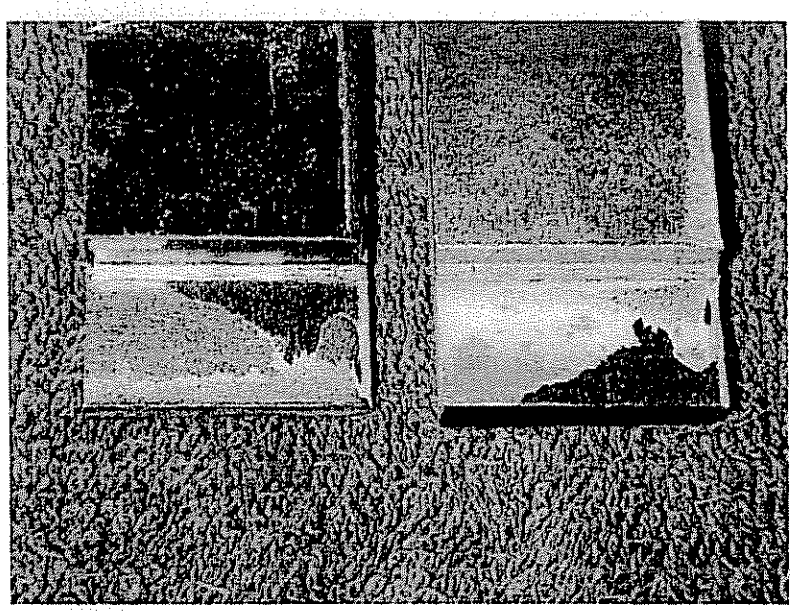

Figure 3.15 A photo of multiple failure modes. Adhesive to steel is the most visible with cohesive in composite and cohesive in adhesive as well.

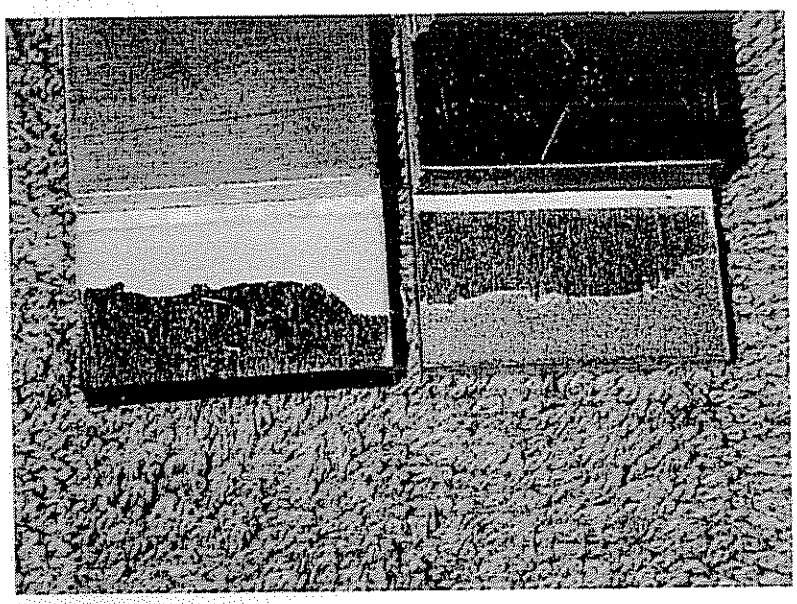

Figure 3.16 Multiple failure modes showing half cohesive in composite (black on either adherend) and half adhesive to steel.

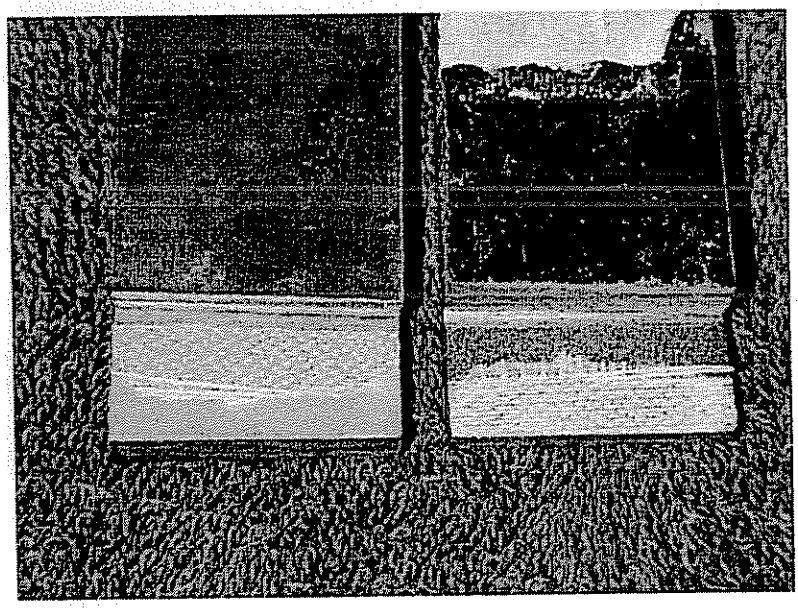

Figure 3.17 An example of an adhesive to steel and cohesive in scrim failure loci with a scrim tear.

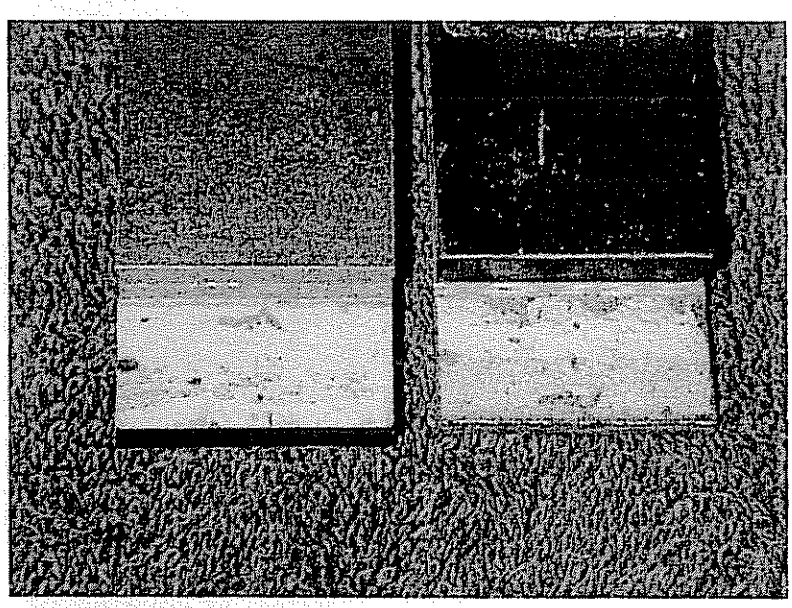

Figure 3.18 An example of cohesive in adhesive failure mode. Note the adhesive on both adherends.

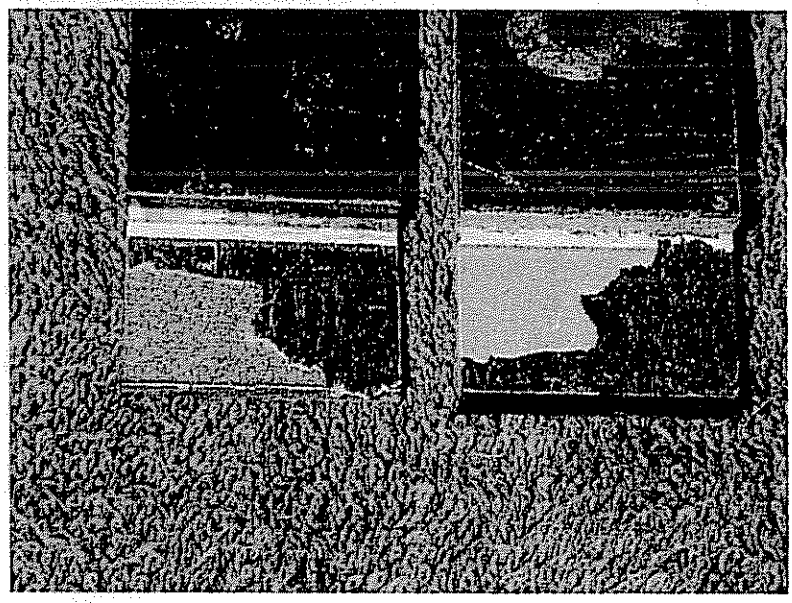

Figure 3.19 An example of cohesive in composite failure shown by composite remnants on the adhesive still bonded to the steel.

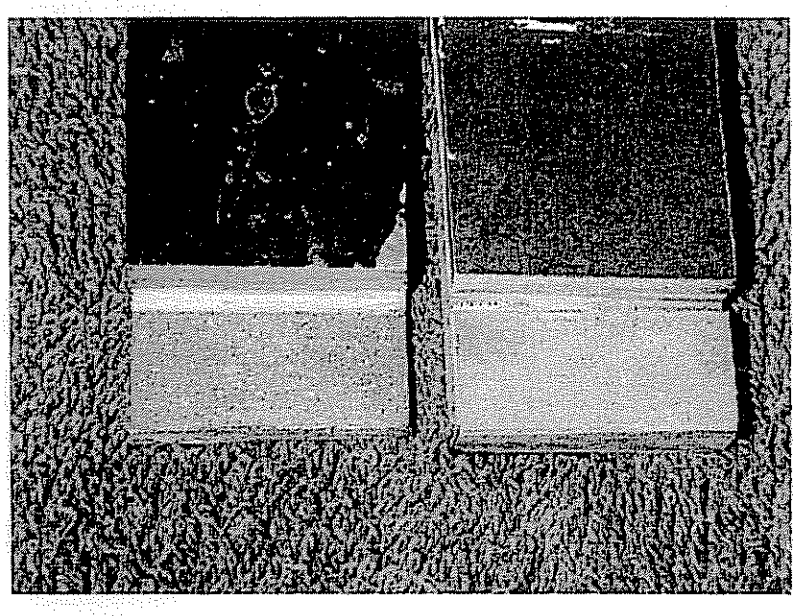

Figure 3.20 A photo of cohesive in DelDOT primer failure. Note the tan-gray color of the primer on either adherend.

Table 3.3 Failure loci listed by sample group in which they occurred.

Major Sample Group	Failure Loci
No primer or scrim used	1, and 4
Primer used but no scrim used	1, 2, 3, and 4
Both primer and scrim used	1, 5, 6, and 7

There were also failure loci unique to Prep DD, which were cohesive in the paint primer and adhesive between the paint primer and the steel. The failed specimens had remains of paint primer on both the steel and the adhesive as shown in Figure 3.20 (cohesive). In the case of an adhesive failure between the primer and the steel, the paint is literally peeled from the surface of the steel during the test.

Clearly, the most desirable failure loci are the cohesive failures since the full strength of the adhesive layer is achieved. Furthermore, cohesive failures also indicate that the interface between layers is not the weak link and our choice of primers, surface preparation, and adhesives are well matched. If poor adhesion to the scrim occurs, the scrim should be chosen with appropriate sizing for a specific adhesive. Additionally, the option exists to fabricate the composite with an integral scrim layer if necessary thereby eliminating that failure mode in an actual application.

From a performance perspective, all failure modes are acceptable as long as the shear strength exceeds the design requirements. Essentially the only

undesirable failure modes are the adhesive failures to either of the adherends or primer adhesively to the steel. However, adhesive failures are indicative of joints that exhibit poor long-term durability under environmental and fatigue loads. The durability of these materials is investigated in Chapter 4.

Note that samples using both the Sika and Plexus adhesives were not tested in this stage. The Sika adhesive was not tested because its performance has already been demonstrated by Chajes et al. (191-201) and has been subsequently approved by the State of Delaware for use in rehabilitations. The Plexus adhesive was eliminated as a candidate due to problems with the application of the adhesive. Following fabrication and adequate curing time, the adhesive that had squeezed out of the samples was still not properly cured. Gillespie experienced similar behavior with this adhesive at a later time. Based on this, it was determined that appropriate confidence could not be placed in the bond between the adherends without further investigation of this effect.

However, an extensive study was conducted for HDR Engineering of MA425 and MA555 with PC 120 primer for retrofitting steel girders. This study revealed that the static mixer caulk gun does not completely mix the two-part adhesive. Pneumatic guns are recommended by Plexus to avoid this problem in the future. Unfortunately, this information was not known prior to downselection. It was later concluded that the Plexus adhesives were viable options for steel girder rehabilitation.

3.7 Experimental Results

After all individual specimens had been tested, their respective shear strength results were compiled by prep method and then averaged for comparison. Shear strength results for samples with a scrim layer, designated by the letter "S" in the preparation method, can be found in Table 3.4 while those samples tested without a scrim layer are contained in Table 3.5. Graphical representations of these results are illustrated in Figures 3.21 and 3.22. Figure 3.23 allows side-by-side comparison of the shear strength of each pretreatment method for those samples with and without the scrim layer.

When examining the data in Table 3.4, it is clear that prep method DDS was the weakest out of all of those tested. Recall that DDS was the sample fabricated using DelDOT's preferred paint primer as an adhesion promoter. It was expected that this group of samples would have the worst performance simply because the primer was intended for paint. Both the adhesion properties and the final surface finish of the primer were not designed to enhance bonding or carry any shear loads. Additionally, the high standard deviation is illustrative of the variation in performance of the samples.

Aside from that, it can be seen that there is no real statistical difference between the remainder of the test sample groups although the samples fabricated using prep method Q demonstrated the highest average shear strength. These results

were very encouraging because McKnight demonstrated that an oven dry enhanced the performance of silane in his test cases. However, in this study, there was no apparent benefit to a high temperature drying of the primer. This was a significant development because it greatly simplifies the field implementation by minimizing the labor and complexity of installation. Through this simplification, it immediately made the rehabilitation scheme more attractive to a potential owner. Furthermore, it might be expected that prep method Q would outperform all other prep methods employing a silane primer because of the additional compounds present that were used to enhance the performance of the silane.

Table 3.4 Experimental results from shear tests on samples with scrim layer.

Preparation Method	Preparation Method Description	Shear Stress (psi)	Standard Deviation (psi)
AS	Baseline	2135	394
BS	Baseline w/ air dried silane	2078	164
CS	Baseline w/ 112°F oven dried silane	2083	182
DS	Baseline w/ 200°F oven dried silane	2150	129
DDS	DelDOT paint primer	1487	329
QS	Q-6106 primer w/ air dry	2277	186

Table 3.5 Experimental results from shear tests on samples without a scrim layer.

Preparation Method	Preparation Method Description	Shear Stress (psi)	Standard Deviation (psi)
A	Baseline	1546	210
B	Baseline w/ air dried silane	2199	490
C	Baseline w/ 112°F oven dried silane	2038	339
D	Baseline w/ 200°F oven dried silane	2377	128

AS	BS	CS	DS	DDS	QS
Baseline w/ scrim	"AS" w/ air dried silane primer	"AS" w/ 112°F oven dried silane primer	"AS" w/ 200°F oven dried silane primer	"AS" w/ DelDOT paint primer	"AS" w/ Q1-6106 air dried primer

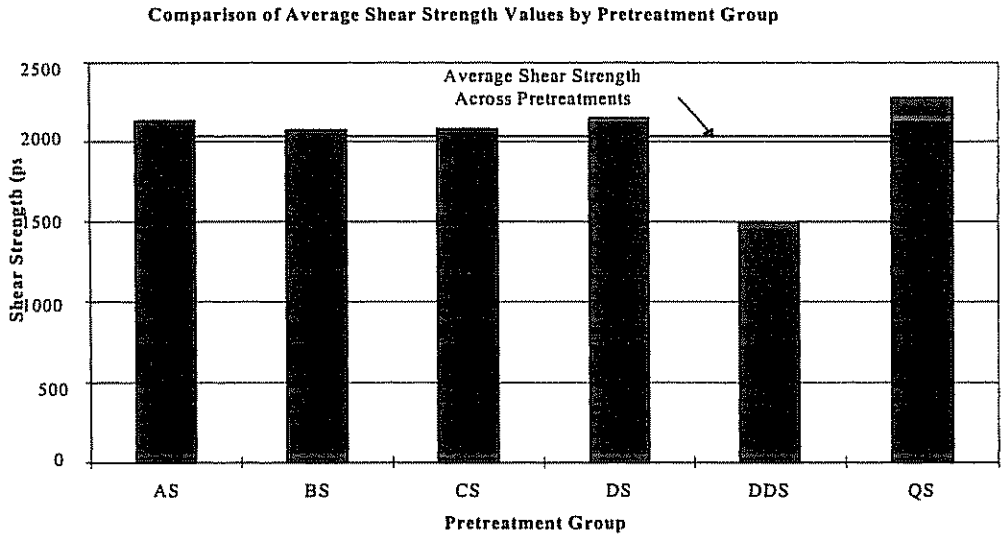

Figure 3.21 Average shear strength of samples with scrim layer across pretreatment group.

A	B	C	D
Baseline pretreatment	"A" w/ air dried silane primer	"A" w/ 112°F oven dried silane primer	"A" w/ 200°F oven dried silane primer
A	**B**	**C**	**D**
Baseline pretreatment	"A" w/ air dried silane primer	"A" w/ 112°F oven dried silane primer	"A" w/ 200°F oven dried silane primer

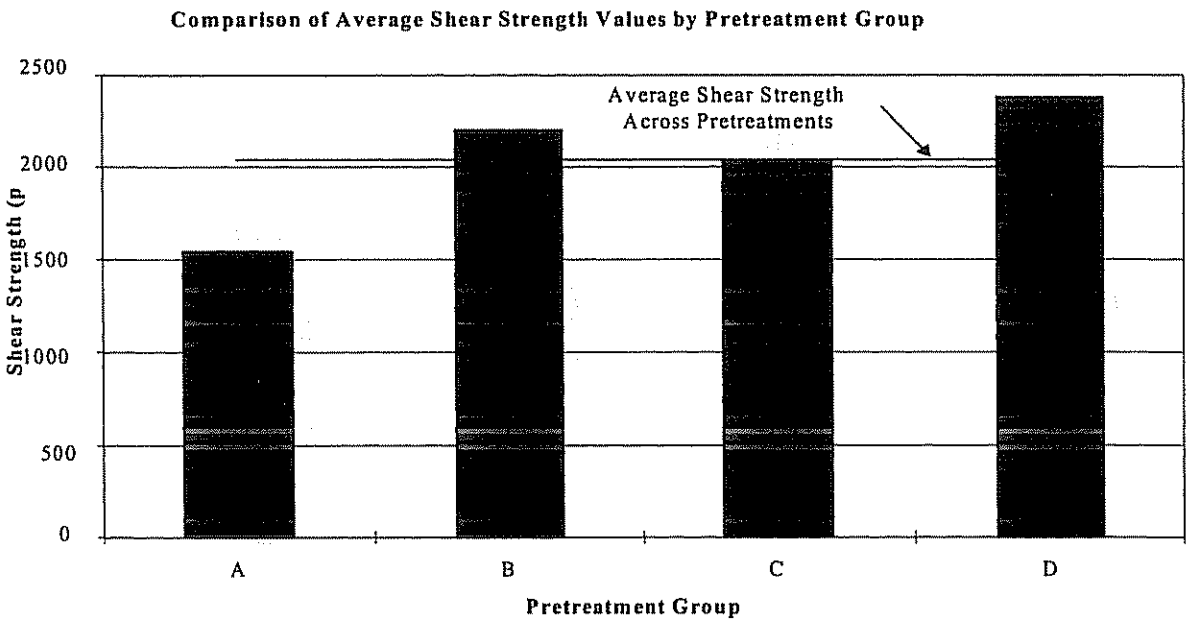

Figure 3.22 Average shear strength of samples without scrim layer across pretreatment group.

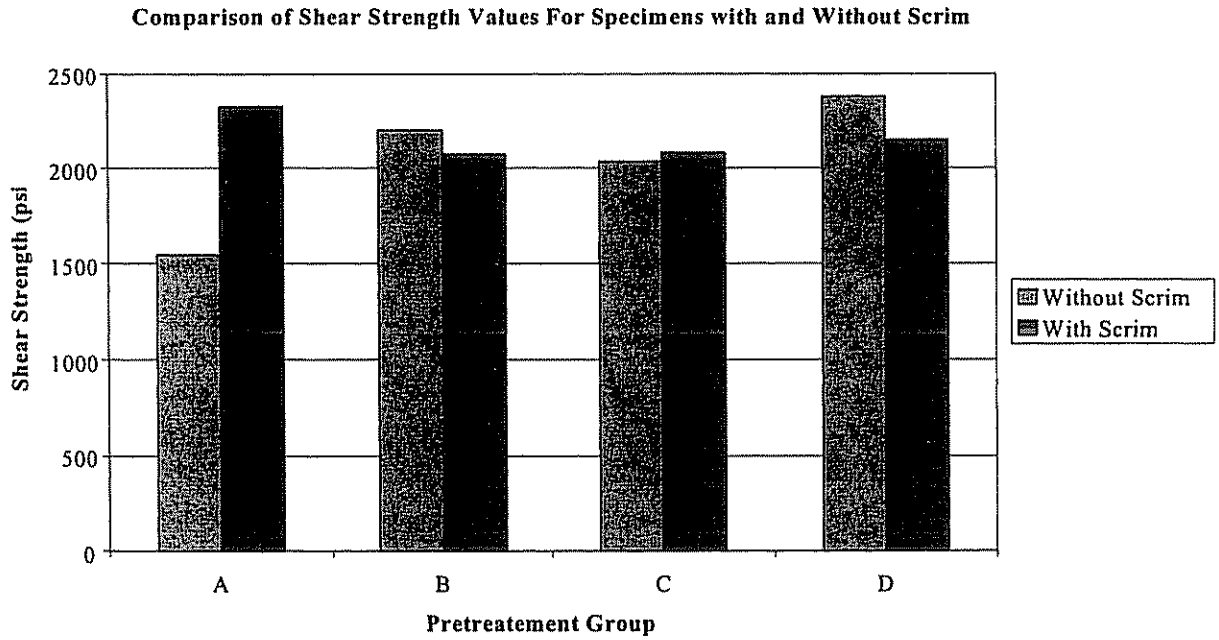

Figure 3.23 Comparison of shear strengths by pretreatment group between samples w and w/o scrim layer.

It is important to note that the strength of the samples tested using the baseline surface preparation, prep method A, could be considered to be artificially high. Certainly the test results indicate a specific level of performance, however it does not address other factors surrounding that specific group. For example, a number of test samples were never actually tested because the bonds failed during the machining process. It is important to note that this did not occur with any of the other samples. Additionally, there were a number of test samples that failed when secured in the test grips before loading had commenced.

When considering all of the samples tested without the scrim layer, three out of six group A samples failed in the grips while only one out of 29 samples failed from groups B, C, and D combined. These factors could be classified as durability issues that will be discussed in greater detail in Chapter 4. Additionally, it suggested that the primer increased the bond durability of the other samples, which was the intent of using primers in the first place.

When comparing the performance of the samples with and without the scrim layers, it can be seen in Figure 3.23 that there was effectively no decrease in the shear strength of the bond. In fact, the samples with the scrim layer had greater shear capacity than those without for prep methods A and C. The large difference in shear strengths for prep method A can be traced to the unreliable behavior of the samples that had been exhibited by the prep method.

Furthermore, those were the first samples tested over the course of the study and the fabrication technique had not yet been perfected which may have contributed to the comparatively low strengths. However the difference between the two classes of prep method Q can be considered to be statistically nonexistent.

Next, the failure surfaces were inspected and a percentage was assigned to each failure locus present through a visual approximation of the amount of surface area affected by each mode. Table 3.6 lists the percentage of failure through the individual modes for each prep method. The values in the table represent the failure loci as established earlier in this section and the letters "ST" represent a scrim tear. Note that the scrim tearing is not considered to be a mode of failure; rather it is a byproduct of an adhesive to scrim failure worth identifying. When studying the table, note that the sum of all of the percentages of failure loci totals to 100% and that "ST" is not included in that determination.

Inspection of the failure modes can be broken down into two major classes within the prep methods, those samples with a scrim layer and those without. Similarly, those major groups also have two subgroups, those fabricated with a primer and those without. Recall that it was established in Chapter 2 that a scrim layer was an effective means to prevent galvanic corrosion effects. Therefore the behavior of the lap shear samples with a scrim layer was of particular interest. Keeping that in mind, the overall results were very favorable.

All samples that had both a silane primer and a scrim layer, those from prep methods BS, CS, and DS, experienced 100% of their failures cohesively in the scrim layer. Furthermore, the last sample set that used a primer with a scrim, samples from prep method QS, experienced nearly 70% of their failures cohesively in the scrim. Recall that cohesive failures were determined to be favorable modes of failure.

Conversely, those fabricated with a scrim but without a silane primer, prep methods AS and DDS, had significant failures in modes deemed undesirable. Nearly 50% of those samples prepared using method AS failed adhesively to the steel. Furthermore, the samples using the DelDOT paint primer as an adhesion promoter experienced nearly 100% of their failures directly related to the primer; either adhesively to the steel or cohesively within the primer.

Similar results were also experienced by those samples that were fabricated without a scrim; recall they fell under the second major classification. Samples using a silane primer applied by methods B, C, and D respectively experienced 86.7%, 68.0%, and 95%, of their failures in favorable modes of either cohesively in the primer or cohesively in the composite. Once again, the samples prepared by method A without a primer had the least favorable failure modes with 72.5% of their failures coming adhesively to the steel.

These results should prove to be significant with respect to the durability aspect of bond performance. Regardless of failure locus, as long as the bond exceeds the minimum required shear strength, the preparation method can be considered acceptable. However, the mere strength of a joint does not necessarily mean it will perform favorably under service conditions. This area of bond performance will be explored further in Chapter 4.

When the shear strengths were plotted vs. bond line thickness, it was illustrated across all samples that the thickness of the bond had no apparent effect on strength. However, this can be misleading because it is well known that very thin and very thick bond lines typically result in a decrease in shear capacity. It should be more appropriately stated that the strength was not affected by the thickness of the bond lines of the samples in this study.

Figure 3.24 does an excellent job exhibiting this observation. It shows that the strengths seen by a majority of individual samples are tightly banded independent of bond thickness. Furthermore, the individual sample with the highest overall shear strength had the second thickest bond line. It is noteworthy to point out that all samples had similar bond thickness envelopes with the exception of samples in prep method DD. This was attributable to the additional thickness of the paint primer layer relative to the thickness of a silane primer layer.

Table 3.6 Failure loci of ASTM D 3165 lap shear samples.

	Failure Loci as Established in Section 3.6							
Prep	**(1)**	**(2)**	**(3)**	**(4)**	**(5)**	**(6)**	**(7)**	**ST**
AS	46.2 %	---	---	---	53.8 %	---	---	12.5 %
BS	---	---	---	---	100%	---	---	---
CS	---	---	---	---	100%	---	---	---
DS	---	---	---	---	100%	---	---	13.1 %
DDS	---	---	---	---	2.5%	22.5 %	75%	---
QS	30.6 %	---	---	---	69.4 %	---	---	---
A	72.5 %	---	---	27.5 %	---	---	---	---
B	12.5 %	0.8%	67.1 %	19.6 %	---	---	---	---
C	32.0 %	---	62.5 %	5.5%	---	---	---	---
D	5.0%	---	79.4 %	15.6 %	---	---	---	---

LEGEND

Sample Preparation Method		**Failure Locus**	
AS	Baseline	**(1)**	Adhesive to steel
BS	"AS" w/ air dried silane	**(2)**	Adhesive to composite
CS	"AS" w/ 112°F oven dried silane	**(3)**	Cohesive in adhesive
DS	"AS" w/ 200°F oven dried silane	**(4)**	Cohesive in composite
DDS	DelDOT paint primer	**(5)**	Cohesive in scrim
QS	Q-6106 primer w/ air dry	**(6)**	Cohesive in DelDOT paint primer
A	Baseline	**(7)**	Paint primer adhesive to steel
B	"A" w/ air dried silane	**ST**	Scrim tear
C	"A" w/ 112°F oven dried silane		
D	"A" w/ 200°F oven dried silane		

It can be seen that the samples without the scrim are shown to have bond thickness less than approximately 0.0175 in and those with the scrim exhibit a thickness greater than 0.0175 in. This was to be expected for two reasons. First, the scrim has a thickness of 0.004 in therefore the addition of the scrim would automatically increase the bond line thickness by this amount. Second, the samples without the scrim were fabricated with a layer of adhesive applied only on the steel surface while those with a scrim had a layer of adhesive applied to both adherends. This was done to ensure that the scrim was effectively wet out with the adhesive to guarantee a complete bond as well as complete electrical isolation for galvanic corrosion protection as described in Chapter 2. Therefore the obvious clustering of samples with and without a scrim with respect to bond line thickness was to be expected.

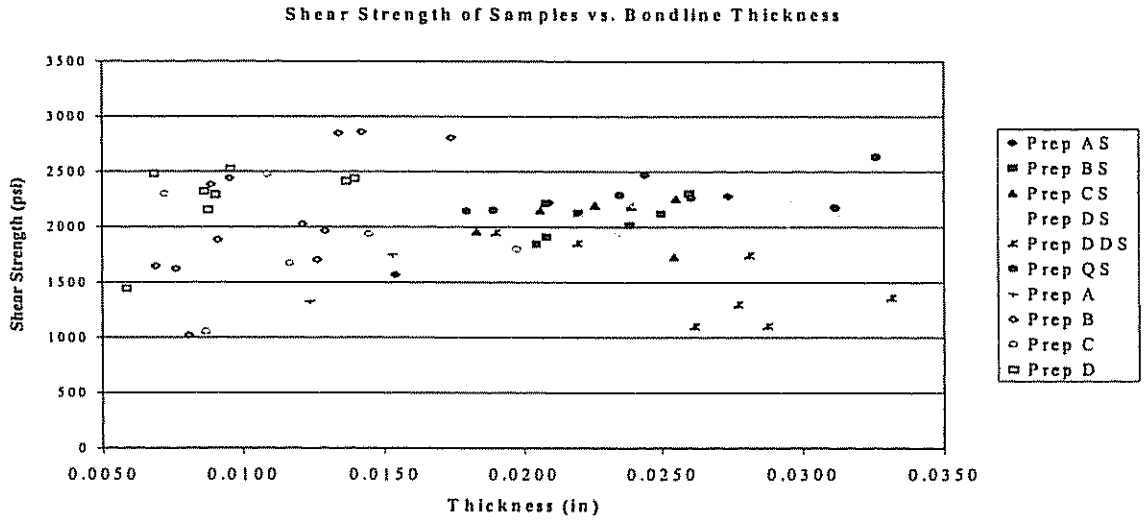

Figure 3.24 Comparison of shear strength vs. bond line thickness across all tested samples.

AS	BS	CS	DS	DDS
Baseline pretreatment w/ scrim	"AS" w/ air dried silane primer	"AS" w/ 112°F oven dried silane primer	"AS" w/ 200°F oven dried silane primer	"AS" w/ DelDOT paint primer
QS	**A**	**B**	**C**	**D**
"AS" w/ Q1-6106 air dried primer	Baseline pretreatment	"A" w/ air dried silane primer	"A" w/ 112°F oven dried silane primer	"A" w/ 200°F oven dried silane primer

3.8 Conclusions

The aim of this chapter was to establish a recommended bonding scheme for the rehabilitation of steel bridge girders through the application of advanced composite materials. First, literature was reviewed to assist in establishing screening criteria and recommendations for adhesives, primers, and surface preparation methods. Tables with these criteria can be found in Sections 3.2 and 3.3. A wide range of adhesives and primers were considered eventually resulting in the selection of three adhesives and three primers for evaluation. Additionally, baseline surface preparation criteria and sample fabrication guidelines were created to ensure consistency across primer and adhesive combinations. A total of eight different bonding combinations were identified with six eventually being tested using ASTM D 3165 Standard Test Method for determining shear strength properties of adhesives. Recall that Edberg and Ammar had previously established minimum acceptable shear strength of 600 psi for adhesively bonding composite materials to steel bridge girders and that was determined to be the target strength of this study. All successful candidates were carried over to the durability phase (Chapter 4) of testing to finalize recommended bonding combinations for a full-scale rehabilitation.

The lap shear testing revealed that all six of the tested adhesive/ primer combinations exceeded the minimum acceptable strength of 600 psi. In fact, five out of the six exceeded 2000 psi in shear. The only preparation method not to achieve this level of performance was the combination of the DelDOT paint primer and the Ciba-Geigy AV8113 adhesive (DDS), which averaged just less than 1500 psi. However, there was some suspicion cast upon the reliability of the results of the baseline preparation methods (AS and A) due to the disproportionately large number of samples that either failed during machining or simply when they were tightened in the test grips. Despite the poor performance of the DelDOT primer and the unreliable nature of the baseline combination, all prep methods were graduated to the durability testing of Chapter 4. Therefore the final selection was made only after the combined performance of the samples in both strength and durability had been determined.

In addition to evaluating the strength of the various bonding combinations, four of the six prep methods were tested to determine the effect the presence of the fiberglass scrim had on bond strength. A group of samples were fabricated

without the fiberglass scrim for prep methods A, B, C, and D. After testing these samples it was determined that all of the groups had statistically equivalent performance because the results fell within three standard deviations of each other across pretreatments groups. Again, pretreatment A, the baseline pretreatment, posed concerns because of the comparatively large standard deviations exhibited by the sample sets. Additionally, it was graphically demonstrated that the samples fabricated with a primer performed better than those without. It was also determined that it was reasonable to assume that the two untested combinations would perform similarly.

Furthermore, the failure loci of the samples were considered when evaluating the strength of the bond. Either a cohesive failure in the composite, in the adhesive, or in the scrim layer was considered to be the most desirable mode of failure. It was demonstrated that a simple silane primer was effective in forcing the failure into one of these three "desirable" modes. A significant majority of all samples with silane primer and a scrim failed cohesively in the scrim. Similarly, those samples with a silane primer yet without a scrim layer failed predominately cohesively in the adhesive with additional "desirable" failures cohesively in the composite.

Finally, bond thickness was considered with respect to shear strength. After testing had been completed on all samples, maximum shear stress values were plotted vs. bond line thickness in an attempt to draw a correlation between the two data sets. It was clearly demonstrated over the range of thickness of the samples in this study, that bond line thickness had no bearing on shear strength.

It was demonstrated that the corrosion barrier developed in Chapter 2 provided, at a minimum, equivalent strength and, in most cases, greater strength than samples without the scrim layer. Therefore it can be concluded that the addition of a fiberglass scrim for corrosion protection is a viable option for rehabilitation from a pure strength standpoint as well.

Based on the results presented in this chapter, a preferred pretreatment and preparation method can be recommended. First, the adequate preparation of the surface of the adherends is essential. This includes cleaning of any steel surfaces to near-white metal and abrasion of the composite surface along with a solvent wipe to remove any residual particulates from the cleaning process.

Next, a primer consisting of silane mixed in de-ionized water applied to the surface of the steel and allowed to air dry proved to be effective and most easily implemented in the field. The silane based Dow Q1-6106 performed well and can be considered to be an acceptable alterative to silane alone.

Third, Ciba-Geigy AV8113 adhesive applied to both bonding surfaces performed best with respect to wetting out the recommended scrim layer despite some drawbacks with respect to workability. SikaDur 30 adhesive exhibited adequate strength as well, however the aggregate in the paste and high viscosity requires

additional diligence over the Ciba-Geigy adhesive with respect to wetting out the scrim.

Finally, a 120-fiberglass scrim layer was demonstrated in Chapters 2 and 3 as an effective protection against galvanic corrosion without compromising bond strength therefore it is recommended to implement this feature as well. To simplify field installation and to introduce a higher level of quality control, it is strongly suggested to introduce the scrim layer during the manufacturing of the composite. However, this is not necessary and a field installation of the scrim between the adherends was demonstrated to work effectively.

Chapter 4: DURABILITY INVESTIGATION

4.1 Introduction

Recall that a variety of primer and adhesive combinations were tested using ASTM D 3165 lap shear specimens with the results discussed in Chapter 3. Based on the results of those tests, specific adhesive/ primer combinations could be recommended for field implementation. However, these preliminary recommendations are from a strength standpoint, which addresses only one component of performance. The other component, durability, is necessary because a strong joint is essentially worthless if it is unable to endure the conditions under which it will be exposed.

A durability investigation was conducted as a continuation of the evaluation of the performance of the adhesive bond to steel. It was determined that the Mode I fracture behavior of bonded joints in various environments would accomplish this. ASTM standard wedge specimens (ASTM D 3762-79) were fabricated and tested for durability for each of the leading adhesive/ pretreatment combinations investigated in Chapter 3. It is significant to note that these samples behave in a similar fashion to those of the ASTM standard double cantilever beam (DCB) specimen of ASTM specification D 5528.

The main difference between the samples is the method in which the load is imparted to the adherends. A DCB specimen is typically loaded dynamically using a universal testing machine such as an Instron where the ends of the specimen are forced open to propagate a crack between the adherends. Wedge specimens are loaded statically through the insertion of a mechanical wedge at the bond interface. Examples of the two specimen types are illustrated in Figure 4-1.

In either case, strain energy is imparted into the system through the deflection of the adherends, or cantilever beams, due to the crack opening displacement (COD). In most cases, this strain energy will cause a crack to develop in the adhesive layer, or bond line, and arrest at a specific length. In the case of the wedge specimens, the COD is constant because the adherends are not further separated once the wedge has been inserted. This is particularly advantageous because for constant COD, shorter cracks indicate tougher bonds (McKnight, 38). In addition, the crack tip/ bond line is continuously subjected to the environment and is effective in assessing durability. Additional details regarding fracture mechanics and how they are applied with respect to adhesives and polymers can be found in texts by Anderson, Broek, and numerous titles from Kinloch.

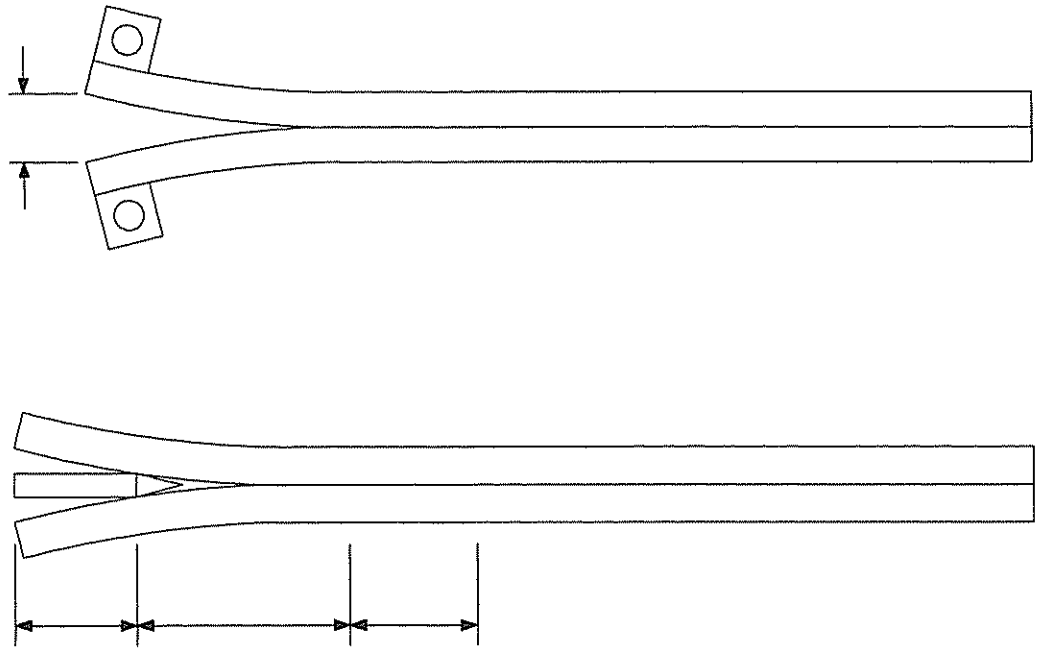

Figure 4.1 Examples of ASTM standard double cantilever beam specimen (top) and ASTM standard wedge specimen.

These samples were exposed to both a hot/ wet environment and a freeze/ thaw environment. The hot/ wet environment consisted of temperatures at approximately 122°F and 85% relative humidity while the freeze/ thaw environment cycled between 0°F and 40°F. In accordance with the specification, crack extensions were measured and recorded over time. These values for crack growth were later converted to values for opening mode interlaminar fracture toughness, G_{IC}, for the adhesives to allow comparison between the sample types.

4.2 Adhesive Selection

Recall the following criteria discussed in Chapter 3 to select adhesives for evaluation in this work:

- ASTM D-1002 Shear Strength
- ASTM D-638 Tensile Strength and Modulus
- Pot Life
- Workability
- Glass Transition Temperature (T_g)
- Room Temperature Cure

- Availability
- Shear Elongation

These criteria consider the design, ease of erection, cost, and performance of retrofit applications. Long-term durability was the final criteria required to make a final installation recommendation and will be determined over the course of this chapter.

The ASTM strength characteristics were significant for obvious reasons; it is desirable to have adequate performance of the rehabilitation. Specifically, Edberg and Ammar previously established minimum shear strength of 600 psi through finite element models for adhesively bonding composite materials to steel bridge girders (this stress level would be specific to each individual bridge design). There was not a specified minimum tensile strength established, rather this information was used to help differentiate performance of the studied adhesives. Shear modulus and elongation to failure were properties that were regarded to be of secondary concern. Steel rehabilitation offers significant shear areas over relatively thin bond lines so load transfer will be efficient for the typical range of adhesives. However at stress concentrations (e.g. splices and terminations) it is desirable to have adhesives with high elongation to failure as this class of materials will be tough and more resistant to fatigue crack growth in the adhesive.

Pot life is significant in this application because it controls the overall size of a practical rehabilitation. It is imperative that all components are in place before the adhesive cures. A longer pot life naturally provides more working time and therefore allows a larger rehabilitation to be performed. A minimum of 30-40 minutes is recommended for a team to complete a 20-30 foot installation. Workability ties directly into pot life with respect to its significance. If an adhesive proves difficult to work with it follows that a specific installation would take longer to be completed than an identical repair with a more "user friendly" adhesive. It follows that the longer it takes to perform a repair of specified area or length, the more significant the pot life of the adhesive becomes. Therefore it is desirable to have and adhesive that is easy to work with.

The glass transition temperature, T_g, is another property of the adhesive that is of significance. The rehabilitation is of no use if the adhesive softens and loses stiffness and strength above T_g. Maximum temperatures for civil engineering applications are on the order of 130°F and that was selected as our minimum value for T_g. Adhesives that cure at room temperature and provide values of T_g greater than our service temperature are highly desirable. Due to the physical nature of the installation, it is greatly simplified if an adhesive can fully cure without the aid of external heating devices. The use of heating blankets and other means of providing adequate heat to guarantee proper curing of concrete are industry practice, however, the complexity and cost of the rehabilitation is reduced through an adhesive with a room temperature cure.

Finally, the availability of the adhesive is something that needs to be taken into consideration. It serves no purpose to recommend a rehabilitation that requires a component that is not readily or widely available. Therefore the adhesive selected should be one that is commercially available from a number of suppliers and in a variety of geographic locations to facilitate implementation of this repair scheme.

Based on these criteria, three adhesives were selected for consideration and Table 4.1 illustrates how their manufacturer data compares. Ciba-Geigy AV8113 epoxy was specifically recommended for this application (Rajagopolan, Immordino, and Gillespie 229) therefore it was considered to be the preferred adhesive. Similarly, Mertz and Gillespie (8) and Gillespie, et al. (234) used it in their work in steel rehabilitation, which laid the foundation for this study. Another epoxy, SikaDur 30, was considered because it was part of a proprietary composite rehabilitation system designed by Sika. Finally, Plexus MA 425 was investigated because of other benefits inherent to a methacrylate adhesive (i.e. high elongation and toughness). All three of the adhesives tested were two-part adhesives that were readily available and currently used in various industries.

The Ciba-Geigy AV8113 adhesive components were available in quarts or in five-gallon units and mixed in a 1:1 ratio by mass. For industrial applications, meter-mixing equipment can be used to automate the mixing phase. The resin was a stiff, ochre colored paste while its accompanying hardener was an ice blue colored material. When mixed, the epoxy was a characteristic green color and was slightly stiffer than the hardener by itself. It spread fairly readily, but was very tacky and sometimes difficult to work with. Conversely, the SikaDur 30 displayed very good workability. It consisted of a 3:1 ratio and was sold in 3/4-gallon kits that consisted of two pre-measured containers to ensure the proper mix. Both parts of the adhesive were gray; one (the larger part) was a very light gray and the other (the smaller component) was significantly darker. The adhesive appeared to have some small aggregate, possibly sand, as a component that made the material grainy. It had the consistency and workability of a cement paste or grout. Considering that the adhesive was originally part of Sika's CarbuDur system used in strengthening concrete with composites, it was not surprising that the adhesive had these physical properties.

Table 4.1 Manufacturer data listing the selection criteria of the three screened adhesives.

Criteria	Ciba-Geigy AV8113	SikaDur 30	Plexus MA425
ASTM D-1002 Shear Strength	2660 psi 18 MPa	3600 psi 24.8 Mpa	1500-1800 psi 10.3-12.4 MPa
ASTM D-638 Tensile Strength	2280 psi 15.7 MPa	3600 psi 24.8 Mpa	2000-2500 psi 13.8-17.2 MPa
ASTM D-638 Tensile Modulus	15.6 ksi 108 MPa	650 ksi 4482 MPA	40-50 ksi 276-345 MPa
Pot Life	60 minutes	70 minutes	30-35 minutes
Glass Transition Temperature (T_g)	194°F 90°C	130°F 55°C	218°F 103°C
Room Temperature Cure Time	16 hours	24 hours	80-90 minutes (75% strength)
Tensile Elongation	25%	1%	120%-140%
Cost per 5 gal.	Resin: $350 Hardener: $515	$563 for complete kits	Resin: $436 Hardener: $585
Availability	Yes	Yes	Yes

The Plexus MA 425 adhesive required a 10:1 ratio of adhesive to activator and was sold in 380 ml pre-measured cartridges, in five-gallon containers of each component, and even in 50-gallon drums for larger applications. The 380 ml cartridge was rather innovative. It had the appearance of a caulking tube that had a second smaller concentric, or co-axial, tube in the center. The creamy white colored resin filled large outer tube while the ice blue colored hardener was contained in the narrow middle tube. A long mixing nozzle with interior baffles to combine the two components was attached to one end of the cartridge. The whole assembly was then placed in a proprietary caulk gun equipped with two plungers. When the trigger was squeezed, both plungers moved simultaneously forcing the components into the nozzle in the correct proportion. After mixing, the adhesive was bright blue in color, less viscous than both the Ciba Geigy and Sika adhesives, and had excellent workability.

4.3 Primer Selection

Similar to the adhesive selection, the primer selection process for the samples was conducted in Chapter 3 as well. Recall that a great deal of literature is available on the topic of surface preparation for adhesive bonding. The literature

survey concluded that some type of primer must be used to create a bond that is both strong and has environmental durability. In selecting primers for this work, it was necessary to select primers that were compatible with the types of adhesives being used on steel. Specifically, a primer designed for use with epoxies was required by both the Ciba-Geigy and Sika adhesives while Plexus manufactured a primer specifically for use with its MA425. Additional criteria included methods of application, drying requirements, present applications, environmental compatibility, as well as cost and availability. Primers from a number of companies (3M, Dow, Essex, Plexus) and a number of applications (industrial, automotive, structural) were considered, however, the following three were best suited to the application. Table 4.2 lists the manufacturer data for the selected primers with respect to the aforementioned criteria.

McKnight (284-287) Rajagopalan (226-229), and Kinloch (Structural 269-312) have all demonstrated the benefits of using a silane-based primer. Therefore silane Z-6040 for epoxies from Dow Corning was selected as the preferred primer. The priming solution was made by mixing 1% by weight of the silane with de-ionized water that had a pH in the range 4.5-5.0 and stirring for a minimum of 30 minutes.

The second primer used in this research was a silane-based chemical recommended by Dow called Q1-6106. This compound contained a melamine based hexamethoxymethylmelamine resin. Melamines are sometimes referred to as urea-formaldehydes and primarily serve as crosslinking catalysts (Sax 737). In other words, the melamine-based chemical was in the primer as a transport mechanism to ensure that the silane was in the proper "location" to carry out its function. This chemical was clear in color and had the consistency of Karo syrup. The Q1-6106 was mixed 5% by weight with methanol and stirred for a minimum of 30 minutes to form the primer.

Plexus PC 120 primer was recommended by the manufacturer for use with its MA 425 adhesive. Again, this Plexus product offered some user-friendly features. First, the primer was available in a ready to use state; there was no mixing involved, just open the container and apply. More significantly, however, was the fact the primer was red in color. This pigment was very useful in showing what surface area had been primed and what areas had not been coated to ensure complete coverage.

In addition to the traditional "adhesive primers," a paint primer was also evaluated. It was considered because every attempt to customize the installation process to current DelDOT procedures would facilitate future implementation. DelDOT paint specifications 605616, 605619, and 605620 call for the use of a micaceous iron oxide based moisture-cured urethane paint system. Approved primers for this system are Wasser MC-Miozinc and Xymax Bridge Zinc. Since both were approved equals, only the Wasser MC-Miozinc was used.

Table 4.2 Manufacturer data listing the selection criteria of the three screened primers.

Criteria/ Properties	Z-6040 Silane	Q1-6106 Adhesion Promoter	Plexus PC120 Primer
Appearance	White to slightly yellow	Clear	Red
Physical Form	Low-viscosity liquid	Slightly viscous fluid	Low-viscosity liquid
Viscosity	3	850	2
Specific Gravity at 77°F	1.07	1.19	0.81
Refractive Index	1.428	1.510	N/A
Flash Point, closed cup (°F)	>213	120 (minimum)	53
Type	Glycidoxy (epoxy) functional methoxy silane	100% active coupling agent	Proprietary chemical primer and conditioner
Primary Uses	Coupling agent to improve adhesion of organic resins to inorganic surfaces	Coupling of reinforcing agents to plastics; adhesion promoter for plastics and metals	Coupling agent to be used in conjunction with Plexus MA420 adhesive
Mixing Agents	1% by mass with de-ionized water	5% by mass with methanol	None
Mixing Procedure	Min. 30 minutes	Min. 30 minutes	None
Recommended Drying Procedure	15 minute air dry	15 minute air dry	Air Dry
Cost for five gallon pail	$544	$718	$390

4.4 Sample Preparation and Bonding Schemes

Minimum material preparation procedures were established in Chapter 3 and were applied to the wedge specimen samples of this chapter as well. Prior to

bonding, all adherends were prepared using the same baseline bonding scheme. This particular combination consisted of the following:

- Bead blast of the steel bonding surface to near-white metal to remove any corrosion, oils, or mill byproducts
- Bead blast of the composite bonding surface to remove the smooth finish per the guidelines set forth in Section 2.5.1.2
- Solvent wipe of both adherends to remove any residual particles from bead blasting process
- Apply Ciba-Geigy AV8113 adhesive and allow 24 hour room temperature cure

Variations of the baseline bonding scheme were then established to evaluate adhesive/ primer combinations. Each combination was given identifiers as follows:

A: Baseline

B: Baseline with Z-6040 primer coat and 15-minute air-dry

C: Baseline with Z-6040 primer coat and 15-minute air-dry with 30 minute oven drying at 112 °F

D: Baseline with Z-6040 primer coat and 15-minute air-dry with 30 minute oven drying at 200 °F

Q: Baseline with Q1-6106 primer coat and 15-minute air-dry

P: Baseline prep substituting Plexus MA 425 adhesive and PC 120 primer with 15-minute air-dry

DD: DelDot approved Wasser MC-Miozinc paint primer

Sika: Identical to prep method "B" with the substitution of SikaDur 30 adhesive for the Ciba-Geigy AV8113

Note that care must be taken when applying the primer coat to ensure only a thin layer has been applied. If the primer layer is too thick, cohesive failure within the primer may occur and limit shear strength. Following all 15-minute periods of air-drying, the steel plates were dried with forced air prior to bonding or prior to oven drying to ensure no unintentional build-up of primer.

4.5 Sample Fabrication

The procedure used to fabricate the ASTM D 3762 wedge specimen samples was nearly identical to that employed to assemble the ASTM D 3165 lap shear specimens of Chapter 3. Characteristics unique to the wedge specimens required variations to the fabrication process. Per the specification, an unbonded region at one end of each sample was required to facilitate the

introduction of the wedge as well as introduce an initial flaw in the bond. This unbonded region was created by using a 1 inch wide strip of Teflon tape. The tape was placed at one end of both the steel plate and each of the composite strips after the bonding surfaces of the adherends had been bead blasted and solvent wiped (Step 2, Section 3.5).

Additionally, it was necessary to match the stiffness of each adherend to facilitate determination of G_{1c}. Recall that the stiffness of a body is the product of its modulus of elasticity and moment of inertia, or EI. Since the modulus of elasticity, E, of each adherend was fixed, the only variable remaining was the moment of inertia, I. The adherends used in this study possessed a constant thickness; 0.125 in for the steel and 0.210 in for the composite. Based on the machining properties of each material, it was determined that it would be significantly easier to match I of the composite to that of the steel. The following derivation is offered for matching the material stiffness.

Start with the stiffness of each component:

$$E_s I_s = E_c I_c \qquad \text{Eq. 4-1}$$

where the subscripts s and c represent the properties of the steel and composite respectively. Substituting the moment of inertia of each material into Eq. 4-1 yields:

$$E_s\left(1/12 b_s h_s^3\right) = E_c\left(1/12 b_c h_c^3\right) \qquad \text{Eq. 4-2}$$

where b_i is the width and h_i is the thickness of each material.
Since an individual sample will be cut from a fabricated panel, it is safe to assume that the thickness of each sample will be constant and identical. The constants on either side of the equation cancel leaving:

$$E_s h_s^3 = E_c h_c^3 \qquad \text{Eq. 4-3}$$

Note that the stiffness of each component has been reduced to the product of its modulus of elasticity and its thickness cubed. Previously we determined it was more desirable to machine the composite as opposed to the steel; therefore, we should solve Eq. 4-3 for h_c. It follows that:

$$h_c = \sqrt[3]{\frac{E_s h_s^3}{E_c}} \qquad \text{Eq. 4-4}$$

Substituting known values yields:

$$h_c = \sqrt[3]{\frac{(29.0x10^6)(0.125)^3}{16.3x10^6}} = 0.1515\ in$$

This value of h_c=*0.1515 in* is the thickness to which the composite needs to be machined in order to match the stiffness between both materials. A surface grinder was used to remove material from the surface of the composite until the desired thickness was achieved.

The remaining steps in the fabrication process were performed as described in Section 3.5 including the application of the primers and adhesives. Similar to the lap shear samples, each panel yielded four (4) individual wedge samples that were cut out of the center of each strip of composite bonded to the steel. The samples had nominal dimensions of 6 inches in length, 1 in width, and with a 1 in unbonded region at one end of all samples. Additionally, note that all samples were fabricated with the 120-fiberglass scrim recommended in Chapter 2 as a galvanic corrosion inhibitor.

In addition to the fabrication of the actual samples, the wedges themselves required fabrication. Stock aluminum with 1/8 in nominal thickness and 1 in nominal width was cut to approximately 1 in lengths for each individual "wedge." Approximately 1/4 in on either side of one edge of each aluminum square was beveled to create the actual wedge. The individual dimensions varied from one wedge to the next, therefore, each was scored with a number and the respective dimensions were recorded. These dimensions were later used on when determining Mode I fracture toughness values for each individual sample.

4.6 Experimental Procedure

Two environments were selected to simulate the thermal loading that would be imparted on the joint under service conditions in an attempt to evaluate its durability. These environments were selected to simulate the thermal loading that would be imparted on the joint under service conditions. The first was a Hot/ Wet (H/W) environment in which the specimens were exposed to temperatures of 122°F (50°C) and 85% relative humidity. Specimens from each preparation type were stored in a high temperature/ high humidity chamber for the duration of this phase of testing.

Additional samples were conditioned in a Freeze/ Thaw (F/T) environment that simulated the cyclic freezing and thawing that routinely occurs during the winter months. The environmental chamber was programmed to a seven-hour cycle that consisted of four hours of freezing at 0°F (-18°C) and an ensuing three-hours of thawing at 40° (4°C). All F/T samples were immersed in de-ionized water during their exposure to ensure the samples completely were completely frozen. In addition to the thermal loads imparted by the F/T environment, a mechanical load was introduced as well. It is common knowledge that water

expands by 10% as it freezes. As the water in the joint froze, the ice forming at the crack tip would expand to impart a mechanical load along with the wedge previously inserted and further progress the crack.

The tests were initiated by gradually forcing an aluminum wedge between the two adherends using constant pressure. Initial crack lengths, a_0, due to the insertion of the wedge were recorded and then the respective samples were exposed to the individual environments. Subsequent crack lengths, a_i, were measured to establish a time history of the development of the crack.

Crack lengths for those specimens placed in the H/W environment were recorded at 15-minute intervals up to one hour and then at 30-minute intervals up to three hours of exposure. The frequent early intervals of measurements allowed the capture of the initial performance of the joint where most of the crack growth was expected to occur. Beyond that, measurements were taken at total elapsed times of 24 hours, 77 hours, 168 hours, and then periodically thereafter.

F/T crack lengths were recorded based on number of cycles as opposed to total elapsed time. This was done for two reasons; first, it would have been impossible to take recordings in the sample's frozen state. Second, it was desirable to measure crack growth in complete cycles to establish probable life expectancy of a rehabilitation based upon the number of cycles to failure. Crack length readings were taken at one, three, and four cycles (approximately one day) initially, and then at 17 cycles and then occasionally thereafter.

After crack growth data had been recorded, it was converted to a G_{IC} fracture toughness for each sample at each reading using equation Eq. 4-5

$$G_{Ic} = \frac{3Ed^2h^3}{16a_i^4} \qquad \text{Eq. 4-5}$$

where E is the modulus of elasticity of the adherend, d is the thickness of the wedge, h is the thickness of the adherend, and a_i is the crack length at any given time. It is significant to note that all variables remained constant for the duration of the exposure with the exception of crack length, a_i. Therefore, it is shown that fracture toughness is inversely proportional to the crack length raised to the fourth power.

Anderson states that a key assumption in "fracture mechanics is that fracture toughness is independent of the size and geometry of the cracked body" (16). Therefore, it is valid to assume that any slight geometry differences between samples due to variability in fabrication can be neglected. Furthermore, it follows that the results obtained in the laboratory are directly applicable to future field rehabilitations.

Resultant values for average fracture toughness were then plotted against time for the samples exposed to the two separate environments. The units of time

varied based on the environment; for H/W, time was in hours while it was recorded as cycles (7 hours per cycle) for the F/T environment.

4.7 Experimental Results

After all individual specimens had been tested, their respective G_{Ic} fracture toughess results were compiled by prep method and then averaged for comparison. Resultant values for average fracture toughness were then plotted against time for the samples exposed to the two separate environments. The units of time varied based on the environment; for H/W, time was in hours while it was recorded as cycles (7 hours per cycle) for the F/T environment. Graphical representations of the results for the samples conditioned in the H/W environment are illustrated in Figures 4.2 through 4.4. Similarly, the graphed F/T results are shown in Figures 4.5 through 4.7. In both cases, the first plot illustrates the initial behavior of the samples; up to 20 hours for the H/W samples and up to 20 cycles for the F/T samples. Similarly, the second chart shows the trends by the samples through an "early-mid range" of the exposure for each type; time up to 100 hours for the H/W samples and up to 100 cycles for the F/T samples. Finally, the last chart in each series depicts the full time history of each experiment in an attempt to show long-term behavior. Note that hot/ wet testing was carried out in stages due to the large number of individual samples (27 total). Because of this, the data points in long-term plot are not necessarily coincident for each prep method beyond the first 100 hours of exposure. However, this does not affect the results in any way.

First, consider the results of the hot/ wet environment as presented in Figure 4.2 covering the first 20 hours of sample exposure. It is clearly shown that there are two levels of initial fracture toughness among the samples tested. The first clustering contains the samples prepared with a silane Z-6040 primer and Ciba-Geigy AV8113 adhesive, prep methods B, C, and D while the second grouping included all remaining prep methods.

In the first group of samples, the method used for drying the silane primer is what distinguished one sample class from the next. Recall method B calls for a 15-minute air-drying of the primer while methods C and D employ drying at temperatures of 112°F and 200°F respectively. Note that the initial values range from approximately 1.275 to 1.55 in-lb/ in^2 and that all samples experience an initial energy dissipation that was significant. The samples prepared by methods B and D stabilized at approximately 1.000 in-lb/ in^2 immediately thereafter and stayed steady through the first 20 hours. Samples prepared using method C continued their gradual reduction in fracturetoughness through the first five hours and then stayed fairly steady through the first 20 hours as well, although some continued loss of fracture toughness was displayed.

Unlike the first group of results, there was no unifying characteristic that would allow a general description to the overall class of the samples. These samples included those made with prep methods A, Q, DD, and Sika. Recall that prep

method A was the baseline of surface abrasion and solvent and was the initial step used for all other sample fabrication. Prep method Q substituted Dow primer Q1-6106 for the silane primer but still used the Ciba-Geigy AV8113 adhesive. "DD" was the designation for the sample category that used a DelDOT paint primer as its primer while the samples prepared using method "Sika" were similar to method A with SikaDur 30 adhesive substituted for the Ciba-Geigy AV8113 adhesive.

A	B	C	D
Baseline pretreatment w/ scrim and AV8113	Baseline w/ air dried silane Z-6040 primer	Baseline w/ 112°F oven dried silane Z-6040 primer	Baseline w/ 200°F oven dried silane Z-6040 primer

DD	Q	Sika
Baseline w/ DelDOT paint primer	Baseline w/ Q1-6106 air dried primer	Baseline with SikaDur 30 adhesive in place of AV8113

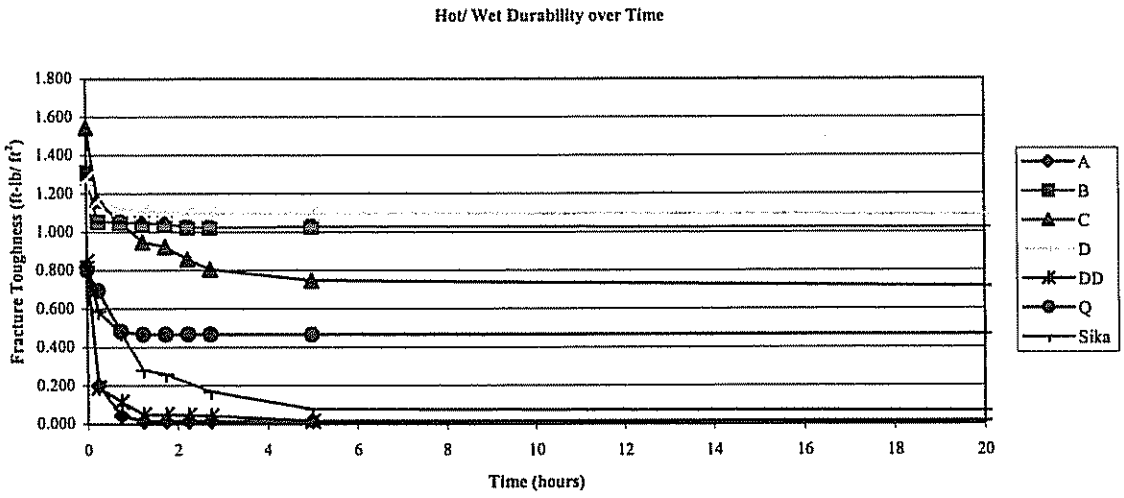

Figure 4.2 Durability over the first 20 hours of exposure for samples in an environment of 122°F and 85% RH.

A	B	C	D
Baseline pretreatment w/ scrim and AV8113	Baseline w/ air dried silane Z-6040 primer	Baseline w/ 112°F oven dried silane Z-6040 primer	Baseline w/ 200°F oven dried silane Z-6040 primer

DD	Q	Sika
Baseline w/ DelDOT paint primer	Baseline w/ Q1-6106 air dried primer	Baseline with SikaDur 30 adhesive in place of AV8113

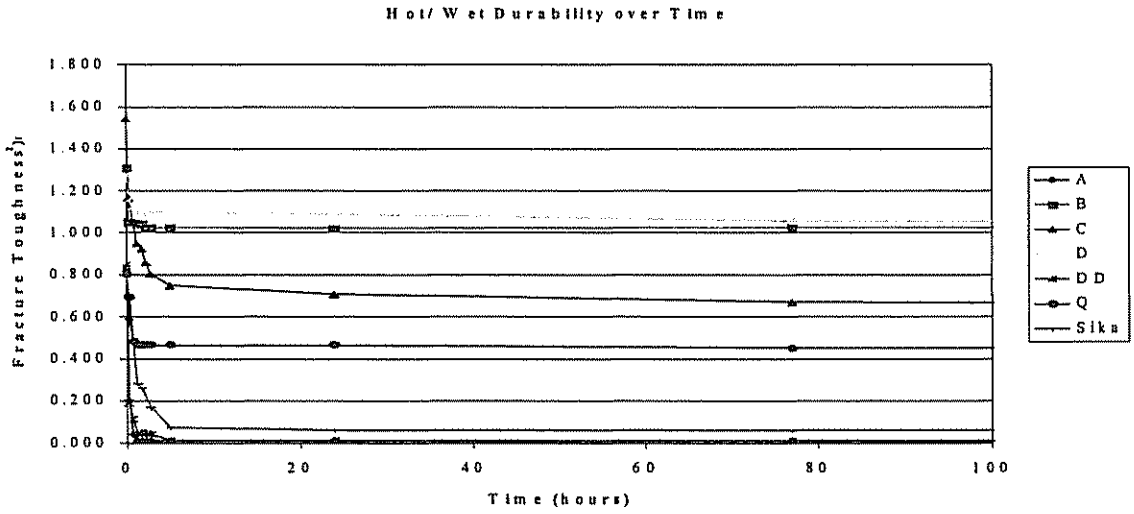

Figure 4.3 Durability over the first 100 hours of exposure for samples in an environment of 122°F and 85% RH.

A	B	C	D
Baseline pretreatment w/ scrim and AV8113	Baseline w/ air dried silane Z-6040 primer	Baseline w/ 112°F oven dried silane Z-6040 primer	Baseline w/ 200°F oven dried silane Z-6040 primer

DD	Q	Sika
Baseline w/ DelDOT paint primer	Baseline w/ Q1-6106 air dried primer	Baseline with SikaDur 30 adhesive in place of AV8113

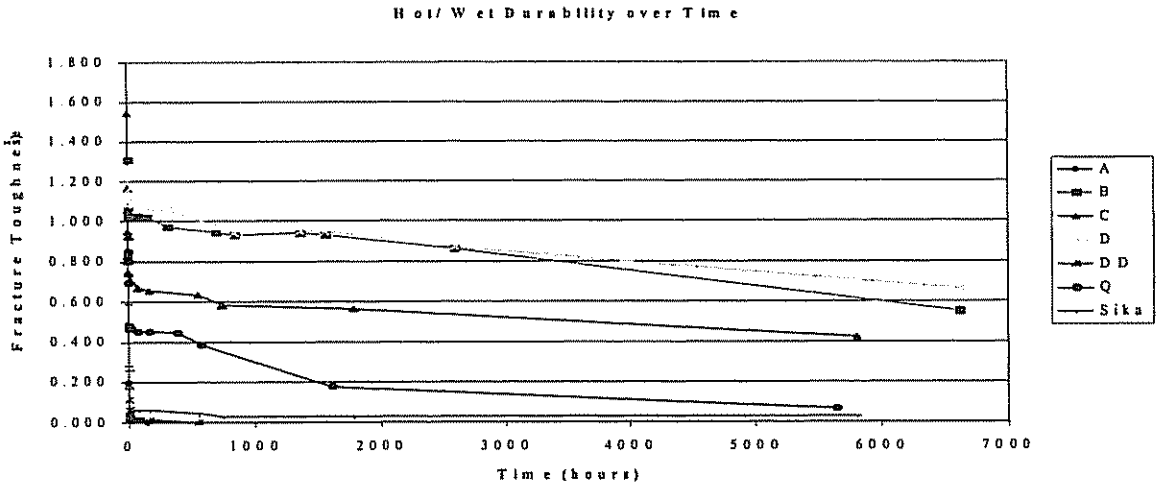

Figure 4.4 Durability over the full duration of exposure for samples in an environment of 122°F and 85% RH.

A	B	C	D
Baseline pretreatment w/ scrim and AV8113	Baseline w/ air dried silane Z-6040 primer	Baseline w/ 112°F oven dried silane Z-6040 primer	Baseline w/ 200°F oven dried silane Z-6040 primer

DD	Q	Sika
Baseline w/ DelDOT paint primer	Baseline w/ Q1-6106 air dried primer	Baseline with SikaDur 30 adhesive in place of AV8113

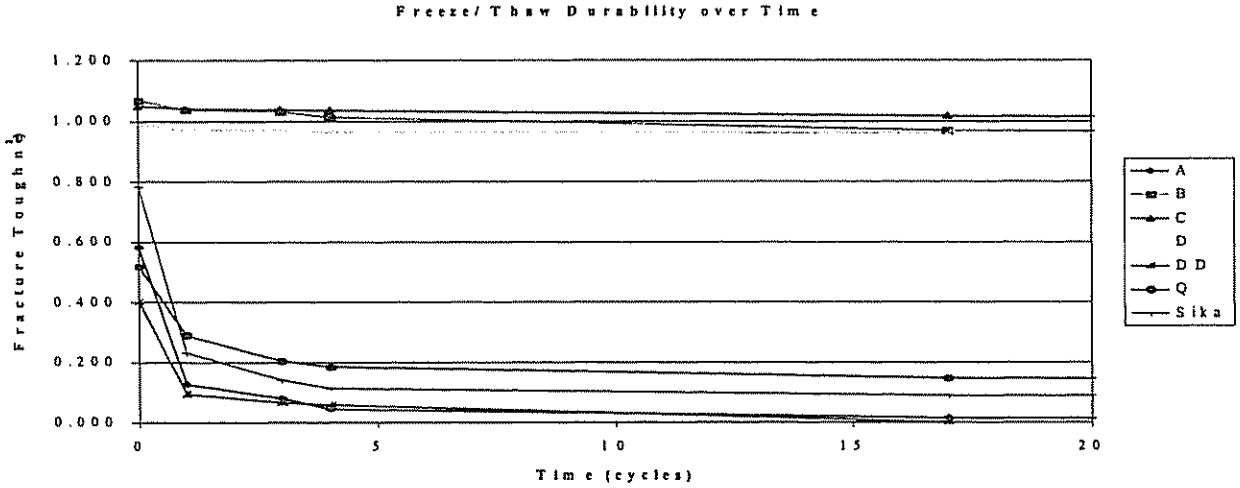

Figure 4.5 Durability over the first 20 cycles of exposure for samples in a freeze/ thaw environment (0°F to 40°F).

A	B	C	D
Baseline pretreatment w/ scrim and AV8113	Baseline w/ air dried silane Z-6040 primer	Baseline w/ 112°F oven dried silane Z-6040 primer	Baseline w/ 200°F oven dried silane Z-6040 primer

DD	Q	Sika
Baseline w/ DelDOT paint primer	Baseline w/ Q1-6106 air dried primer	Baseline with SikaDur 30 adhesive in place of AV8113

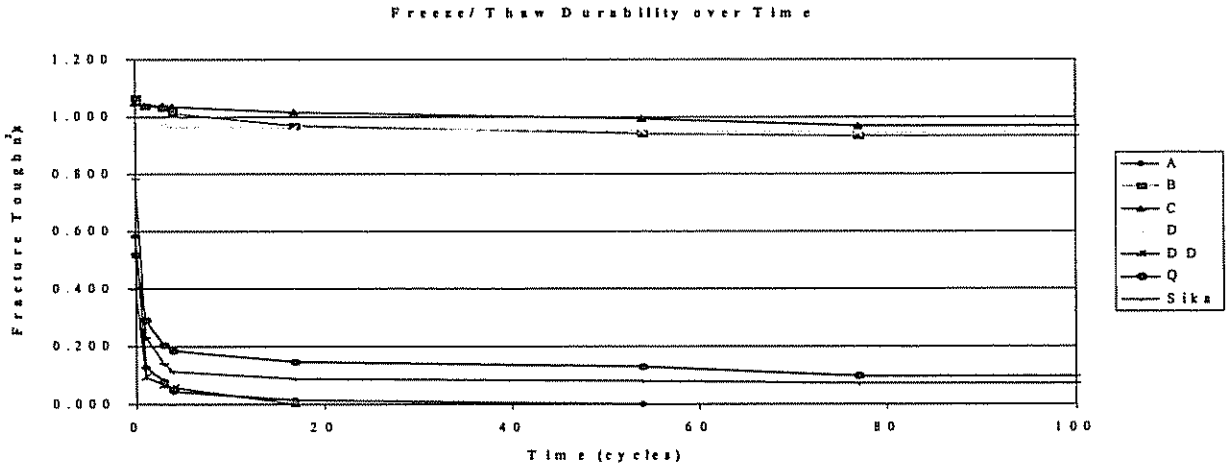

Figure 4.6 Durability over the first 100 cycles of exposure for samples in a freeze/ thaw environment (0°F to 40°F).

A	B	C	D
Baseline pretreatment w/ scrim and AV8113	Baseline w/ air dried silane Z-6040 primer	Baseline w/ 112°F oven dried silane Z-6040 primer	Baseline w/ 200°F oven dried silane Z-6040 primer

DD	Q	Sika
Baseline w/ DelDOT paint primer	Baseline w/ Q1-6106 air dried primer	Baseline with SikaDur 30 adhesive in place of AV8113

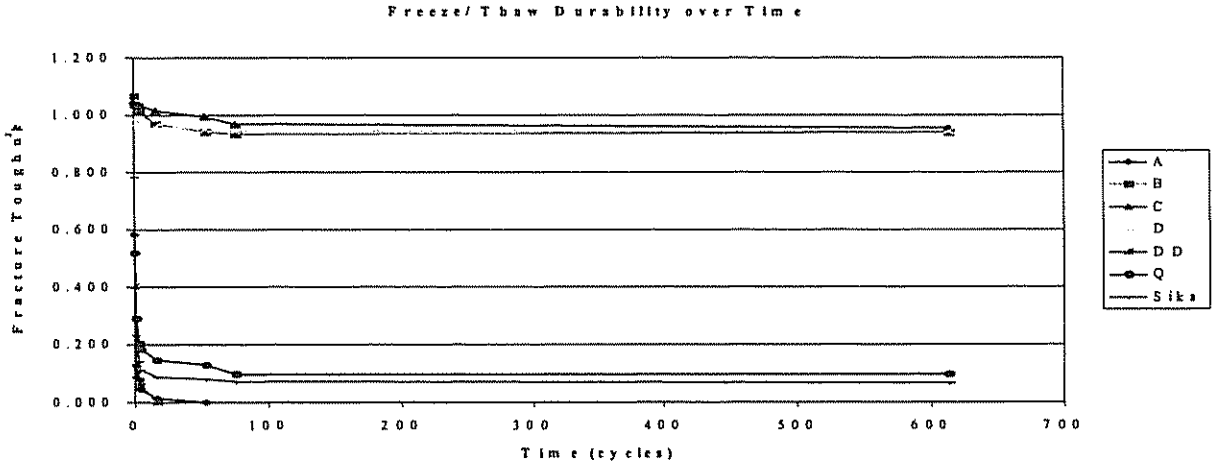

Figure 4.7 Durability over the full duration of exposure for samples in a freeze/ thaw environment (0°F to 40°F).

This clustering of sample types had a significant initial drop much like those samples in the first grouping as well as similar overall behavior. Amazingly, the average value for initial fracture toughness, G_{Ici}, was practically identical for all of the remaining sample groups at approximately 0.800 in-lb/ in^2. Despite this tight clustering, this G_{Ici} was significantly smaller in magnitude than the initial fracture toughness values of their counterparts at only slightly greater than half of that of the first group described. Sample classes A, DD, and Q behaved similar to B and D by exhibiting a sharp initial drop and then quickly stabilizing for the remainder of the first 20 hours. However, samples from A and DD dropped more significantly and stabilized at values less than 0.100 in-lb/ in^2 while Q leveled off at approximately 0.500 in-lb/ in^2. Meanwhile, the last remaining sample group in this cluster, Sika, behaved almost identically to prep method C however it too stabilized at a much lower level of toughness at approximately 0.075 in-lb/ in^2.

Unlike the first grouping, however, there were a number of individual samples that had fractured completely along the gage length very early in the exposure. For prep method A, three of the four samples were completely fractured within the first 75 minutes of exposure. Two of the four samples fabricated with the DelDot primer had completely failed within 75 minutes while a third sample

failed under five hours of exposure. Even a sample fabricated with the silane based Q1-6106 primer had failed within the first 75 minutes as well. Of the remaining unfractured samples, the last sample for both prep methods A and D was on the order of 0.060 in-lb/ in^2. Similarly, one of the three remaining samples from class Q was on the order of 0.060 in-lb/ in^2 while the other two had stabilized at approximately 0.900 in-lb/ in^2. Even though none of the samples fabricated using the SikaDur 30 adhesive had completely failed, all four samples were barely holding together with fracture toughness values all below 0.100 in-lb/ in^2.

Despite the fact that one of the four of the samples prep method Q had failed very early and with a second sample dangerously close to failure, the primer warrants a closer look. Recall that the average fracture toughness of the group stabilized on the order of 0.500 in-lb/ in^2. With two samples, for all practical purposes, with a fracture toughness of 0 in-lb/ in^2, the remaining two samples must have stabilized on the order of 1.000 in-lb/ in^2 in order to maintain that average. This value of 1.000 in-lb/ in^2 is comparable to those exhibited by the averages of the samples made using prep methods B and D. It is possible that there were other factors contributing to the low fracture toughness (impure primer mixture, primer application errors, outdated primer, etc.) that yielded results that are not necessarily representative of the behavior of the primer/ adhesive system.

Next, consider Figure 4.3 that illustrates the exposure time history of the H/W samples through the first 100 hours of exposure. There were not any significant developments over this period. Sample groups B and D continued to exhibit fracture toughness above 1.000 in-lb/ in^2, however prep method D showed a trend of slightly decreasing strength. Prep methods C and Q remained nearly constant through the next 80 hours of exposure as well. Prep method C exhibited a trend of slight reduction similar to prep method D, however only at a lower order of magnitude. Very little was expected out of the samples in fabricated by the remaining prep methods and that is exactly what was exhibited. Prep method Q lost an additional sample to complete fracture somewhere between 24 and 77 hours while prep method A had its final sample fracture between 77 and 150 hours. Additionally, the minimal average toughness for all sample groups after 20 hours of exposure was essentially unchanged through 100 hours as well.

Figure 4.4 includes the entire time history of sample exposure under the hot/ wet conditions. Beyond 100 hours of exposure, all sample groups exhibited some additional loss of fracture toughness. Prep methods B and D continued to have the highest residual fracture toughness throughout the extent of the testing. After approximately 140 hours, prep method B experienced a decline in toughness that occurred at varying rates through 315 hours. The crack growth stabilized from 315 hours through 1500 hours at approximately 0.950 in-lb/ in^2 and then grew steadily for the balance of the exposure (over 6600 total hours). Prep method D exhibited crack stability through 315 hours when it too experienced additional crack growth that continued through 840 hours where it

was at the same order of magnitude as prep method B. Interestingly, prep D behaved very similarly to prep B through the balance of exposure; ultimately the group as a whole exhibited the least crack growth out of all sample groups tested and had a final fracture toughness value of approximately 0.660 in-lb/ in^2.

Prep method C continued the steady crack growth through 550 hours that it had shown over the first 100 hours. Between 550 hours and 750 hours, the average crack growth of the growth increased in rate, but it stabilized and grew at a slower rate than groups B and D but continued to decline through 5800 hours, the balance of its exposure period. Similarly, prep method Q continued its slow loss of fracture toughness through 380 hours of overall exposure time. Around 380 hours of exposure, one of the remaining two samples from group Q experienced additional crack growth at a higher rate than its mate that continued through the end of exposure. Shortly thereafter, the second sample experienced an increase in crack growth as well thereby explaining the significant loss of fracture toughness the average plot exhibited through the end of its exposure.

The remaining three prep method groups limped to an inauspicious finish. Recall that all samples prep method A had fully fractured within the first week of exposure. Similarly, the DD prep method experienced its final sample fracture by the end of the first week of exposure as well. Meanwhile, two of the four Sika samples failed by the end of the first month and the remaining two defiantly retained their minimal fracture toughness through the end of the exposure.

At the end of the hot/ wet exposure, it was clear that there were prep methods that had outperformed the others. The samples fabricated using prep methods B and D, a silane Z-6040 primer either air-dried or oven dried at 200°F respectively used in conjunction with the Ciba Geigy adhesive, demonstrated significantly more favorable fracture toughness characteristics than all other prep methods. Their initial loss of fracture toughness was lower than any of the other prep methods studied and were on the same order of magnitude. Furthermore, they maintained their remaining fracture toughness more consistently than the others as well.

Prep method C, a silane Z-6040 primer oven dried at 112°F, performed similarly to those of methods B and D except it experienced a larger initial loss of fracture toughness (on the order of 0.400 in-lb/ in^2). Similarly, prep method Q is worthy of additional consideration in light of the fact that it appears there were problems in the fabrication of the samples due to the unexpected initial failure of half of its samples. When investigating the prep method without the samples that failed early, it was observed that its behavior closely followed that of the preferred prep methods B and D.

Ultimately prep method B is favored above all other methods at this stage of the investigation because of its performance and the fact that its application involves only air-drying which greatly facilitates field installation. The balance of the performance investigation will focus on the behavior of the wedge specimens

under freeze thaw conditions. The final adhesive and primer recommendations will be made after this stage of the research an used in a simulated full-scale rehabilitation.

Next, consider the results of the freeze/ thaw exposure as presented in Figure 4.5 for the average performance of the samples by group through the first 20 cycles. Recall that one cycle of freeze/ thaw exposure consisted of four hours of "freezing" at 0°F followed by three hours of "thawing" at 40°F for a total cycle time of seven hours. It can readily be seen that the average behavior of the sample prep methods can once again be broken down into two groups, those that were fabricated using a silane Z-6040 primer and those that were not.

Similar to the H/W results, the samples from prep methods B, C, and D that used the silane primer had higher initial values for fracture toughness than the other sample classes tested. As a matter of fact, the F/T results were even more tightly banded together than those from the H/W exposure and ranged between 0.989 and 1.067 in-lb/ in^2. However, unlike the H/W samples, these groups did not experience significant reduction in fracture toughness over the first 20 cycles (140 hours) of exposure. Some slight loss in fracture toughness was experienced, however all of the three sample groups remained banded around 1.000 in-lb/ in^2. It is significant to note that this was the same level of fracture toughness exhibited by the best performing sample groups (A and D) from the H/W testing.

Results for the remaining samples, prep methods A, DD, Q, and Sika, were not nearly as tightly grouped as the other F/T samples or their counterparts from the H/W exposure. However, their similar behavior over the first 20 cycles enables them to be considered simultaneously. Their average G_{Ic} values ranged from 0.783 in-lb/ in^2 for the Sika prep method to 0.403 in-lb/ in^2 for prep method DD with the samples from A and Q starting with 0.583 in-lb/ in^2 and 0.518 in-lb/ in^2 respectively. However, after only one freeze/ thaw cycle, all sample classes experienced a significant decrease in fracture toughness; decreases on the order of 75% for prep methods A, DD, and Sika, and approximately 50% for prep method Q. These losses continued for all of the four sample groups for the balance of the first 20 cycles, but not at nearly the same rate of toughness loss. Note that three of the four samples from prep method A failed completely under 20 cycles (one after only one cycle) and the only sample from prep DD failed before the end of 20 cycles as well. Prep method DD had only one sample actually tested to offer some idea of its F/T behavior even though three samples is typically considered a minimum. However, this will not affect the evaluation of its results since it had already been eliminated from consideration after strength testing and H/W exposure.

Figure 4.6 depicts the performance of the sample groups through the first 100 cycles (700 hours) of F/T exposure. Similar to the plot over the same range for the H/W samples, not significant developments were experienced. The first group of samples , prep methods B, C, and D, continued their predictable behavior of limited crack growth with only sample class C showing any

appreciable energy loss over this period. Similarly, the remaining groups held constant over this same range as well. Only one additional sample failed during this period and it was one of the samples fabricated under prep method Q between 54 and 77 cycles. Otherwise, there were no further developments. Once again, note that samples from prep methods B, C, and D were keeping pace with the top samples from the H/W tests described earlier.

The final chart, Figure 4.7, captures the full time history of all of the samples exposed under F/T conditions, which included a total of 614 cycles over the course of six months (almost 4300 hours). Unlike the H/W samples, there were no further developments as the exposure extended. The average crack length, and hence the fracture toughness, of all sample groups remained surprisingly steady. Prep methods B, C, and, D remained bunched together at approximately 0.950 in-lb/ in^2 while the samples from prep methods Q and Sika held steady below 0.100 in-lb/ in^2. Minimal crack growth was exhibited by these last two sample groups and it can be concluded that all of the remaining samples from each class would have ultimately failed had the exposure been permitted to continue. Recall that prep methods A and DD were eliminated within the first 50 cycles.

4.8 Conclusions

The research documented in Chapter 4 was a continuation of the testing initiated in Chapter 3 to evaluate the performance of the steel to composite adhesive bond. The collective aim of both chapters was to recommend adhesive and primer combinations to be used in the rehabilitation of steel bridge girders with advanced composite materials. Chapter 3 established surface preparation standards as well as adhesive and primer combinations while it addressed the first component of performance, strength, through ASTM D 3165 lap shear tests. Chapter 4 continued this performance evaluation through the testing of ASTM D 3762 wedge specimens in both hot/ wet (122°F and 85%RH) and freeze/ thaw (cyclic temperatures between 0°F and 40°F) environments. All of the six prep methods considered in the lap shear testing were evaluated in both of the chosen environments and were joined by a seventh, the Sika prep method.

Early results from the H/W environment clearly set the tone for the results of the research in this chapter. Through only five hours of exposure, all samples fabricated with a silane Z-6040 primer, prep methods B, C, and D, clearly outperformed those that were fabricated without the silane primer, prep methods A, DD, Q, and Sika. Furthermore, the samples from groups B and D performed slightly better than those from C. This trend was reinforced as the H/W exposure continued. Despite groups B, C, and D losing some of their fracture toughness in the latter stages of exposure, it was evident that they outperformed the samples fabricated without the silane primer.

Nearly identical behavior was exhibited by the samples in the F/T testing as well. Once again, samples fabricated using a silane Z-6040 primer (B, C, and D)

markedly outperformed those without it (A, DD, Q, and Sika). More importantly in this phase of testing, there was less separation between the three groups of samples using the silane primer than those from the H/W environment. Additionally, their performance did not diminish towards the end of their exposure as with the H/W samples.

The fact that the performance could be broken down to those samples fabricated with a silane Z-6040 primer and those without was not surprising. The driving force of introducing the primer was to enhance the strength and durability of the bond. It is clear that this was exhibited. Coincidentally, the peak levels of fracture toughness were on the order of 1.000 in-lb/ in^2 for the best-performing samples from both environments.

Now that both components of performance, strength and durability, have been evaluated, a final primer/ adhesive combination can be determined. Independent of the primer and adhesive combination used, recall that it was critical for a baseline surface preparation included the abrasion of each adherend followed by a solvent wipe. Based on the results of Chapters 3 and 4 either prep method B, baseline surface prep with an air-dried silane Z-6040 primer, or prep method D, baseline surface prep with a 200°F oven-dried silane Z-604 primer, should be used. Note that both prep methods were used with the Ciba-Geigy AV8113 two-part epoxy adhesive. It is clear that the air-drying prep method B would be the preferred choice over elevated temperature dried prep method D based on the comparative simplicity of its field implementation.

In addition, an alternate adhesive of SikaDur 30 is also recommended. This is not readily evident from its performance in the durability phase of testing; however the sample preparation should be investigated further. Recall that the Sika samples were essentially baseline samples with no primer, only a different adhesive. Taking that fact into consideration, the Sika samples should be compared directly to the samples from prep method A. When this comparison was conducted, it was evident that the Sika samples outperformed those using prep method A from a durability standpoint. While all samples fabricated using the Ciba-Geigy AV8113 adhesive without primers failed in both durability environments, only one H/W sample and no F/T samples using the SikaDur 30 adhesive fractured fully. Because of this observed performance of the Sika adhesive, it is recommended that it be investigated further with pretreatments and considered for future applications.

Based on the cumulative results of the performance studies, two adhesives will be used with each with two primers for the full-scale rehabilitation. The selected adhesives are Ciba Geigy AV8113 and SikaDur30 while the primers are silane Z-6040 and the Q1-6106 adhesion promoter. Chapter 5 will outline the procedure used for the full-scale rehabilitation.

Chapter 5: FULL-SCALE REHABILITATION

5.1 Introduction

The strength investigation of Chapter 3 and the durability investigation of Chapter 4 have established a recommended adhesive/primer combination for field implementation. A preferred combination of Ciba-Geigy AV8113 adhesive used with an air-dried layer of silane Z-6040 primer was the result of the research conducted in these chapters. Additionally, acceptable alternatives to this particular combination include SikaDur30 and Dow Corning Q1-6106 adhesion promoter for the adhesive and primer, respectively. Note that these alternatives can be used with either adhesive or primer. Also recall that Chapter 2 recommended the introduction of a fiberglass scrim for galvanic corrosion protection. In this portion of the study, these developments were combined with previously established techniques to perform the simulated rehabilitation.

Gillespie et al pioneered this specific rehabilitation scheme through cooperative research between the University of Delaware and Lehigh University. Under this work, researchers successfully demonstrated that composite materials could be bonded to steel bridge girders under simulated field conditions. PennDOT donated four decommissioned, heavily corroded steel bridge girders to the universities for research purposes. Two of the four were used in the original study while the remaining two girders were retained for use in this research. More information regarding these girders is provided in Section 5.2.

In the original work, a team of five graduate students successfully performed the repair on the two girders. Pre-repair elastic testing of the girders quantified the loss of stiffness of the members when compared to a theoretical stiffness of a new girder derived from the cross sectional properties of the member. Testing of the girders after the rehabilitation revealed that the stiffness had been renewed to as much as 97% of their original values while the original load carrying capacity could be restored or even exceeded.

It is important to note that the original research only considered one type of adhesive, Ciba-Geigy AV8113, and only one preparation method, cleaning of bonding surfaces with an abrasive blast and solvent wipe. This bonding scheme can be considered equivalent to the baseline preparation method (Prep Method A) of Chapters 3 and 4. The same repair procedure used in the original research was performed for this study except that the recommendations from Chapters 2 through 4 were incorporated.

Prior to the implementation of the recommendations of this research to a simulated rehabilitation, the girders were tested in four-point bending. This established a baseline level of stiffness for each member that was compared to theoretical values in order to quantify the level of lost stiffness due to corrosion.

After the rehabilitation, the girders were again tested in four-point bending and the results were compared to the pre-repaired results to demonstrate the benefit of the composites; the discussion of this aspect of the research is contained in Chapter 6. Finally, future research will evaluate the performance of the repaired girders under fatigue loading as well as under long-term environmental conditions.

5.2 History

The four girders that were donated by PennDot were from a bridge built circa 1940 over Rausch Creek in Valley View, PA with a span of approximately 32 feet. Inadequate vertical clearance over the stream created a very aggressive corrosion environment due to the accumulation of mist from the creek on the bottom portion of the girders. This accumulation was particularly bad on the downstream side of the structure. In 1995 the bridge was replaced after years of deterioration and after posting, shoring, and underpinning could no longer guarantee the safety and function of the bridge.

Unfortunately, original plans were unavailable for the structure. A survey of historical rolled shapes produced in that era conducted by the initial team of researchers provided original section properties for the girders. Each girder had an approximate depth of 24 in with a web thickness of 0.430 in and flange width of 9.035 in. The shape was similar to modern I shapes except that the flanges tapered from 0.924 in at the web to 0.565 in at their outer edges. A cross section of the girder as well as its section properties can be found in Figure 5.1.

Physically, the girders were ideal candidates for rehabilitation. The bottom sides of the tension flanges were heavily corroded along their length to the point where the flange thickness was reduced to less than 0.250 in as shown in Figure 5.2. This corrosion continued on the top of the tension flange and up the sides of the web as well. As one might expect, the level of corrosion on the web was reduced the further away the section was located from the stream and can be seen in Figure 5.3. Finally, the compression flanges were found to be in noticeably better condition primarily because they were encased in the deck concrete. Figure 5.4 illustrates the general condition of the girders.

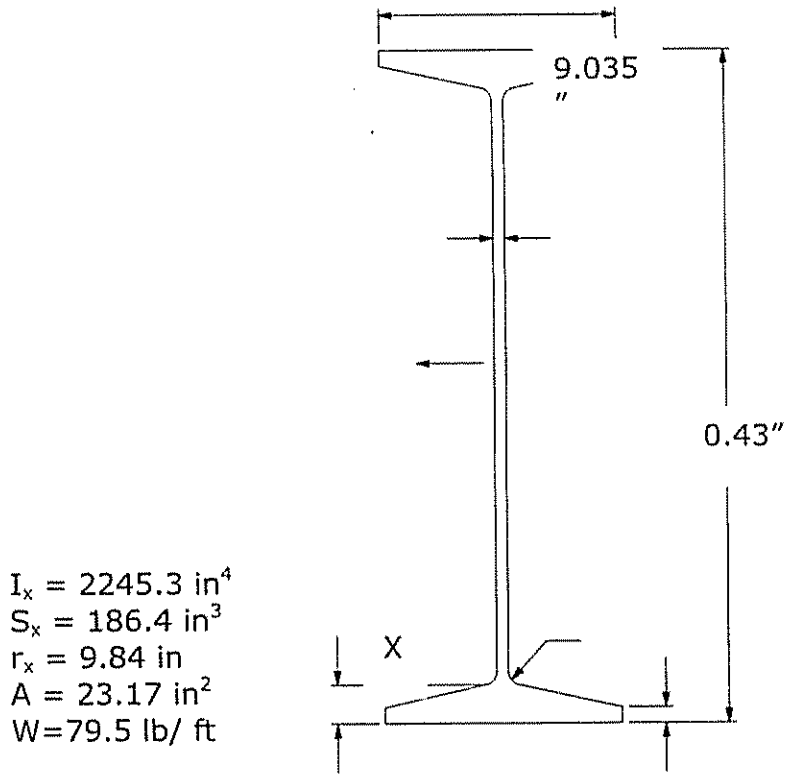

Figure 5.1 Original cross section of girder used in the full-scale rehabilitation.

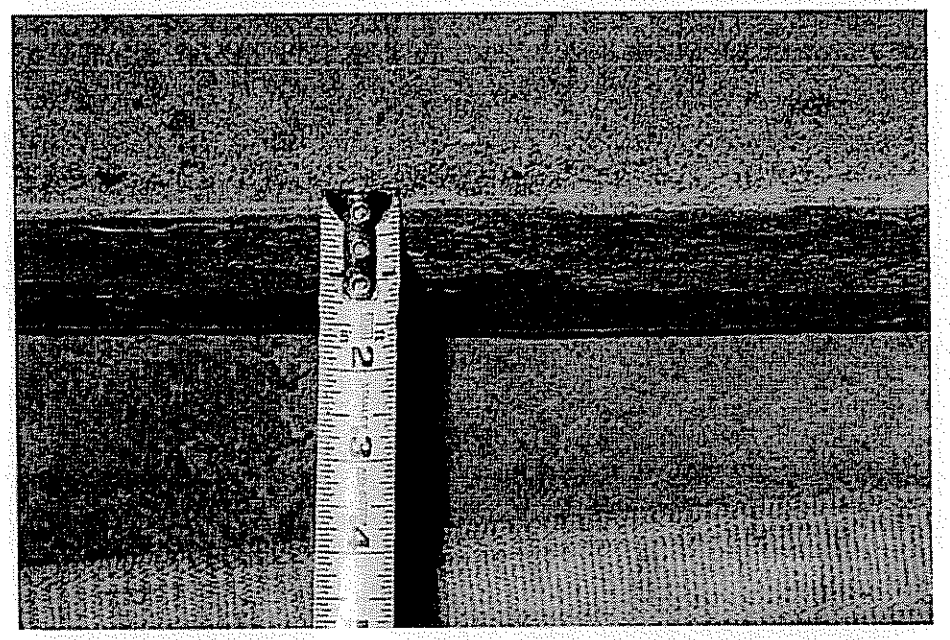

Figure 5.2 Effects of corrosion on flange thickness.

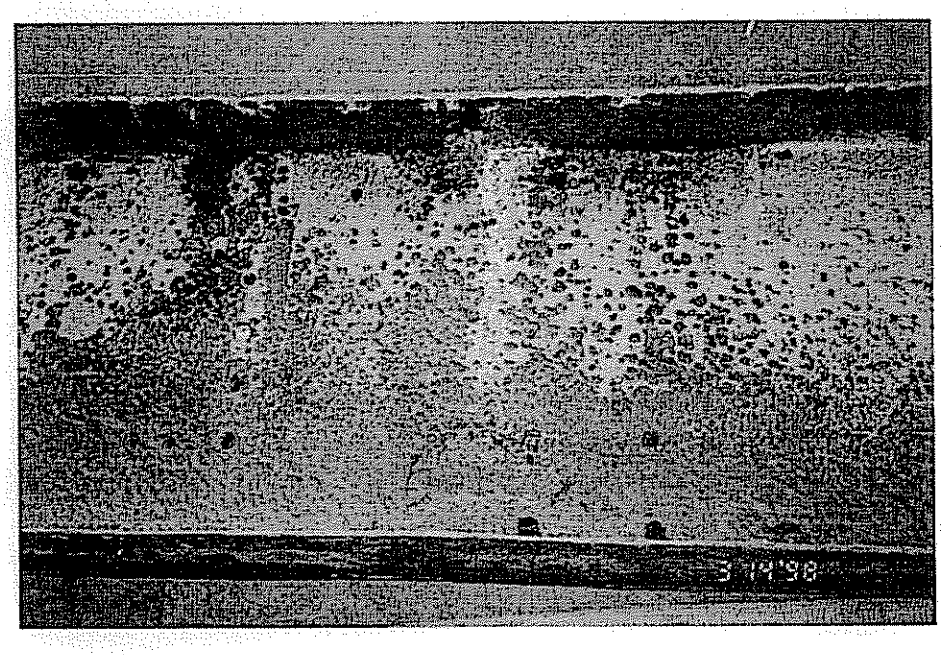

Figure 5.3 Corrosion of the girder web.

5.3 Methodology

The methodology used to rehabilitate the girders was similar to the one that was implemented during the initial research at Lehigh and the University of Delaware. Enhancements were made to the procedure based on the results of this research as presented in Chapters 2 through 4. The primary goal was to demonstrate the benefit of strengthening a steel bridge girder through the application of advanced composite materials.

The methods used to fabricate the lap shear and wedge test samples were expanded in order to apply them to the full-scale specimens. However, the overall process was still the same. In order to maximize the benefits of the rehabilitation, composite was bonded to both the top and bottom of the tension flange. Note that the girders were rehabilitated tension flange up. Although this was not representative of field conditions it was done in order to coordinate with other laboratory research and facilitate the process. Additionally, the initial researchers demonstrated that this rehabilitation procedure could be performed in over-head conditions as would be required in the field therefore eliminating the necessity of this type of procedure. The following list of rehabilitation steps describes the specific procedure used for the materials selected for this rehabilitation. Modification to these steps may be necessary if different materials are used.

(1) Prior to starting rehabilitation, ensure that all necessary materials, tools, and safety equipment are assembled.

(2) Cut the required amount of composite to the appropriate length. In this case, the 9 in flange required six strips of 1.44 in wide composite to provide maximum coverage. Figures 5.5 and 5.6 show the spool of composite material used in the rehabilitation behind the installation team and author respectively.

(3) Mix the required quantity of primer. In this case, quantities of each recommended primer, silane Z-6040 and Q1-6106, were both used to evaluate relative performance.

(4) Clean the bonding surfaces of the steel girders to state DOT specifications for surface preparation for applying coatings.

(5) Wipe the surface of the cleaned steel with a solvent to ensure that any residue from the cleaning process had been removed.

(6) Abrade the surface of the composite material based on the recommendations from Section 2.5.1. Recall that included 20-30 psi bead blast applied two to three inches from the surface of the material.

(7) Align the composite strips abraded side down on a flat surface.

(8) Bond 1 in x 1 in blocks of wood at 12 in increments to the aligned composite strips using a hot glue gun. This creates a rigid assembly that is much easier to apply the adhesive to and much easier to bond to the steel girder. Furthermore, the wood blocks provide a clamping surface in order to protect the composite material.

(9) Wipe the surface of the abraded composite with a solvent to ensure that any residue from the abrading process had been removed. Figure 5.9 depicts the steel girder and the composite assembly prior to rehabilitation.

(10) Apply the primer to the surface of the cleaned steel girder flange (Figure 5.8).

(11) Mix the adhesive per manufacturer's specifications. The Ciba-Geigy AV8113 required mixing in equal parts by mass (Figure 5.9) while the SikaDur 30 adhesive was available in pre-measured packages. Figure 5.10 shows to workers mixing the Ciba-Geigy adhesive used in the rehabilitation.

(12) Apply an even coat of adhesive to the abraded surface of the composite (Figures 5.11 and 5.12).

(13) Blow any excess primer from the surface of the girder flange to prevent build up of primer (Figure 5.13). Ensure that the primer had dried for a minimum of 15 minutes before performing this step. Note that this may not be necessary under field conditions where the flange is overhead.

(14) Apply an even coat of adhesive to the surface of the girder flange. Ensure that any surface irregularities due to corrosion have adequate adhesive coverage (Figure 5.14).

(15) Measure and cut the required length of 120 fiberglass scrim as shown in Figure 5.15.

(16) Apply the scrim to the surface of the plate girder. Ensure that there are no trapped pockets of air between the scrim and the girder and that the scrim is smooth against the girder surface (Figure 5.16). Bunching or other irregularities in the scrim could compromise the bond integrity.

(17) Lift the composite assembly into place and align with the girder flange. The process of placing the composite assembly on the surface of the girder is shown in Figures 5.17 to 5.19.

(18) Attach the composite to the girder using C-clamps at each wooden block. Ensure that the clamps are tight to wet out the scrim (Figure 5.21) and to squeeze out (Figure 5.22) any excess adhesive. Retighten clamps as necessary after adhesive has squeezed out to guarantee a full bond.

(19) Spread the adhesive that had squeezed out of the bond line around the all edges of the composite to create a fillet in order to insulate the composite from the steel. Recall this was a recommendation from Chapter 3 to prevent galvanic corrosion at the edges of the composite.

(20) Allow the adhesive to bond for a minimum of 24 hours before removing the C-clamps. Figure 5.23 shows a girder that has been rehabilitated during the adhesive cure stage with all C-clamps tightened. (21) Remove the wooden blocks by striking a hammer against the side of the block to shear the glue.

(22) Repeat steps 1 through 20 on the opposite side of the tension flange for each girder requiring strengthening.

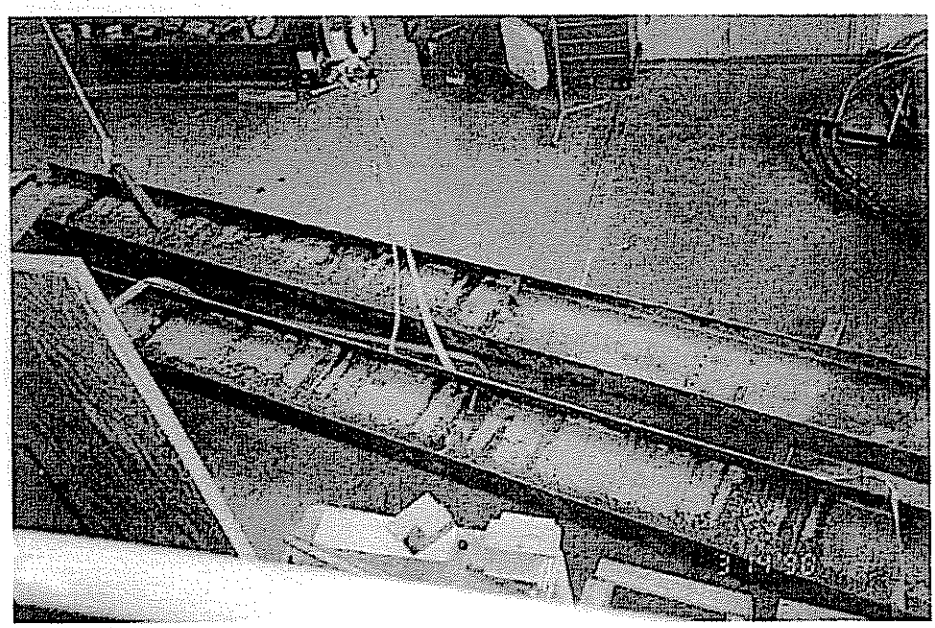

Figure 5.4 Overall condition of corroded girders.

Figure 5.5 Rehabilitation team.

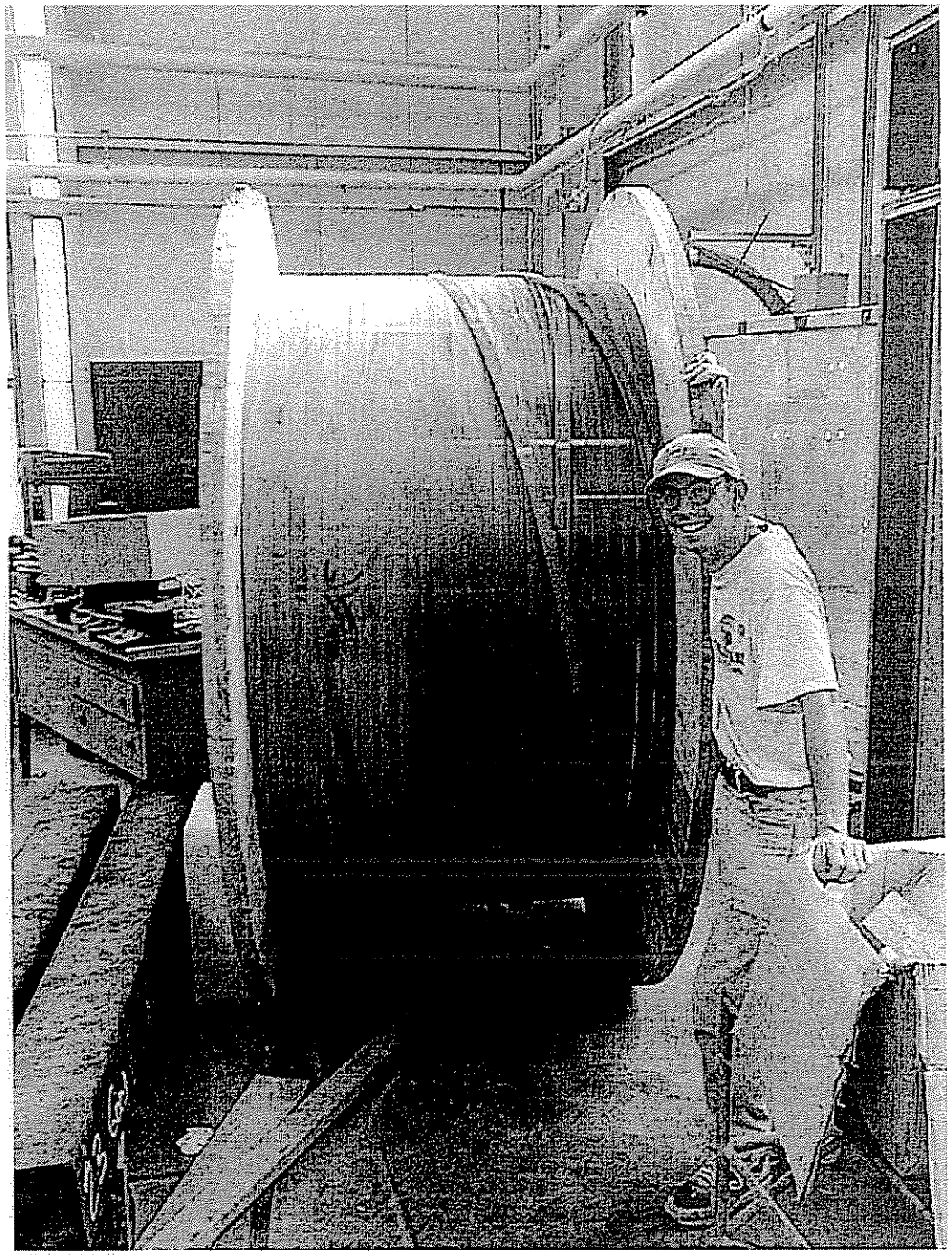

Figure 5.6 Author with spool of composite used in this rehabilitation.

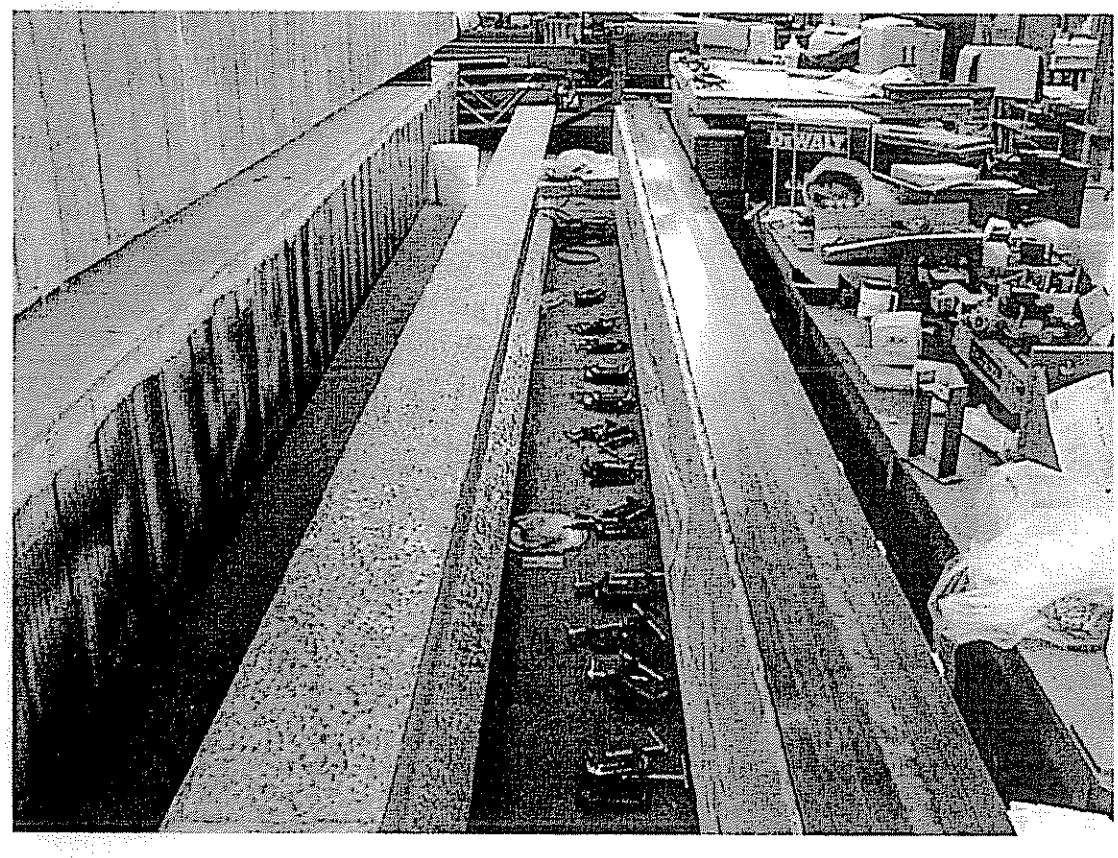

Figure 5.7 Cleaned girder surface (left) and composite assembly (right) prior to bonding. Note the C-clamps on the floor to be used in step 18.

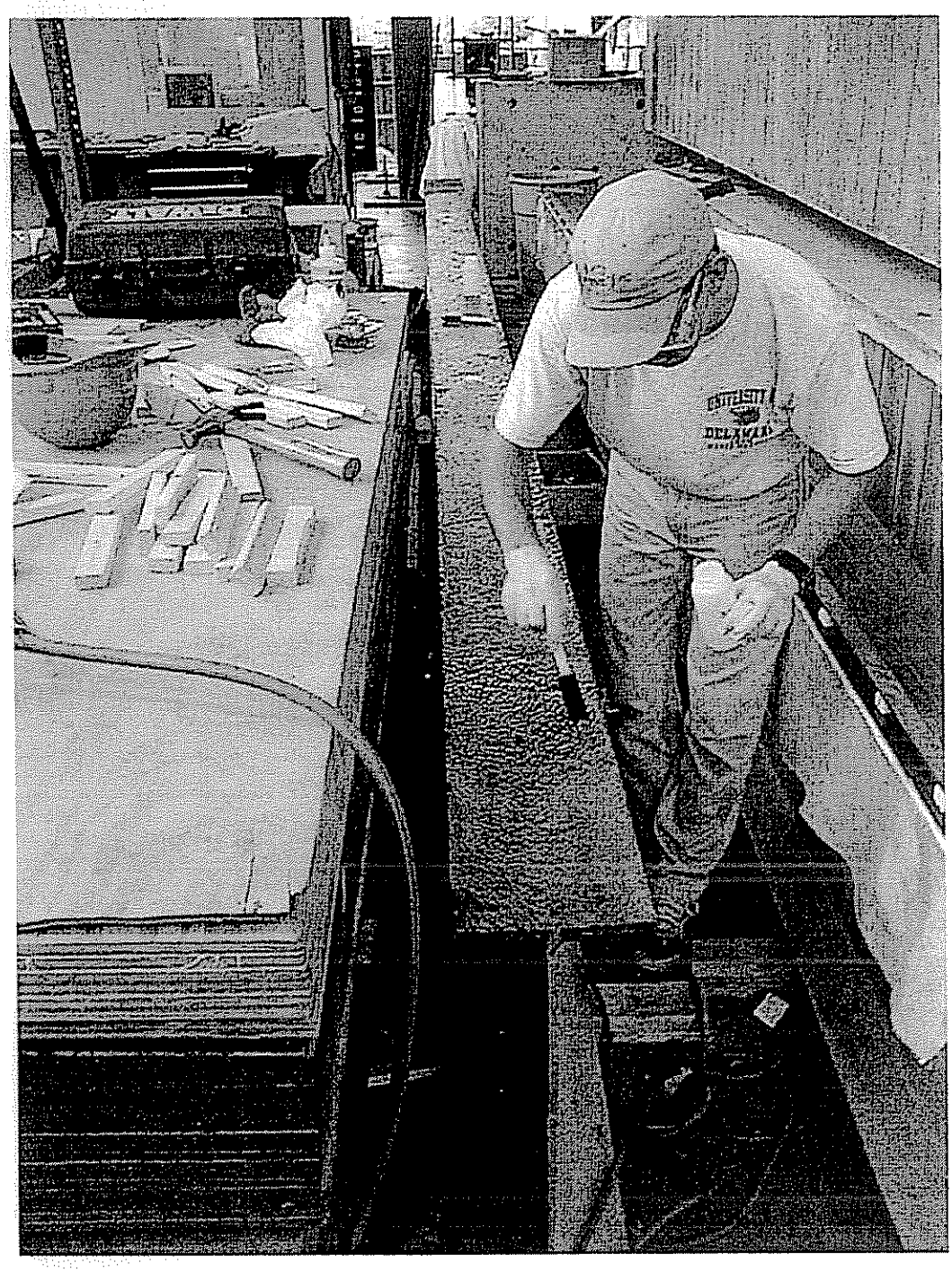

Figure 5.8 Application of primer to surface of tension flange.

Figure 5.9 Weighing the parts of adhesive to ensure a proper mix. On the floor in the background, note the individual components awaiting mixing.

Figure 5.10 Mixing the two parts of adhesive in preparation for bonding.

Figure 5.11 Application of the adhesive to the composite assembly. Note the wooden blocks underneath the composite.

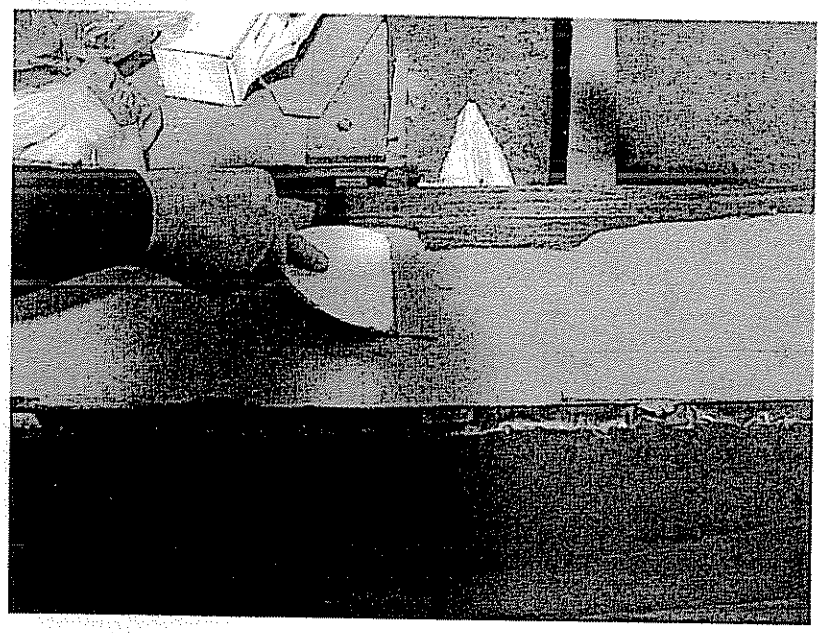

Figure 5.12 Smoothing out the adhesive to ensure an even coat on the composite.

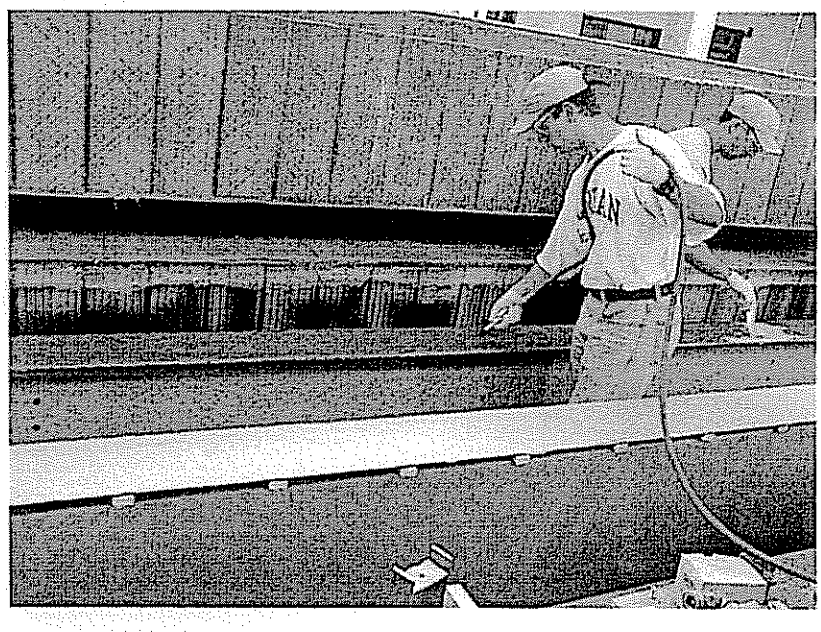

Figure 5.13 Dispersion of any excess primer using a stream of compressed air.

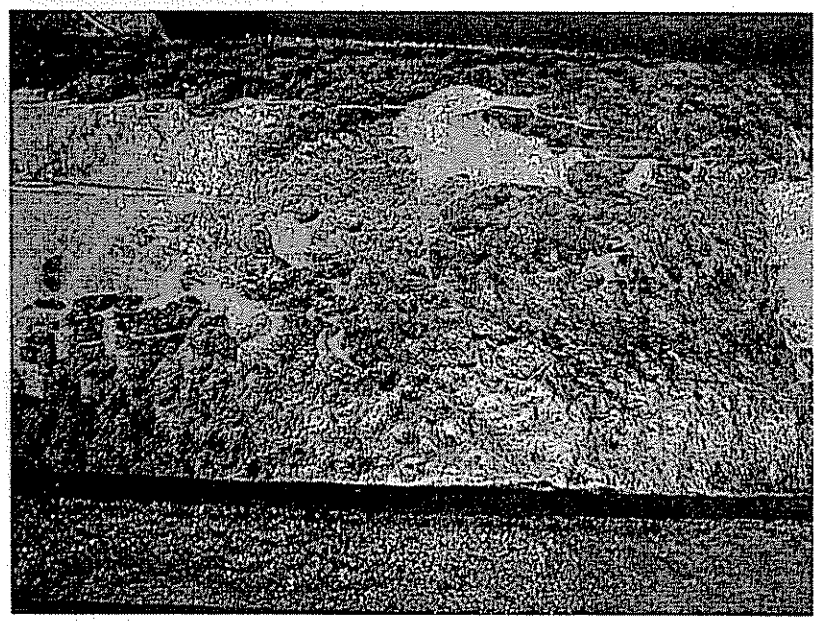

Figure 5.14 Pitted flange surface due to corrosion. Care was required to ensure complete adhesive coverage.

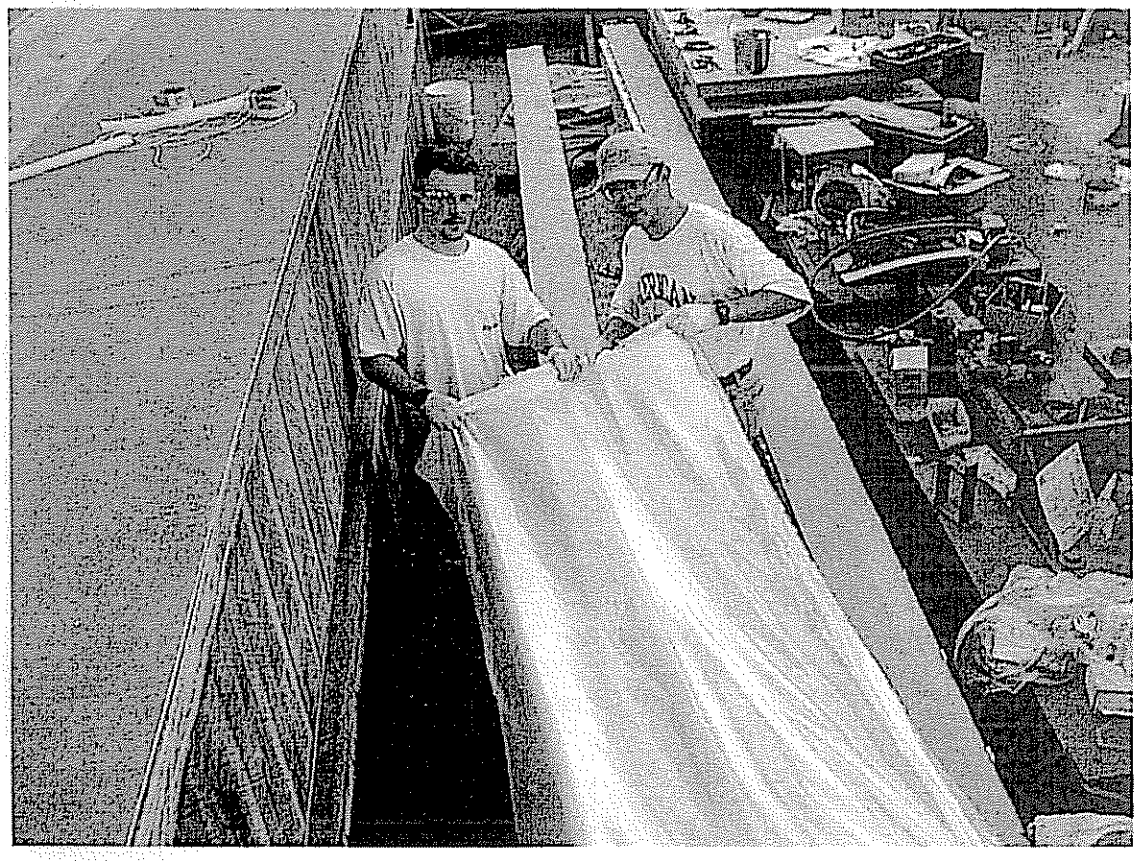

Figure 5.15 Pulling out 120-fiberglass scrim to place in bondline as a galvanic corrosion inhibitor.

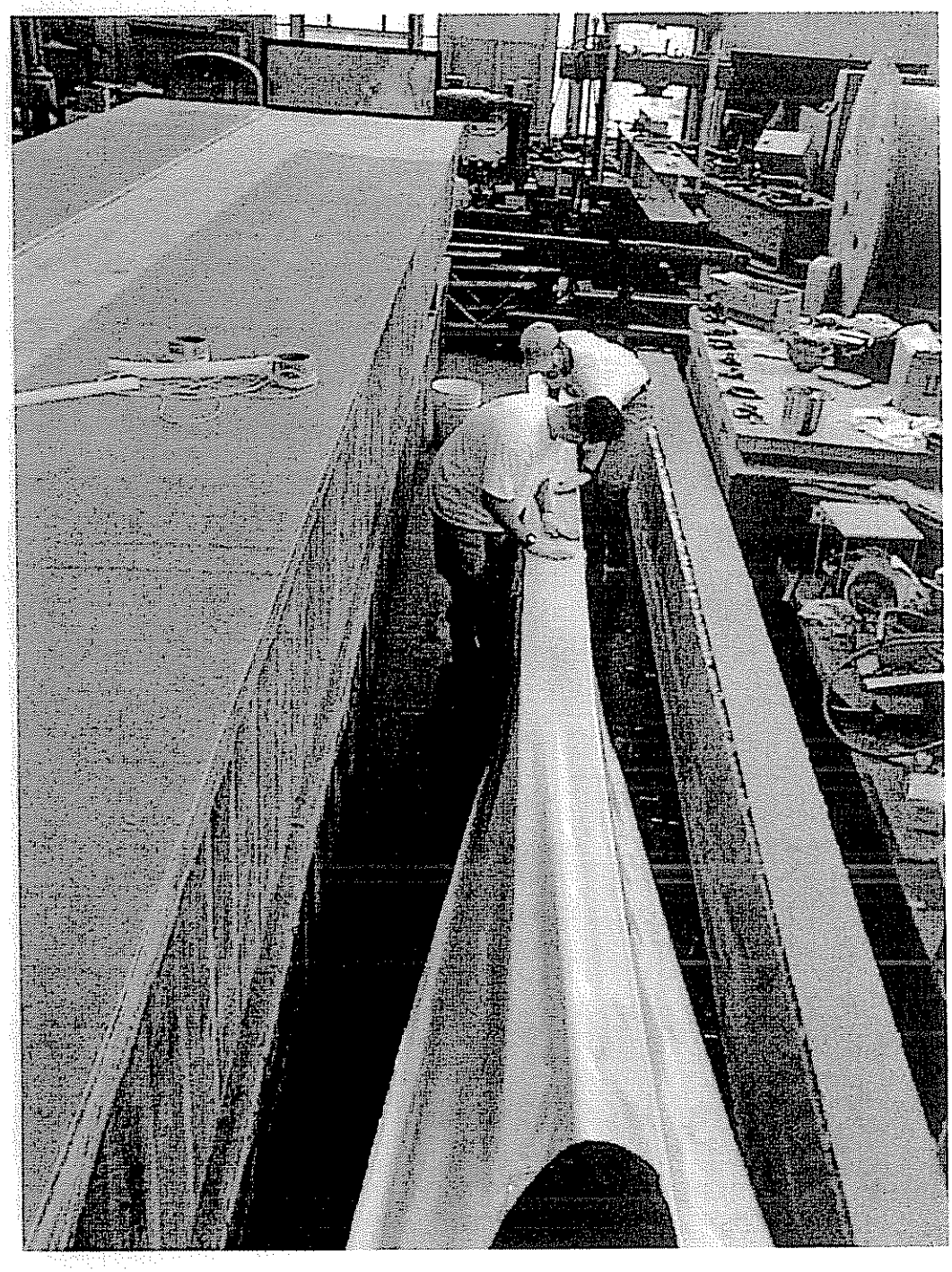

Figure 5.16 Smoothing out the surface of the scrim to ensure that there are no air pockets or surface irregularities that could effect bond integrity.

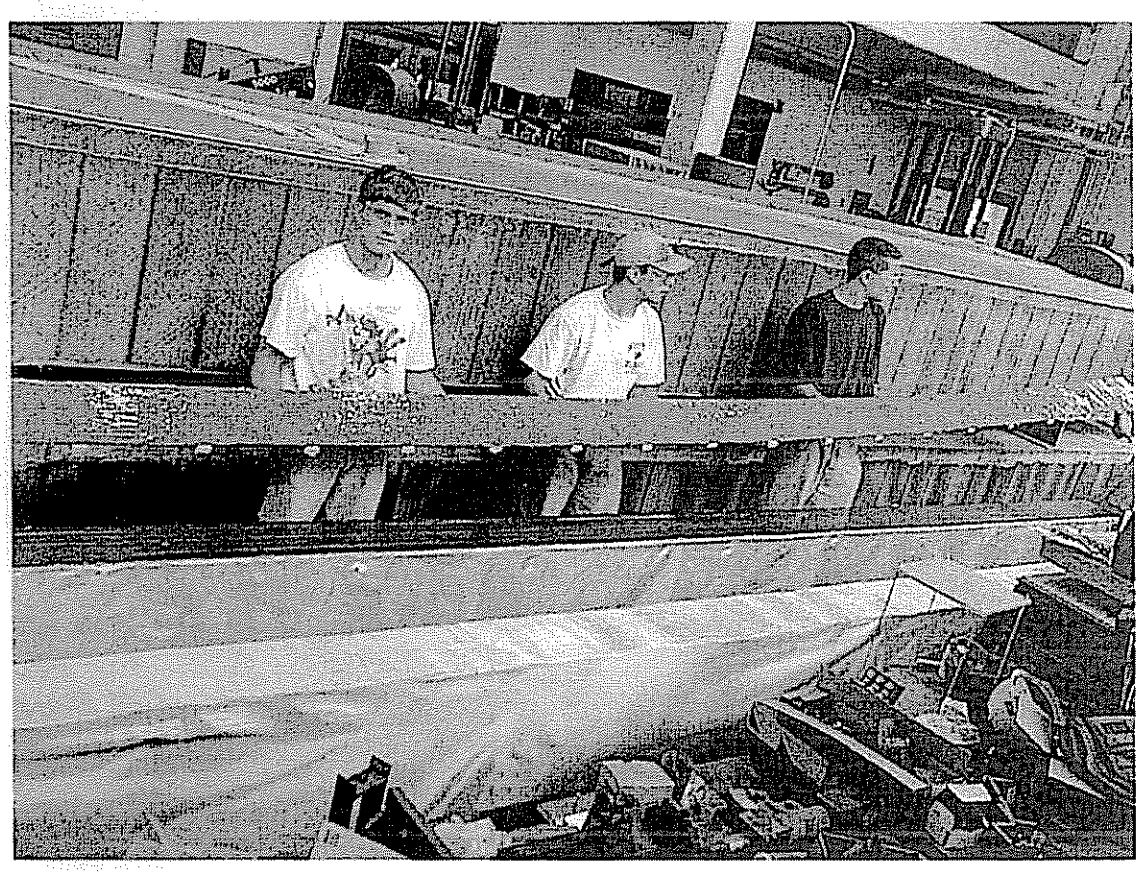

Figure 5.17 Lifting the composite assembly with full coat of adhesive prior to bonding to steel.

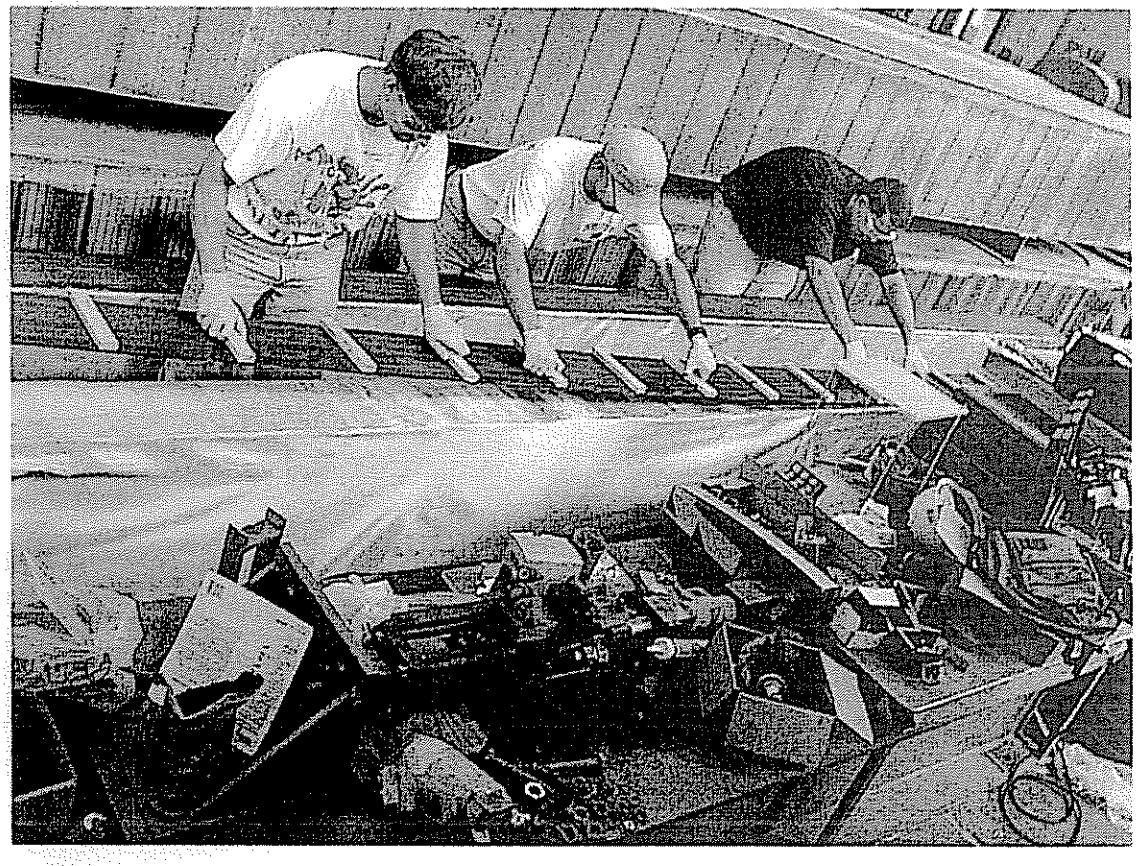

Figure 5.18 Placing the composite assembly on the surface of the girder taking care to ensure its alignment. Note the workers holding on to the wooden blocks and the scrim on the girder surface.

Figure 5.19 The composite assembly in its final location prior to clamping.

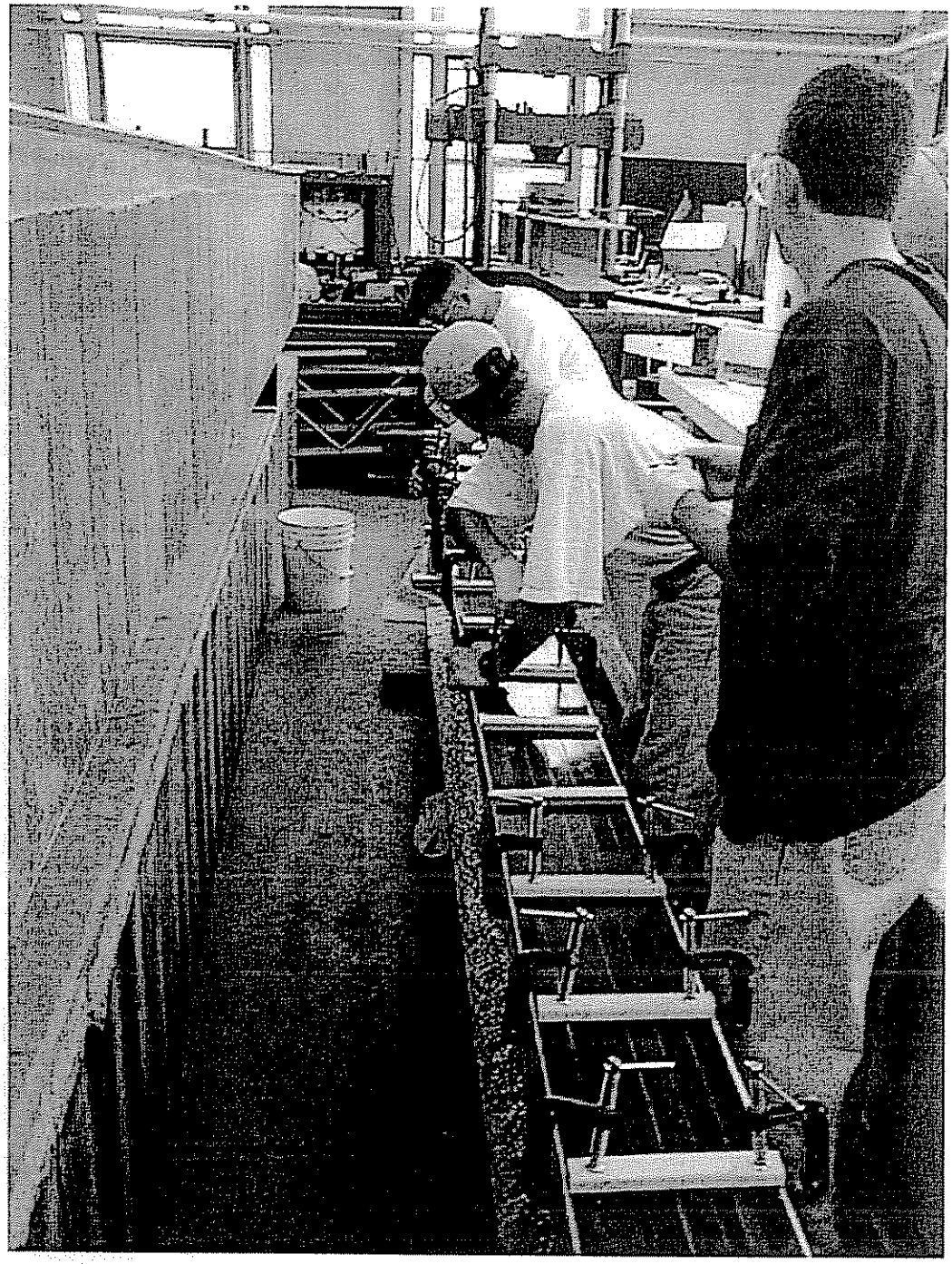

Figure 5.20 Tightening C-clamps on the wooden blocks and flange along the length of the girder.

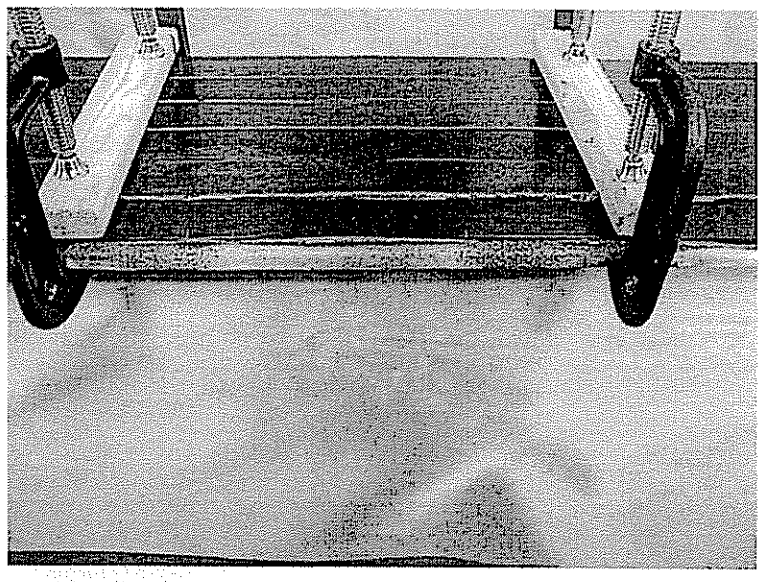

Figure 5.21 Close-up of adhesive squeezing through the scrim layer in the bond line indicating that it has been fully wet out.

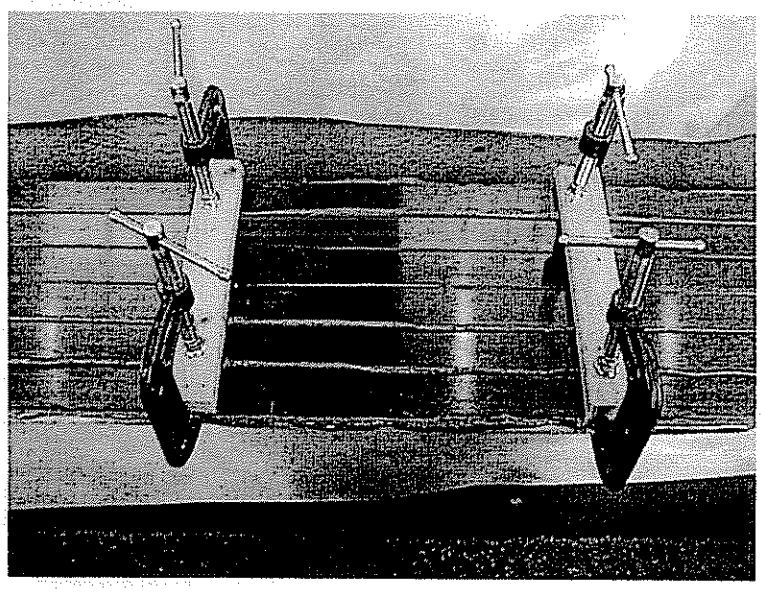

Figure 5.22 Close-up of adhesive squeezing out between composite strips and on the edge of the assembly indicating adequate adhesive at the interface to fully bond the adherends.

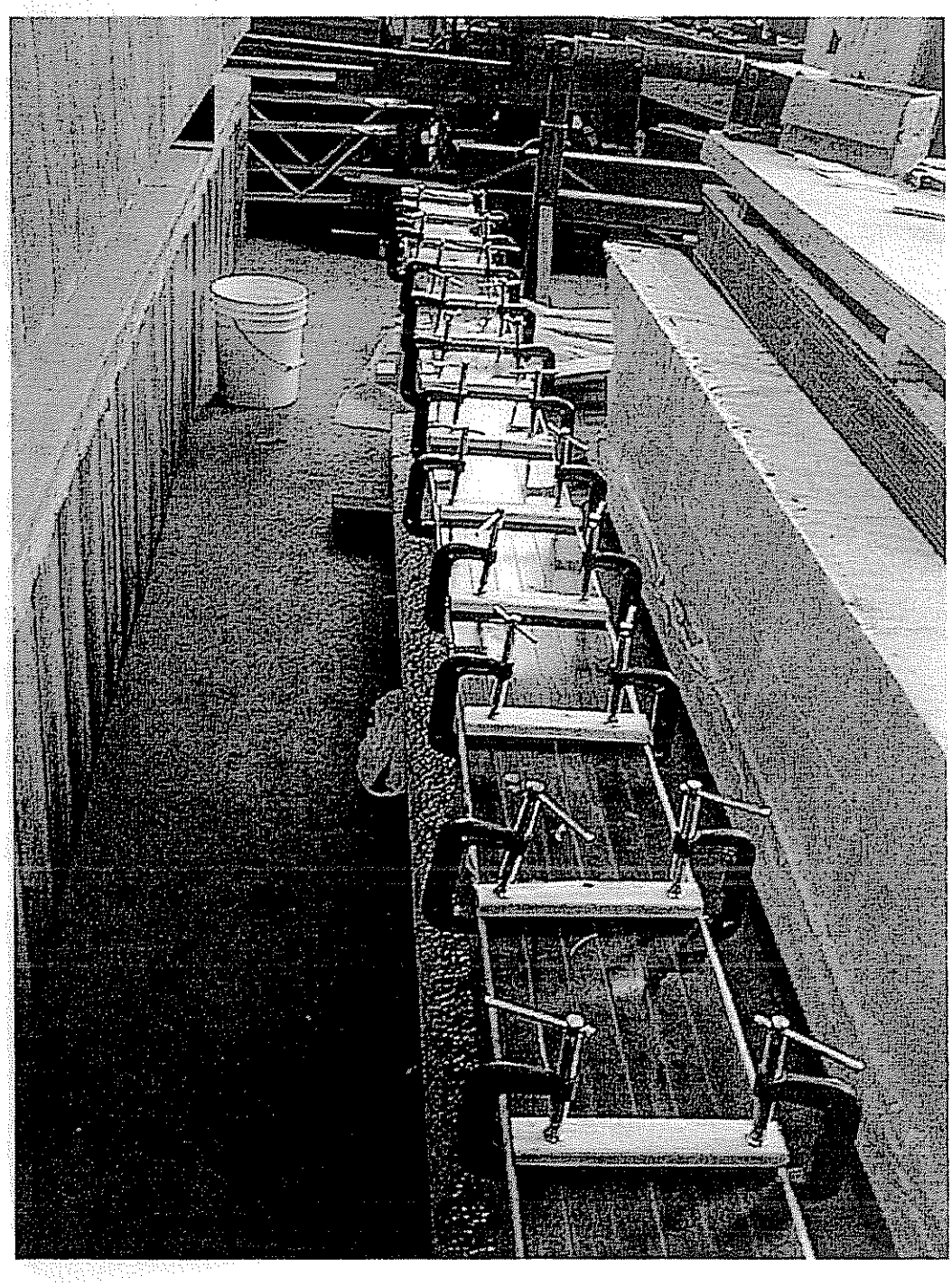

Figure 5.23 Completed rehabilitation with all clamps tightened while adhesive cures.

5.4 Conclusions

The two remaining girders were rehabilitated during this stage of the research. In order to assess the relative performance between adhesives under long-term

conditions, both the Ciba-Geigy AV8113 and SikaDur 30 adhesives were used. Additionally, one half of each girder was primed with either primer such that their long-term performance with either adhesive could be monitored as well. Additionally, it was proven that a team of five workers with limited familiarity with the installation process could easily perform the rehabilitation within the constraints of the procedure.

Many steps within the repair process are time sensitive therefore it is imperative that the procedure has been well planned prior to implementation. For example, the primers used have minimum stirring times to ensure complete mixing throughout the solution as well as minimum drying times in order to perform effectively. Similarly, the adhesives have finite working times before they begin to cure therefore it is important to complete all necessary steps in that window of workability. If the adhesive begins to cure prior to the C-clamps being tightened, for example, the rehabilitation would be a failure because a proper bond could not be guaranteed.

Chapter 6: FULL-SCALE GIRDER TEST PROGRAM

6.1 Introduction

Chapter 5 discussed the procedure used to rehabilitate steel bridge girders developed in this research. In this chapter, full-scale testing of the girders is discussed. Pre-rehabilitation testing was performed in order to evaluate the condition of the girders relative to an identical theoretical girder that had no section loss due to corrosion. These results were also used to establish a baseline level of performance to compare with the post-rehabilitation test results. Post-rehabilitation testing was performed on the same girders after receiving the composite repair in an attempt to evaluate the benefits of this type of rehabilitation.

6.2 Elastic Stiffness of the Girder

In order to compare the performance between individual girders and between the different states (theoretical, pre-repair, and post-repair), a quantity for comparison must be established. In this study, the elastic stiffness, k, of the girder was selected for comparison purposes. Elastic stiffness can be defined by the following equation

$$k = \frac{P}{\Delta_m} \qquad \text{Eq. 6-1}$$

where P is the load applied to the girder and Δ_m is the mid-span deflection of the girder. Because k is a function of deflection, it varies for each test based on the loading configuration. In this research, a four-point bending test configuration was selected for two reasons. First, four-point bending affords a constant moment region between the load points, which can be useful for experimental instrumentation and measurements. Second, four point bending was easily implemented in the University of Delaware Structures Laboratory using the MTS test frame. Additionally, the load can be applied using one or two actuators depending upon coordination of the test frame with other concurrent research.

Because four-point bending was selected, mid-span deflection was defined from beam bending theory as

$$\Delta_m = \frac{Pa}{24EI}\left(3L^2 - 4a^2\right) \qquad \text{Eq. 6-2}$$

where P is defined as the total load applied to the beam, a is the distance from the end of the test section to the load point, E is the flexural modulus of the material, I is the moment of inertia of the cross section of the girder, and L is the length of the test section. In order to apply this equation, the assumptions were made that the loading was applied symmetrically and that shear deformation was negligible compared to the flexural response. Actual mid-span deflection could be experimentally measured using a linear voltage displacement transducer (LVDT) placed at mid-span of the beam or using the displacement data from the load actuator if only one actuator was used during the testing. Once Δ_m had been obtained the elastic stiffness of the girder could be calculated and the results could then be compared to theoretical values to quantify the stiffness loss due to corrosion.

In addition to obtaining a value for elastic stiffness, Eq. 6-2 could also be solved for flexural modulus, EI. Rearranging terms to solve for flexural modulus yields:

$$EI = \frac{Pa}{24\Delta_m}\left(3L^2 - 4a^2\right) \qquad \text{Eq. 6-3}$$

Flexural modulus is also a useful way to evaluate the section loss due to corrosion. Because the modulus of elasticity of the material, E, is constant, the moment of inertia, I, can be computed. Moment of inertia is a function of the cross sectional area of the member and the overall section loss can be determined by comparing to values for the original section.

6.3 Pre-Rehabilitation Testing

Recall that the girders were tested prior to rehabilitation in order to determine the lost stiffness when compared to an identical uncorroded girder. Recall that all girders were tested in four-point bending. For the pre-rehabilitation testing, a 20-foot span length was used with the loads applied six feet from either end creating an eight-foot constant moment region in the center. The beam was loaded by using one actuator in contact with a spreader beam that was supported by two neoprene pads on the compression flange of the girder. A maximum load of 40 kips was applied to this spreader beam to impart two 20-kip loads on the girder. The beam deflection was recorded by placing an LVDT at the mid-span of the girder. Two tests were performed for each girder and the average results can be found in Table 6.1. Figures 6.1 and 6.2 contain the load deflection curves for the pre-rehabilitation testing of both girders.

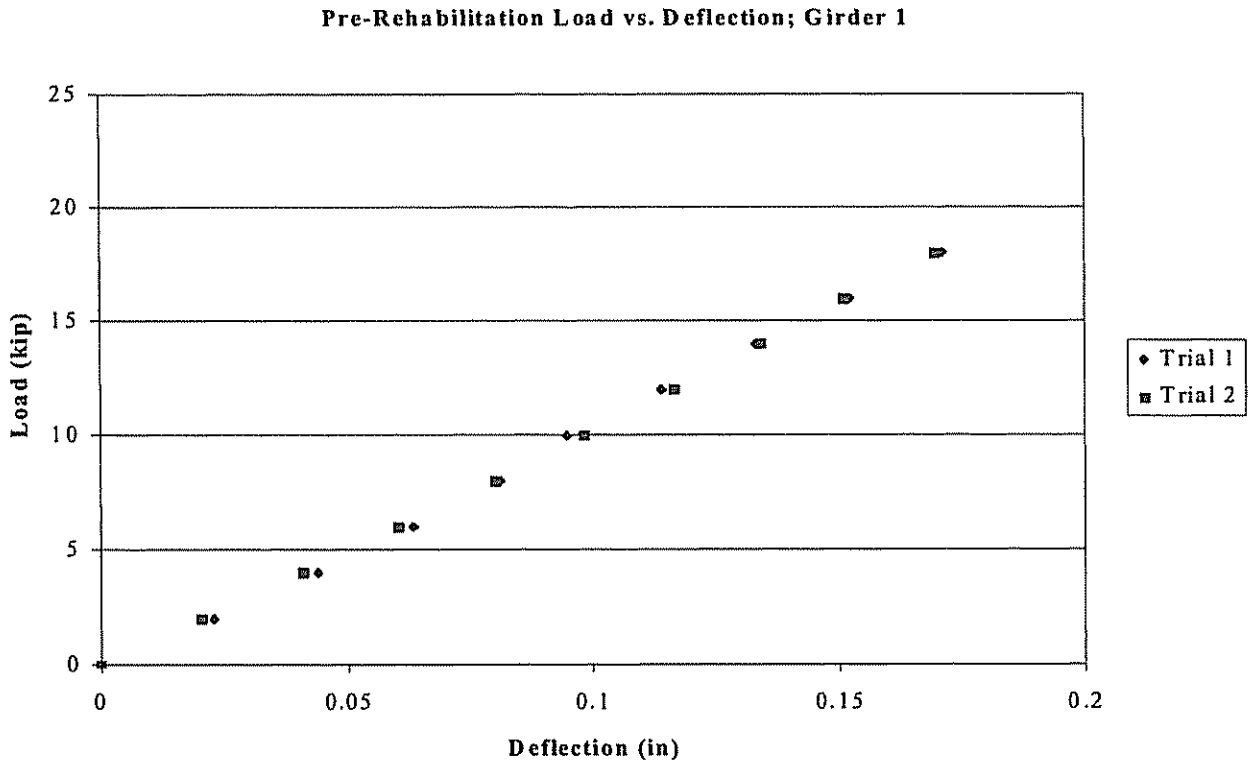

Figure 6.1 Load-deflection data for the pre-rehabilitation testing of Girder 1.

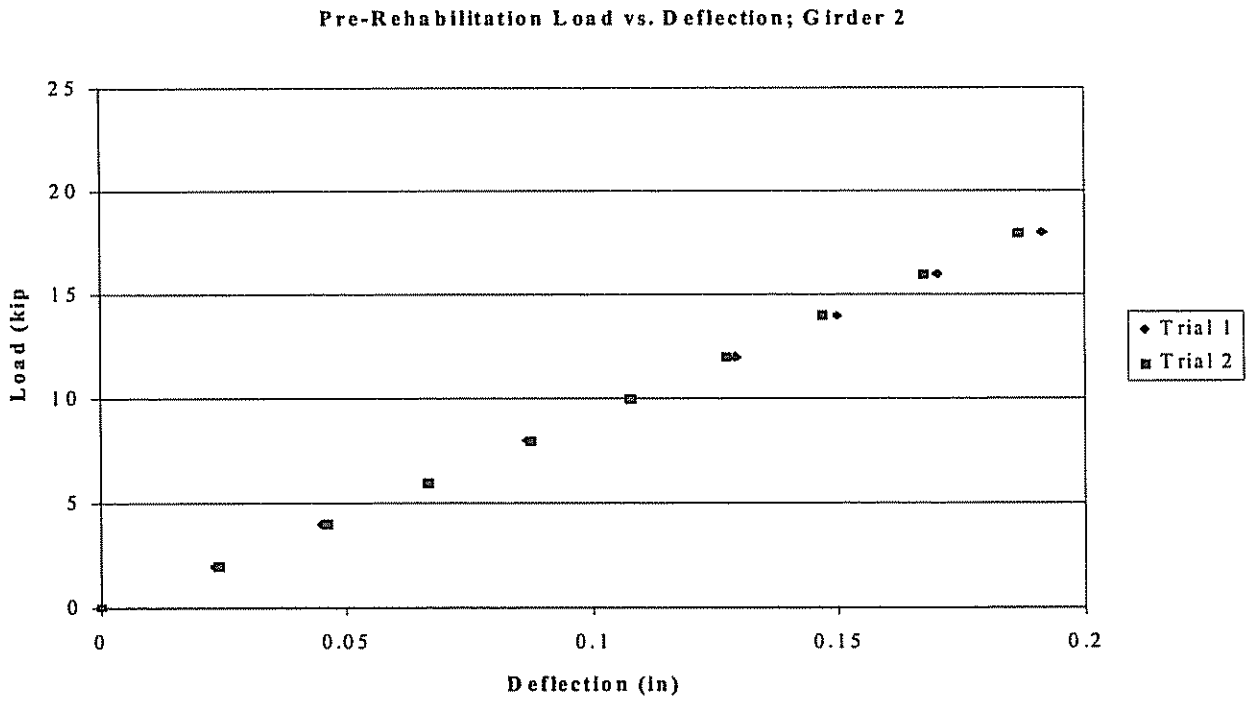

Figure 6.2 Load-deflection data for the pre-rehabilitation testing of Girder 2.

Table 6.1 Results from pre-rehabilitation girder testing.

	k	*EI*	% of original
Theoretical	142.7	$6.51x10^7$	100%
Girder 1	105.6	$4.82x10^7$	74.0%
Girder 2	95.2	$4.34x10^7$	66.7%

6.4 Post-Rehabilitation Testing

Similar to the pre-rehabilitation testing of Section 6.3, the testing performed on the repaired girders was conducted in four-point bending. Similar to the pre-rehabilitation testing, the post-rehabilitation testing used a 20-foot span length. Because the MTS test frame was configured differently at the date of the second test, a different loading configuration was used. For this test set-up, the loads were applied eight feet from either end creating a four-foot constant moment region in the center of the test length. In this case, the beam was loaded using two actuators in direct contact with the compression flange of the girder. Again, beam deflection was recorded by placing an LVDT at the mid-span of the girder. A minimum of two tests per girder was performed and the average results can be found in Table 6.2. Unfortunately, out of plane bending was experienced due to the change in stiffness of the section as a result of the

rehabilitation. Because adequate transverse support was not an option, the loads to which the girders were tested was on the order of six kips as opposed to the 20 kips from the initial testing. This difference in loading had no bearing on the test results because the stiffness was measured in the linear-elastic range of the material. After obtaining a value for the flexural stiffness, *EI*, of the repaired girders, a load-deflection history for the repaired girders was generated based upon the original test configuration to facilitate evaluation of the test results.

Table 6.2 Results from post-rehabilitation girder testing.

	k	*EI*	% of original
Theoretical	119.7	$6.51x10^7$	100%
Girder 1	109.9	$5.98x10^7$	91.8%
Girder 2	124.5	$6.78x10^7$	104%

Note that the theoretical value for elastic stiffness, *k*, for the post-rehabilitation testing was not the same as the value from the pre-rehabilitation testing. Recall that *k* is function of deflection, which is dependant upon the test configuration. Because the test configuration was different for the two groups of tests, it follows that the elastic stiffness would vary for each group of tests as well. However, the flexural modulus, *EI*, is independent of test set-up and is therefore a more reliable quantity for comparison between tests. Figures 6.3 and 6.4 contain the load deflection curves for the post-rehabilitation testing of both girders

6.5 Experimental Results

After both the pre- and post-rehabilitation testing had been completed, the results were compiled for comparison in Table 6.3. When examining the results contained within this table, the benefits of the composite rehabilitation were evident. The repaired Girder 1 renewed stiffness from 74% to 91.8% of the theoretical stiffness. Similarly, Girder 2 experienced a significant increase in stiffness from 66.7% to 104% of the theoretical stiffness. The repair scheme was so effective that it exceeded the original stiffness of a similar new girder by 4%. Figure 6.5 contains a direct comparison of the average values for the pre-rehabilitation and post-rehabilitation test results.

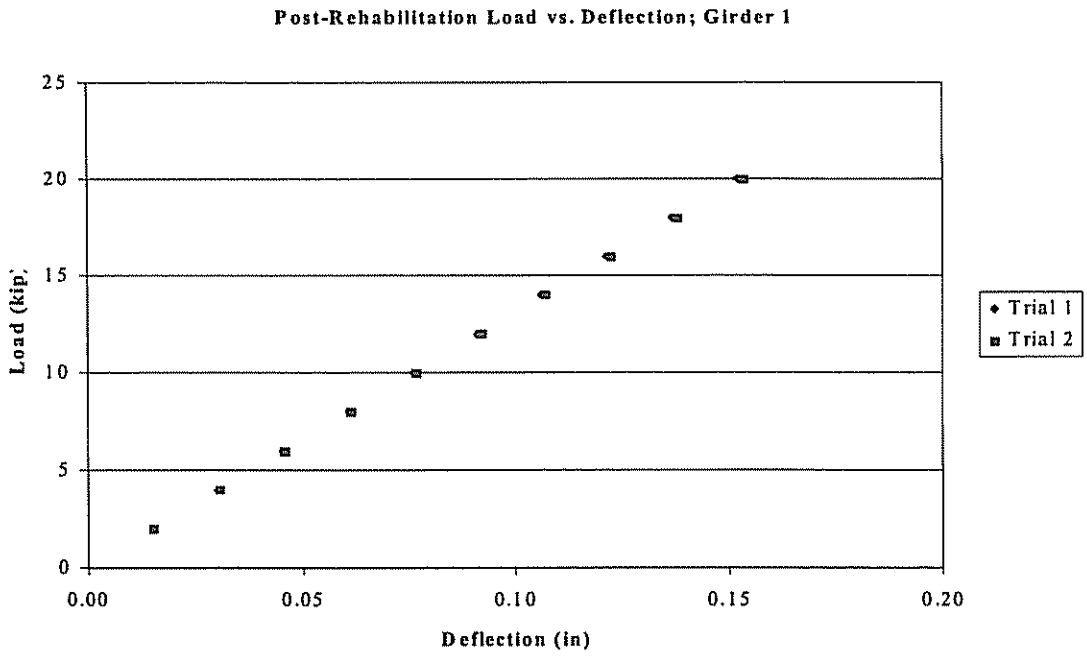

Figure 6.3 Load-deflection data for the post-rehabilitation testing of Girder 1.

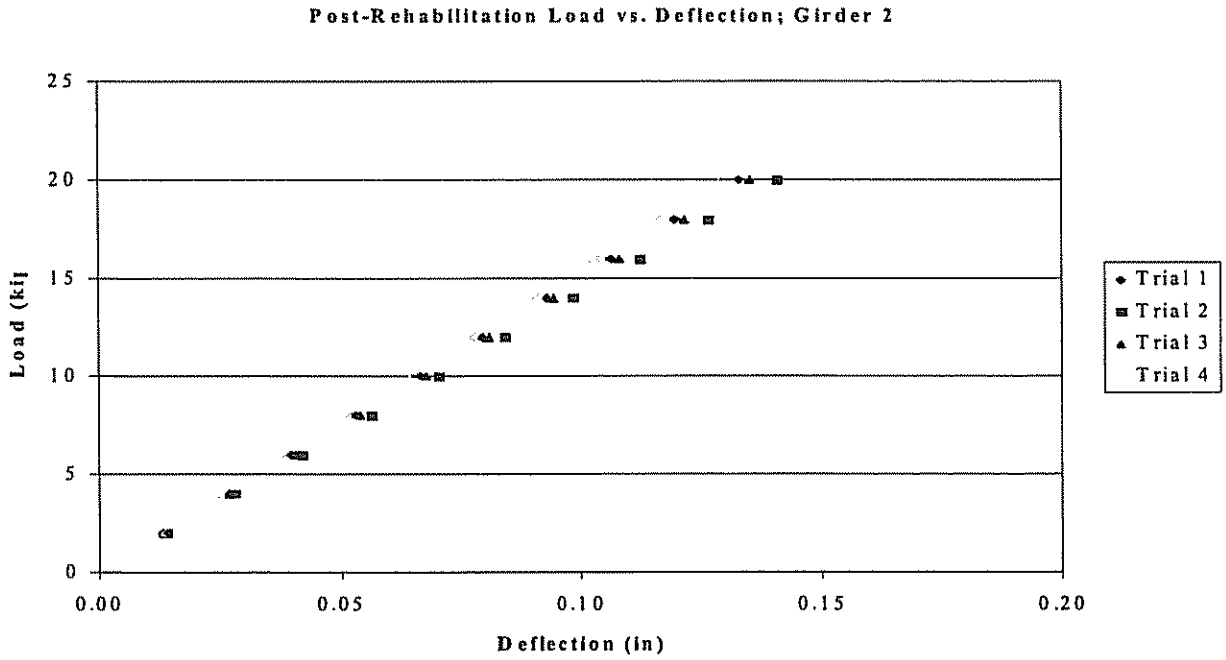

Figure 6.4 Load-deflection data for the post-rehabilitation testing of Girder 2.

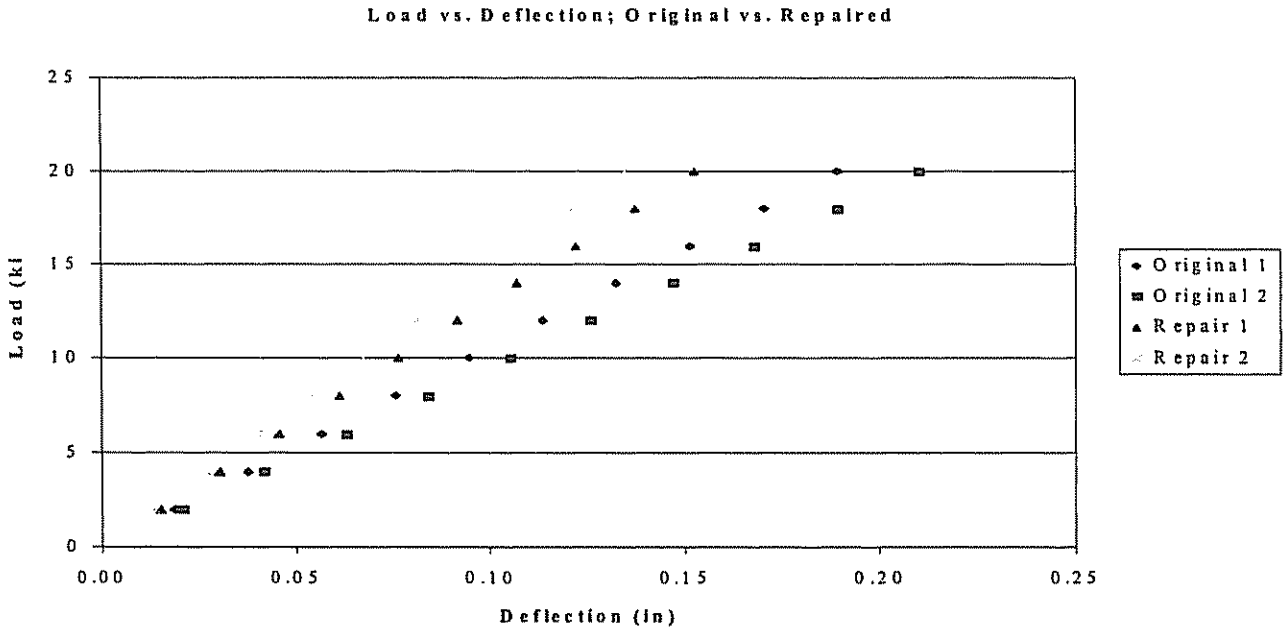

Figure 6.5 Comparison of average load-deflection data for pre-rehabilitation and post-rehabilitation test results.

Table 6.3 Comparison of test results before and after rehabilitation.

		k	*EI*	% of Original
Girder 1	Theoretical	142.7	$6.51x10^7$	100%
	Pre-Rehab	105.6	$4.82x10^7$	74.0%
	Post-Rehab	131.0	$5.98x10^7$	91.8%
Girder 2	Theoretical	142.7	$6.51x10^7$	100%
	Pre-Rehab	95.2	$4.34x10^7$	66.7%
	Post-Rehab	148.6	$6.78x10^7$	104%

6.6 Conclusions

Chapter 6 focused on the evaluation of the benefits of using composites to rehabilitate deficient steel bridge girders. Four-point bending was utilized in order to determine the elastic stiffness and flexural modulus of the beams prior to rehabilitation. These values were then used to evaluate how much stiffness had been lost over time when compared to a new girder. This pre-rehabilitation testing showed that the girders possessed only 74.0% and 66.7% of their original stiffness when compared to an identical new girder.

After the rehabilitation was performed, the beams were again tested to evaluate the increase in stiffness as a result of the composite rehabilitation. The first girder tested showed its stiffness was restored from 74.0% to 91.8% of its original performance. The rehabilitation exhibited an even more dramatic effect on Girder 2 by restoring all lost stiffness, from 66.7% to 104%, and even exceeding the original value by 4%. This testing conclusively demonstrates the benefits of this type of rehabilitation.

Note that these results compare favorably to those obtained by Gillespie, et al (238) in their original research. This is significant because it demonstrates that the addition of the scrim layer for galvanic corrosion protection as well as the introduction of the improved pretreatments did not degrade the overall performance. In addition to maintaining the desired benefits of the original rehabilitation, the implementation of the new pretreatments and incorporation of the scrim should enhance the overall performance by providing superior strength and long-term environmental durability. Future research should be able to utilize these same rehabilitated girders in a long-term durability study subject to actual environmental exposure, freeze-thaw conditions, and fatigue loading.

Chapter 7: CONCLUSIONS AND RECOMMENDATIONS

7.1 Conclusions

The purpose of this study was to expand upon previously established concepts and techniques for the rehabilitation of steel bridge girders through the application of advanced composite materials. Gillespie and Mertz (3-5) determined that adhesively bonding pultruded composite strips to the tension flange of a steel girder was the most viable option among a variety of concepts examined. This previous research established a rehabilitation scheme that was capable of renewing stiffness and increasing load capacity of steel bridge girders. A variety of other requirements were not considered that affect ling-term durability of the repair. Specifically, aspects such as galvanic corrosion, surface preparation, and bond performance required further investigation that was carried out in this work. Furthermore, the developments attained in this work were applied as a full-scale rehabilitation and corresponding load testing to assess the effects of incorporating the new techniques.

Most significantly, galvanic corrosion was a primary concern with this specific application because the graphite in the composite material and the steel bridge girder are on extreme opposite ends of the galvanic table. In order to prevent the formation of such an electrical circuit, it was necessary to insulate the two materials from one another. In theory, the adhesive alone should be sufficient to isolate the two constituents; however material discontinuities or installation defects could result in local galvanic couples. In order to safeguard against this possibility, a three-ounce 120-fiberglass scrim was introduced in the bond line. Two separate experiments were designed to evaluate the performance of the fiberglass scrim.

The first experiment measured the through thickness conductivity of both steel samples and composite samples. After establishing the presence of current flow, a layer of the fiberglass was bonded to the surface of the composite using the SCRIMP manufacturing process. It was demonstrated that the current flow through the composite was eliminated through the presence of the fiberglass scrim and that the corrosion resistance was significantly improved. In practice, the scrim layer could be added between the adherends during the installation process or incorporated in the surface of the composite during the manufacturing process to ensure greater quality control.

As a consequence of these first galvanic corrosion tests, an improvement in surface preparation needed for the bonding process was discovered. In order to ensure the best possible bond, it is strongly recommended to abrade the bonding surfaces and clean with a solvent. Typically, abrasive blasting of the surface of both the composite and steel will accomplish this. During the conductivity testing, it was observed that the conductivity of the composite

material decreased as the surface was abraded using a glass bead blast. This was counterintuitive because the process of abrading the surface was expected to expose more graphite fibers and therefore increase conductivity. Through examination under a microscope, it was discovered that the pressure used for the bead blast was too great and was actually damaging the composite material by pitting the surface and destroying the reinforcing fibers (i.e. failure would occur in the weakened surface layer during lap shear testing reducing strength). A series of tests were conducted to establish recommended guidelines for the surface preparation of the composite. It was learned that a 20-30 psi bead blast applied 2-3 inches from the surface of the material was effective in abrading the surface without compromising the integrity of the material.

The second galvanic corrosion test involved conditioning eleven representative samples through wet-dry cycling in a 10% aqueous NaCl bath. A total of 220 24-hour exposure cycles were conducted over an equal number of days. The samples included those fabricated with and without a scrim, samples designed to isolate through thickness and edge effects of corrosion with respect to the composite, as well as control samples. Both qualitative and quantitative results were recorded as part of this study. Ultimately, mechanical tests were performed on the composite material alone in order to evaluate the effect of the exposure on this particular material.

Upon separating the bonded samples, the most significant qualitative results were obtained. First and foremost, the composite failed cohesively instead of adhesively at the interface indicating that the chosen bonding scheme withstood the effects of the long-term saturation. Additionally, at some areas where the adhesive did pull away from the steel, an uncorroded, white metal surface was revealed. This observation dramatically illustrated that corrosion at the bond interface had effectively been prevented.

Mechanical testing was performed on conditioned and virgin composite samples to evaluate the effects of the corrosive environment. Both short beam shear (ASTM D 2344) and three point bending (ASTM D 790) were conducted as a part of the testing on both sample types. Analysis of the test results showed that the conditioned composite and the virgin composite exhibited statistically equivalent apparent shear strengths and that the virgin samples exhibited a slightly higher flexural strength. However, the modulus of elasticity across the two groups of sample was virtually identical. These results demonstrate that both the galvanic corrosion protection measures were effective and that the environmental exposure had no adverse effects on the mechanical properties of the composite material.

The galvanic corrosion study was followed by the bond performance phase of this work. Lessons learned during the previous stage were incorporated in the sample fabrication for the bond performance evaluation. In this work, bond performance was defined as strength, characterized using ASTM D 3165 lap shear specimens, and durability, investigated using ASTM D 3762 wedge specimens. Lap shear samples were tested under load control using an Instron

universal testing machine in order to arrive at ASTM D-1002 shear strength values. Similarly, the wedge specimens were exposed to both hot/ wet (122°F and 85% RH) and freeze/ thaw (cyclic temperatures from 0°F to 40°f) conditions in order to assess environmental durability. All samples were fabricated using the same standard procedure that was outlined in Chapter 3.

A baseline pretreatment was used for all samples fabricated throughout this work. This scheme consisted of the abrasion of the faying surfaces followed with a solvent wipe to remove any residue or cleaning particulates. Beyond the baseline material preparation, adhesive and primer candidates were selected after surveying literature and industry practices and using criteria set forth in Sections 3.2 and 3.3 respectively. Note that each primer and adhesive was accompanied by specific guidelines concerning their application and use, which included but was not limited to mixing and drying procedures. A total of eleven different sample types were fabricated and tested where four samples were identical to another four with the exception of the presence of the fiberglass scrim in the bond line. This allowed direct comparison between shear strength values to determine if there was any loss of strength due to the presence of the scrim.

The results of the strength testing showed that only one class of samples, those fabricated using the DelDOT paint primer, performed unfavorably compared to the remainder of the sample classes. Furthermore, the samples fabricated without a primer and implementing only the baseline surface treatment were found to have had a large number of samples that failed in the test grips despite having adequate strength characteristics and was therefore considered "suspect" at best. Additionally, the samples fabricated with the scrim in the bond line exhibited strength characteristics on the order of or even exceeding the values of those fabricated without the scrim therefore it was determined that its presence had no adverse effects on strength.

Despite being able to eliminate one sample class form the environmental durability testing using the wedge specimens, all prep methods were carried forward. It was during this phase of testing that preferred pretreatments and adhesive/ primer combinations were established based on the relative performance of all samples. In both the wedge specimen tests (hot/wet and freeze/ thaw) the samples fabricated using a combination of the Ciba Geigy AV8113 adhesive and Dow Silane Z-6040 primer performed superior to the other sample classes. Specifically, those samples fabricated in which the primer was either air-dried or oven dried at 200°F outperformed all other combinations. Based on the constraints of the application, it was determined that the air-dried silane was preferable due to the simplicity with which it could be implemented in the field. In order to establish several favorable combinations of adhesives and primers, it was suggested that both the Ciba-Geigy AV8113 and SikaDur 30 adhesives should be used in conjunction with both the Dow Silane Z-6040 primer and Dow Q1-6106 adhesion promoter in the next stage of the work, which was the full-scale rehabilitation.

After the adhesives and primers were selected, two full-scale bridge girders that had been taken out of service and donated to the university for research by PennDOT were retrofitted using the procedure outlined by previous researchers and enhanced through this work. The composite was bonded to the surface of the tension flange of the girder in a similar fashion to that which was used to fabricate the test samples, only on a larger scale. The exact procedure was outlined step-by-step in Chapter 5 to allow replication of the procedure in the field.

In the case of these girders, opposite halves of each tension flange was primed with each of the two primers. Conversely, one adhesive was used on either girder. This would allow future evaluation of the performance of each primer/ adhesive combination that was recommended through this work. After the rehabilitation was complete, the girders were tested in four-point bending with the results compared to pre-rehabilitation results in order to assess the overall benefits of the rehabilitation. The results demonstrated that the girders had their stiffness restored from 74.0% of original levels to 91.8% and from 66.7% to 104% of the original stiffness level. This agreed favorably with the results obtained in the original study (Mertz and Gillespie 14) thereby demonstrating repeatability of the process by independent research teams, consistency in the procedure, integrity of the results, and no adverse effects based on the presence of the scrim within the bond line.

7.2 Recommendations for Future Study

Despite the enhancements made in this work to the overall rehabilitation procedure from the original work, there are still some issues that require investigation. The full-scale girders that were rehabilitated should be studied under fatigue loading conditions to evaluate the performance of the rehabilitation under simulated service conditions. Furthermore, the same girders should be exposed to real-time environmental conditions outside of the laboratory for years to come to evaluate the effect of actual weather variations and compare that to the results obtained from the durability study in this work. Additionally, it would be beneficial to investigate the development of stresses in the ends of the composite strips to gain a better understanding of the behavior of this system and to make improvements in the system if necessary. Ultimately, based on the data gathered from the preceding recommendations and based on the information learned through the first two phases, the rehabilitation should be implemented on a bridge that is currently in service. This bridge should then be load rated and monitored to evaluate the overall effectiveness and performance of the structural repair for years to come.

BIBLIOGRAPHY

American Society for Testing and Materials. *Annual Book of ASTM Standards*. Vol. 03.01. Easton, MD: ASTM, 1995.

American Society for Testing and Materials. *Annual Book of ASTM Standards*. Vol. 03.02. Easton, MD: ASTM, 1996.

American Society for Testing and Materials. *Annual Book of ASTM Standards*. Vol. 15.06. Easton, MD: ASTM, 1996.

American Society for Testing and Materials. *Atmospheric Corrosion of Metals*. ASTM Special Technical Publication 767. Baltimore: ASTM, 1982.

American Society for Testing and Materials. *Corrosion in Natural Environments*. ASTM Special Technical Publication 558. Lutherville-Timonium, MD: ASTM, 1974.

American Society for Testing and Materials. *Electrochemical Corrosion Testing*. ASTM Special Technical Publication 727. Baltimore: ASTM, 1981.

Ammar, Nouredine. *Rehabilitation of Steel Bridge Girders with Graphite Pultrusion*. Master's Thesis. Newark, DE: U of Delaware P, 1996.

Anderson, T. L. *Fracture Mechanics: Fundamentals and Applications*. 2nd ed. Boca Raton: CRC Press, 1995.

Askeland, Donald R. *The Engineering and Science of Materials*. 3rd ed. Boston: PWS Publishing Company, 1994.

Aylor, Denise M. "The Effect of a Seawater Environment on the Galvanic Corrosion Behavior of Graphite/ Epoxy Composites Coupled to Metals." *High Temperature and Environmental Effects on Polymeric Composites*. ASTM Special Publication 1174. Virginia: ASTM, 1993.

Barsom, John M., and Stanley T. Rolfe. *Fracture and Fatigue Control in Structures: Applications of Fracture Mechanics*. 2nd ed. Englewood Cliffs, NJ: Prentice-Hall, Inc. 1987.

Beer, Ferdinand P. and E. Russel Johnston, Jr. *Mechanics of Materials*. 2nd ed. New York: McGraw-Hill Inc., 1992.

Bellucci, F. "Galvanic Corrosion Between Nonmetallic Coposites and Metals II. Effect of Area Ratio and Environmental Degradation." *Corrosion* 48 (1992): 281-291.

Boyd, Jack, et al. "Galvanic Corrosion Effects on Carbon Fiber Composites." *Proceedings from the 36th International SAMPE Symposium*. Covina, CA: SAMPE, 1991.

Broek, David. *Elementary Engineering Fracture Mechanics*. 4th ed. Hingham: Nijhoff, 1986.

Carlsson, Leif A., and R. Byron Pipes. *Experimental Characterization of Advanced Composite Materials*. 2nd ed. Lancaster: Technomic, 1997.

Chajes, M. J., et al. "Flexural Strengthening of Concrete Beams Using Externally Bonded Composite Materials." *Construction & Building Materials*. 8 (1995): 191-201.

Chajes, Michael J. Personal Communication. 1996-1999.

Demitz, John R. Personal Communication. 1996-2001.

Eckel, Douglas A. III. Personal Communication. 1997-1999.

Edberg, William. Personal Communication. 1996-1998.

Gillespie, J. W., Jr., et al. "Rehabilitation of Steel Bridge Girders: Large-Scale Testing." *Proceedings from the ASC 11th Technical Conference*. Atlanta: 1996.

Gillespie, John W., Jr. Personal Communication. 1996-2001.

Hack, Harvey P. *Corrosion Testing Made Easy: Galvanic Corrosion Test Methods*. Vol. 2. Houston: NACE International, 1993.

Hack, Harvey P., ed. *Galvanic Corrosion*. ASTM Special Publication 978. Ann Arbor: ASTM 1988.

Harris, Charles E., and Thomas S. Gates, eds. *High Temperature and Environmental Effects on Polymeric Composites*. ASTM Special Publication 1174. Virginia: ASTM, 1993.

Karbhari, V.M. and S. B. Shulley. "Use of Composite for Rehabilitation of Steel Structures – Determination of Bond Durability." *J. of Materials in Civil Engineering* 7 (1995): 239-245.

Kinloch, A. J. *Adhesion and Adhesives: Science and Technology*. New York: Chapman and Hall, 1987.

Kinloch, A.J. *Developments in Adhesives-2*. Englewood, NJ: Applied Science Publishers, Inc., 1981

Kinloch, A. J., ed. *Durability of Structural Adhesives*. New York: Applied Science, 1983.

Kinloch, A. J., and R. J. Young. *Fracture Behaviour of Polymers*. New York: Applied Science, 1983.

Kinloch, A. J., ed. *Structural Adhesives: Development in Resins and Primers*. New York: Elsevier Applied Science, 1986.

Koehn, Enno and Nestor A. Barroeta. "Inventory of Highway Infrastructure Problems Through Bridge Inspection." *J. of Professional Issues in Engineering Education and Practice* 117 (1991): 133-149.

Lyon, S.B., et al. "Accelerated Atmospheric Corrosion Testing Using a Cyclic Wet/ Dry Exposure Test: Galvanic Couples of Aluminum with Graphite Neoprene Rubber, Galvanized Steel, and Steel." Corrosion 45 (1989): 951-957.

McKnight, Steven H. *Influence of Surface Modification on the Processing and Perfromance of Aluminum Adhesive Joints Bonded with Thermoplastic Polymers*. Doctoral Dissertation. Newark, DE: U of Delaware P, 1995.

McKnight, Steven H. Personal Communication. 1997.

Mertz, Dennis R. and John W. Gillepsie, Jr. "Rehabilitation of Steel Bridge Girders Through the Application of Advanced Composite Materials." *IDEA Program Final Report*. 1996.

Mertz, Dennis R. Personal Communication. 1996-1998.

Mistretta, John P. "Rehabilitation of Concrete Bridge Beams with Externally-Bonded Composite Plates. Part II." *Proceedings from the 41st International SAMPE Symposium*. Covina, CA: SAMPE, 1996.

Purvis, Ronald L. and Khossrow Babaei. "Selection Bridge Protection and Rehabilitation Options." *Pacific Rim Trans Tech Conference Proceedings of the ASCE 3rd International Conference on Applications of Advanced Technologies in Transportation Engineering*. Seattle: 1993.

Rajagopalan, G., K. M. Immordino, and J. W. Gillespie, Jr. "Adhesive Selection Methodology for Rehabilitation of Steel Bridges with Composite Materials." *Proceedings from the ASC 11th Technical Conference*. Atlanta: 1996.

Rajagopalan, G. Personal Communication. 1997-2000.

Sax, Irving N. and Richard J. Lewis, Sr., eds. *Hawley's Condensed Chemical Dictionary*. 11th ed. New York: Van Nostrand Reinhold Company: 1987.

Scribner, L.L., and S. R. Taylor, eds. *The Measurement and correction of Electrolyte Resistance in Electrochemical Tests*. ASTM Special Technical Publication 1056. Baltimore: ASTM, 1990.

Sloan, F. E. and J. B. Talbot. "Corrosion of Graphite-Fiber-Reinforced Composites I – Galvanic Coupling Damage." *Corrosion* 48 (1992): 830-838.

Society for the Advancement of Material and Process Engineering. *How Concept . . . Becomes Reality*. Vol 36, Book 2 of 2. Covina, CA: SAMPE, 1991.

Society for the Advancement of Material and Process Engineering. *Materials and Process Challenges: Aging Systems, Affordability, Alternative Applications*. Vol 41, Book 2 of 2. Covina, CA: SAMPE, 1996.

Vinson, J. R., and R. L. Sierakowski. *The Behavior of Structures Composed of Composite Materials*. Boston: Kluwer Academic Publishers, 1987.

Wake, William C. *Developments in Adhesives-1*. London: Applied Science Publishers Ltd., 1977.

Wetzel, Eric. *Assessment of Heating Techniques for Metal to Composite Bonding in Infrastructure Rehabilitation*. Senior Thesis. Newark, DE: U of Delaware P, 1995.

Delaware Center for Transportation
University of Delaware
Newark, Delaware 19716